

# BET bromodomain ligands: Probing the WPF shelf to improve BRD4 bromodomain affinity and metabolic stability

Laura E. Jennings, Matthias Schiedel, David S. Hewings, Sarah Picaud, Corentine M.C. Laurin, Paul A. Bruno, Joseph P. Bluck, Amy R. Scoriah, Larissa See, Jessica K. Reynolds, Mustafa Moroglu, Ishna N. Mistry, Amy Hicks, Pavel Guzanov, James Clayton, Charles Evans, Giulia Stazi, Philip C. Biggin, Anna K. Mapp, Ester M. Hammond, Philip G. Humphreys, Panagis Filippakopoulos, Stuart J. Conway

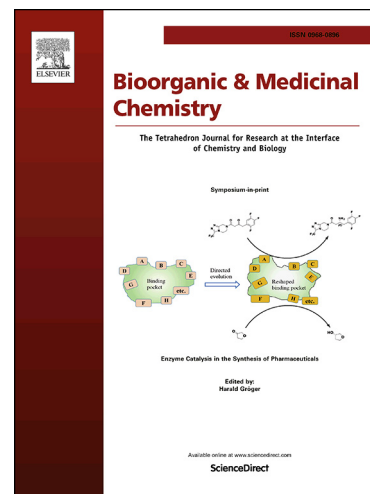
PII: S0968-0896(18)30382-1  
DOI: <https://doi.org/10.1016/j.bmc.2018.05.003>  
Reference: BMC 14345

To appear in: *Bioorganic & Medicinal Chemistry*

Received Date: 23 February 2018  
Revised Date: 30 April 2018  
Accepted Date: 2 May 2018

Please cite this article as: Jennings, L.E., Schiedel, M., Hewings, D.S., Picaud, S., Laurin, C.M.C., Bruno, P.A., Bluck, J.P., Scoriah, A.R., See, L., Reynolds, J.K., Moroglu, M., Mistry, I.N., Hicks, A., Guzanov, P., Clayton, J., Evans, C., Stazi, G., Biggin, P.C., Mapp, A.K., Hammond, E.M., Humphreys, P.G., Filippakopoulos, P., Conway, S.J., BET bromodomain ligands: Probing the WPF shelf to improve BRD4 bromodomain affinity and metabolic stability, *Bioorganic & Medicinal Chemistry* (2018), doi: <https://doi.org/10.1016/j.bmc.2018.05.003>

This is a PDF file of an unedited manuscript that has been accepted for publication. As a service to our customers we are providing this early version of the manuscript. The manuscript will undergo copyediting, typesetting, and review of the resulting proof before it is published in its final form. Please note that during the production process errors may be discovered which could affect the content, and all legal disclaimers that apply to the journal pertain.



# BET bromodomain ligands: Probing the WPF shelf to improve BRD4 bromodomain affinity and metabolic stability

## Authors

Laura E. Jennings<sup>at</sup>, Matthias Schiedel<sup>at</sup>, David S. Hewings<sup>a</sup>, Sarah Picaud<sup>b</sup>, Corentine M. C. Laurin<sup>a</sup>, Paul A. Bruno<sup>c,d,e</sup>, Joseph P. Bluck<sup>a,f</sup>, Amy R. Scorch<sup>a</sup>, Larissa See<sup>a</sup>, Jessica K. Reynolds<sup>a</sup>, Mustafa Moroglu<sup>a</sup>, Ishna N. Mistry<sup>g</sup>, Amy Hicks<sup>a</sup>, Pavel Guzanov<sup>a</sup>, James Clayton<sup>a</sup>, Charles Evans<sup>a</sup>, Giulia Stazi<sup>h</sup>, Philip C. Biggin<sup>f</sup>, Anna K. Mapp<sup>c,d,e</sup>, Ester M. Hammond<sup>g</sup>, Philip G. Humphreys<sup>i</sup>, Panagis Filippakopoulos<sup>b</sup>, Stuart J. Conway<sup>a,\*</sup>

<sup>a</sup> Department of Chemistry, Chemistry Research Laboratory, University of Oxford, Mansfield Road, Oxford, OX1 3TA, United Kingdom.

<sup>b</sup> Nuffield Department of Clinical Medicine, Structural Genomics Consortium, University of Oxford, Old Road Campus Research Building, Roosevelt Drive, Oxford, OX3 3TA, United Kingdom.

<sup>c</sup> Department of Chemistry, University of Michigan, Ann Arbor, Michigan 48109-1055, United States

<sup>d</sup> Life Sciences Institute, University of Michigan, Ann Arbor, Michigan 48109-2216, United States

<sup>e</sup> Program in Chemical Biology, University of Michigan, Ann Arbor, Michigan 48109-2216, United States

<sup>f</sup> Department of Biochemistry, University of Oxford, South Parks Road, Oxford, OX1 3QU, United Kingdom.

<sup>g</sup> CRUK/MRC Oxford Institute for Radiation Oncology, Department of Oncology, University of Oxford, Old Road Campus Research Building, Oxford, OX3 7DQ, United Kingdom.

<sup>h</sup> Department of Chemistry and Technologies of Drugs, Sapienza University of Rome,

Piazzale Aldo Moro 5, 00185 Rome, Italy.

<sup>i</sup> Epigenetics Discovery Performance Unit, GlaxoSmithKline R&D, Stevenage, Hertfordshire, SG1 2NY, United Kingdom

<sup>†</sup> These authors contributed equally to this work.

\*To whom correspondence should be addressed: stuart.conway@chem.ox.ac.uk, telephone: +44 (0)1865 285 109, fax: +44 (0)1865 285 002.

**Abstract**

Ligands for the bromodomain and extra-terminal domain (BET) family of bromodomains have shown promise as useful therapeutic agents for treating a range of cancers and inflammation. Here we report that our previously developed 3,5-dimethylisoxazole-based BET bromodomain ligand (OXFBD02) inhibits interactions of BRD4(1) with the RelA subunit of NF- $\kappa$ B, in addition to histone H4. This ligand shows a promising profile in a screen of the NCI-60 panel but was rapidly metabolised ( $t_{1/2}$  = 39.8 mins). Structure-guided optimisation of compound properties led to the development of the 3-pyridyl-derived OXFBD04. Molecular dynamics simulations assisted our understanding of the role played by an internal hydrogen bond in altering the affinity of this series of molecules for BRD4(1). OXFBD04 shows improved BRD4(1) affinity ( $IC_{50}$  = 166 nM), optimised physicochemical properties (LE = 0.43; LLE = 5.74; SFI = 5.96), and greater metabolic stability ( $t_{1/2}$  = 388 mins).

## 1. Introduction

Lysine acetylation is a prevalent protein post-translational modification (PTM) that occurs throughout the proteome<sup>1</sup> and is similar to phosphorylation in its ability to regulate protein function.<sup>2</sup> The role of acetyl-lysine (KAc) has been heavily studied in histone proteins, with KAc recognised as one of the key “marks” proposed to comprise the epigenetic code.<sup>3, 4</sup> Lysine acetylation state is regulated by lysine acetyl transferases (KATs) and lysine deacetylases (KDACs), while bromodomains are viewed as readers of KAc marks, and mediate chromatin-protein interactions that are frequently involved in transcriptional regulation.<sup>5</sup> There are 61 bromodomains found within 46 bromodomain-containing proteins (BCPs) in the human proteome which, despite having diverse primary sequences, share a common protein fold and structure.<sup>6</sup> The KAc residue binds in a well-defined pocket that, in some bromodomains, contains 5 structurally-conserved water molecules at its base, and possesses a key recognition residue that hydrogen bonds to the KAc; in canonical bromodomains this is an Asn residue. A sustained effort over recent years has resulted in small-molecule ligands being identified for an increasing number of these bromodomains.<sup>7-12</sup> The majority of work has focused on the development of ligands for the bromodomain and extra terminal domain (BET) family of BCPs, comprising bromodomain-containing proteins 2-4 (BRD2-4) and the testis-specific BRDT; each of these proteins contains two adjacent canonical bromodomains. There is also increasing work on the development of ligands for the non-BET bromodomains.<sup>13-16</sup> The BET bromodomains have emerged as exciting therapeutic targets with over 20 clinical trials involving BET bromodomain ligands in progress, primarily focused on oncology indications.<sup>14, 17-19</sup> Here we report further cellular data for our previously reported BET bromodomain ligand OXFBD02 (**1**),<sup>20, 21</sup> and subsequent structure-activity relationship (SAR) studies aimed at optimising the solubility and metabolic stability of this series of compounds. This work resulted in the development of OXFBD04 (**9j**), which displays improved BRD4(1) affinity and substantially enhanced metabolic stability compared to OXFBD02.

## 2. Results and discussion

A common feature of almost all bromodomain ligands is a component that occupies the KAc-binding pocket and mimics the interactions formed by KAc with the bromodomain. Work by us<sup>20-25</sup> and others<sup>26-35</sup> has shown that the 3,5-dimethylisoxazole group is a particularly effective KAc mimic, which has been used as the basis of ligands for the CREBBP bromodomain and the BET family of BCPs (Fig. 1).

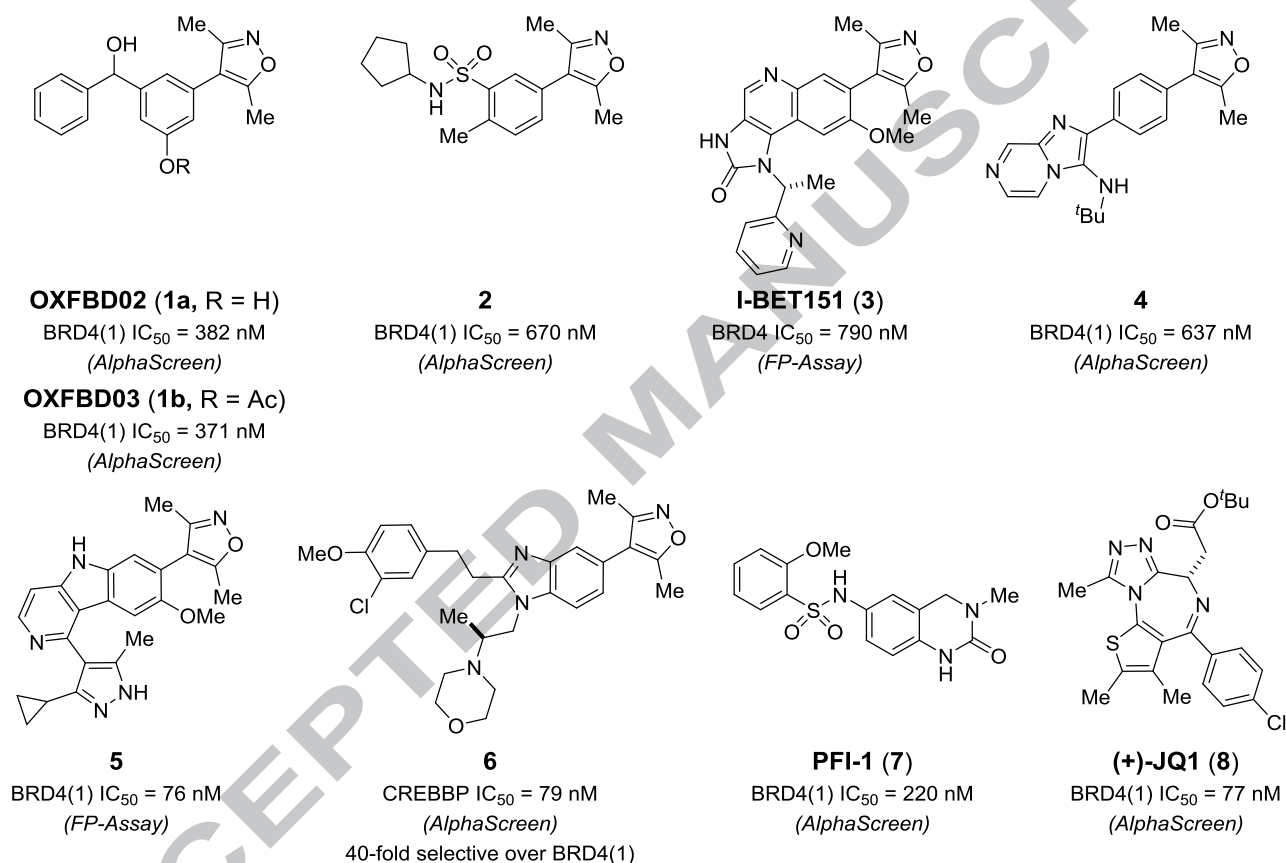


**Fig. 1.** Chemical structures and *in vitro* inhibition data of the 3,5-dimethylisoxazole-based BET bromodomain ligands **1-5**,<sup>21, 26, 27, 31, 33, 34</sup> the 3,5-dimethylisoxazole-based CREBBP bromodomain ligand **6**,<sup>24</sup> and the structurally unrelated BET bromodomain ligands PFI-1 (**7**)<sup>36</sup> and (+)-JQ1 (**8**).<sup>37</sup>

Using a fragment-based approach we previously developed OXFBD02 (**1a**) and OXFBD03 (**1b**) which have IC<sub>50</sub> values of 384 nM and 371 nM in an AlphaScreen assay for the first bromodomain of BRD4 [BRD4(1)], and IC<sub>50</sub> values for cytotoxicity of 794 nM and 616 nM in the MV4;11 acute myeloid leukaemia (AML) cell line, respectively.<sup>20, 21</sup>

## 2.1. Cellular evaluation of OXFBD02 (1)

To determine its activity against a wider panel of cancer cell lines, OXFBD02 (**1a**) was submitted for testing at a single dose against the NCI-60 human cancer cell line screen.<sup>38</sup> Growth inhibition (GI) was determined after 48 h treatment at 10  $\mu$ M, using a sulforhodamine B assay (to indicate cellular protein content). The compound was subsequently evaluated at five concentrations between 10 nM and 100  $\mu$ M to obtain GI<sub>50</sub> values, and to indicate the concentration required (if < 100  $\mu$ M) for total growth inhibition (TGI) (Table S1). A box plot of the data grouped by cancer type is shown (Fig. 2).

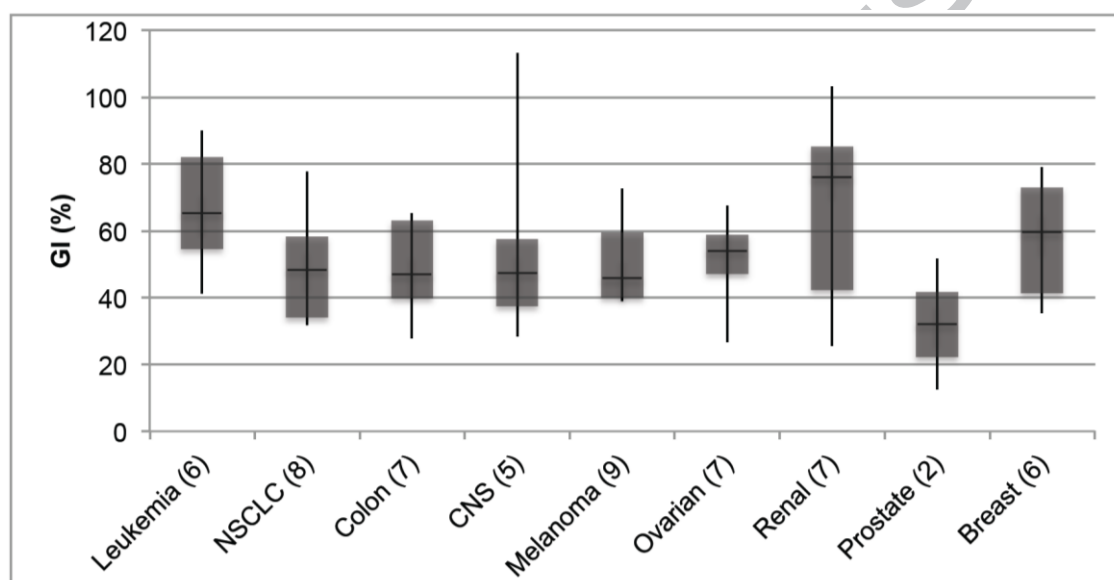


**Fig. 2.** Box plot of growth inhibition (GI) by OXFBD02 (**1a**) in NCI-60 panel. Plot indicates median, range and quartiles of GI by **1a** after 48 h treatment at 10  $\mu$ M in the NCI-60 DTP Human Tumour Cell Screen, grouped by cancer type. The number in brackets is the number of cell lines of each type in the NCI-60 panel. (Graphical representation in analogy to Lucas *et al.*)<sup>39</sup>

Similar to other BET bromodomain ligands, OXFBD02 (**1a**) was particularly effective at inhibiting the growth of leukaemia-, breast-, and renal-cancer cell lines. Calculation of the GI<sub>50</sub> values (see Table S1) allow comparison of OXFBD02 (**1a**) with the NCI-60 data obtained for PFI-1 (**7**, see Fig. 1), which is a chemically-distinct well-characterised BET bromodomain ligand.<sup>36</sup> PFI-1 (**7**) and OXFBD02 (**1a**) display well correlated patterns of cancer cell toxicity (Pearson's product-moment correlation coefficient,  $r = 0.82$ ; Table S1, Fig. S1 and S2).<sup>36</sup> These data suggest that the activity displayed by both compounds results predominantly from interaction with the BET bromodomains, rather than other chemotype-specific off-target cellular interactions.

Beyond its interactions with KAc residues in histone proteins, BRD4 has been reported to bind KAc310 of the RelA subunit of NF- $\kappa$ B. The binding of BRD4 leads to recruitment of cyclin-dependent kinase 9 (CDK9), phosphorylation of RNA polymerase II, and consequent activation of NF- $\kappa$ B-dependent gene expression.<sup>40-43</sup> Disruption of the RelA-BRD4 interaction with the BET ligand (+)-JQ1 (**8**) was previously shown to suppress NF- $\kappa$ B-dependent transcription.<sup>41</sup> To investigate whether OXFBD02 (**1a**) also disrupts the interaction of BET bromodomains KAc310 of RelA, and to assess the cellular effects of OXFBD02 (**1a**) in a functional assay, we employed a luciferase reporter system based on a previously published procedure.<sup>44</sup> This allowed us to determine the effects of BRD4 bromodomain binding on NF- $\kappa$ B-dependent transcription. (+)-JQ1 (**8**, see Fig. 1) was employed as a positive control and exerted a potent suppression of NF- $\kappa$ B-dependent gene expression, whereas the inactive enantiomer (–)-JQ1 did not show significant effects. Addition of OXFBD02 (**1a**) led to a concentration-dependent suppression of NF- $\kappa$ B-dependent gene expression (Fig. 3), indicating that it also disrupts the interaction of the BRD4 bromodomains with KAc310 of RelA. The fact that complete repression of NF- $\kappa$ B-dependent transcription was not observed with either **1a** or (+)-JQ1 suggests that there might be other PPIs involved in this process.

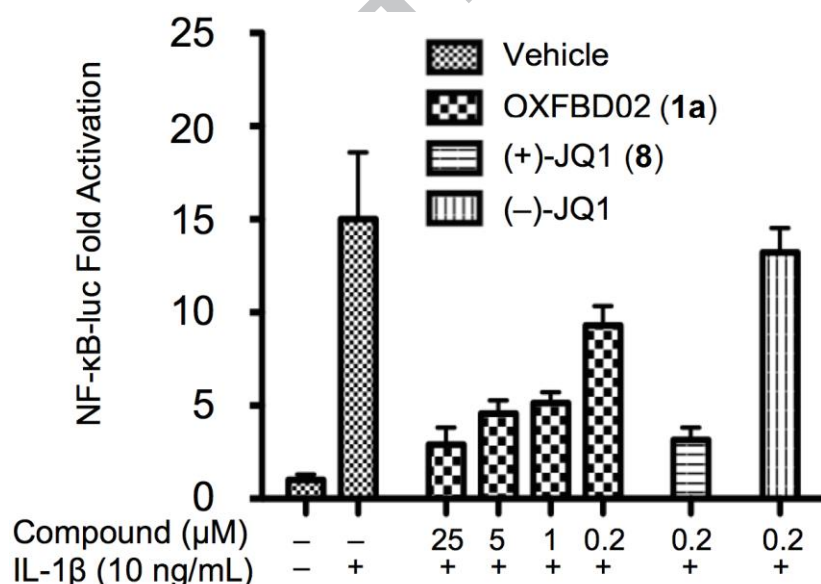


**Fig. 3.** Luciferase reporter gene assay allows assessment of the effect of compounds on NF- $\kappa$ B-dependent gene expression. HeLa cells were transiently transfected with a reporter plasmid containing luciferase and five  $\kappa$ B binding sites. The cells were treated with DMSO as a control (–), or different concentrations (0.2, 1, 5 and 25  $\mu$ M) of OXFBD02 (**1a**), (+)-JQ1 (**8**), or (–)-JQ1 for 12 hours before stimulation with IL-1 $\beta$  (+). The gene expression without stimulation of IL-1 $\beta$  (–) was also measured for the DMSO-treated control. Results

were obtained in quadruplicate and averaged, with error bars signifying standard deviation. OXFBD02 (**1a**) shows a concentration-dependent effect on transcription.

## 2.2. Designing compounds to investigate the WPF shelf-binding region

Taken together the data above indicate that the series of compounds exemplified by OXFBD02 (**1a**) are potentially useful tools to investigate the function of the BET bromodomains in cellular and ultimately *in vivo* settings. With this in mind, we used Metasite 3.1.2 (phase I) and Meteor 2.0.2 (phase I and II) to predict the metabolic liabilities of OXFBD02 (**1a**) (Fig. S3). This analysis indicated that the 4-position of the phenyl ring was the most significant liability, presumably through CYP450-catalysed oxidation. In accordance with this prediction, investigation of the metabolic stability of OXFBD02 (**1a**) in human liver microsomes showed that **1a** is a relatively high clearance compound, with  $CL_{int}$  of 34.8  $\mu\text{L}/\text{min}/\text{mg}$  protein and a cellular half-life of 39.8 mins (Table S2). These data are consistent with work by Sharp *et al.* who showed that, in a direct comparison, 3,5-dimethylisoxazole-based compounds showed the highest affinity for the BET bromodomain, but also poor metabolic stability.<sup>31</sup> Therefore, while optimising our compounds we wished to determine whether poor metabolic stability is an inherent problem with 3,5-dimethylisoxazole-based compounds, or whether by carefully balancing the properties of the whole molecule this apparent liability can be overcome.

Given the structure of **1a**, and the metabolic liability of the *para*-position, the region of the molecule that is most suitable for optimisation is the WPF shelf-binding phenyl ring. It has generally been observed that binding of a lipophilic moiety to this region confers high affinity for the BET bromodomains.<sup>7</sup> However, the lipophilicity of this group has to be balanced with the overall properties of the molecule to ensure that the compound is soluble. Solubility Forecast Index ( $\text{SFI} = \text{clogD}_{\text{pH}7.4} + \#\text{Ar}$ )<sup>45</sup> is a useful parameter for predicting compound solubility, and is especially useful for comparing molecules within a series. OXFBD02 (**1a**) is soluble enough to be used in *in vitro* and cellular settings, and has  $\text{SFI} = 6.6$ , suggesting that new analogues should have an SFI value of 6.6 or lower to ensure useful solubility. In addition,  $CL_{int}$  is hydrophobicity dependent and therefore reducing compound hydrophobicity might help to improve compound metabolic stability.<sup>46</sup>



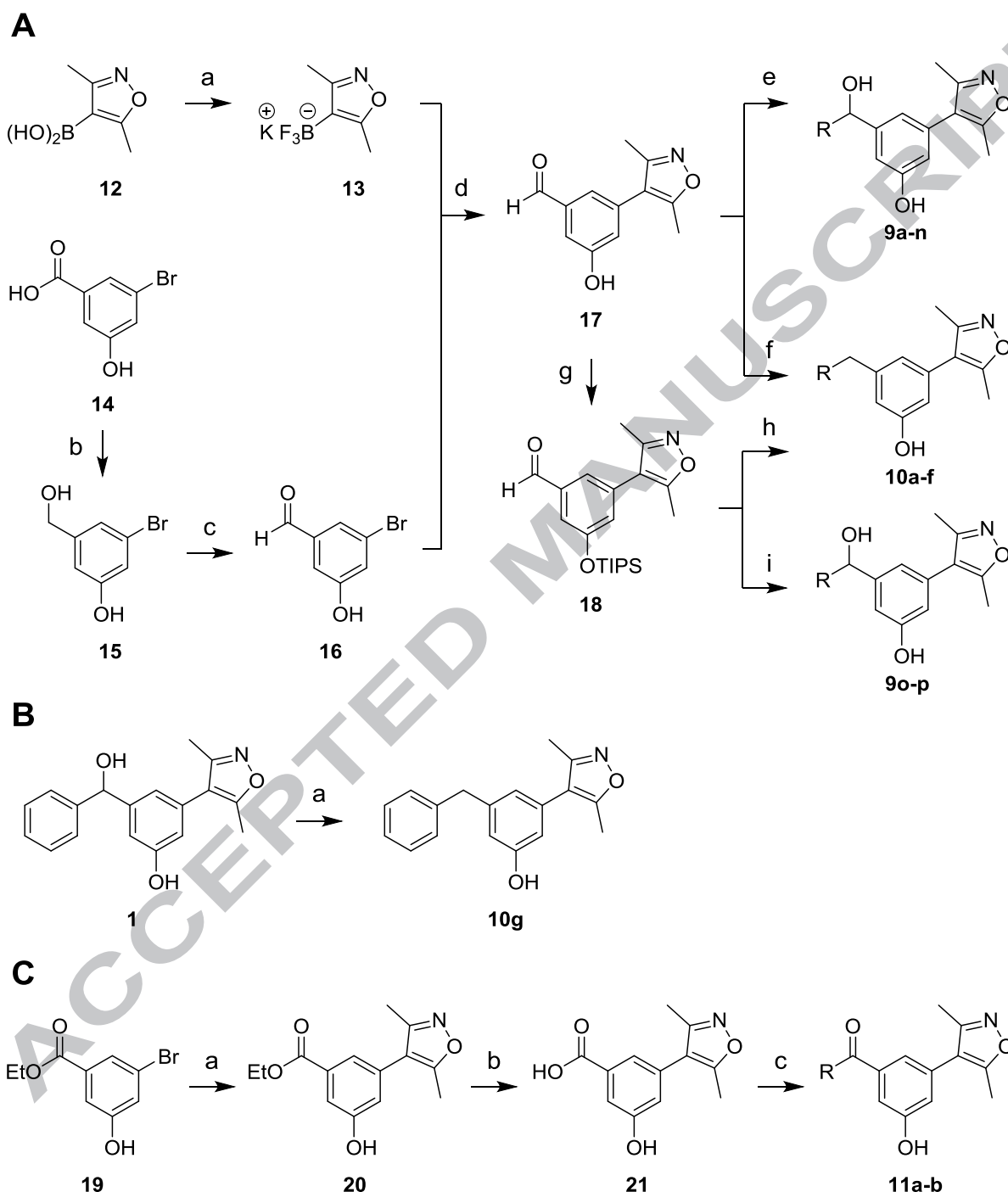
Based on these observations, and cognisant of work by Gehling *et al.*<sup>30</sup> we designed a series of compounds to probe the WPF shelf-binding region of the molecule. In particular we wished to explore blocking the 4-position of the phenyl ring with metabolically stable functionality to be a facile way to overcome the issue of metabolic oxidation.

Compounds with both electron-withdrawing and electron-donating substituents at the 2-, 3-, and 4-position of the ring (**9a-e**, **g**, **l**, **m**, **o**) were designed to probe the optimum electronics and vector for ring substitution. Compound **9f** contains 3,4-dichloro-substitution to determine whether two substituents are tolerated on the phenyl ring. The 2-, 3-, and 4-pyridyl derivatives (**9j**, **k**, **p**) were designed as these compounds have favourable SFI values of 5.9, and the 4-chloro-2-pyridyl derivative (**9n**) was designed to reduce the basicity of the pyridine nitrogen atom ( $pK_a = 2.22$  ( $pK_a$  value of the conjugated acid), predicted using ACD/Labs I-Lab 2.0 software [Algorithm Version: v12.1.0.50374]). We designed compounds with cyclohexyl and cyclopropyl substituents (**9h-i**) to determine whether non-aromatic rings are accepted by the WPF shelf. We also wished to probe whether the secondary hydroxyl group is essential for good BET bromodomain affinity, and so a series of compounds was designed without this functionality, which also allowed the introduction of less polar solubilising groups, mainly *via* reductive amination. In this series, we investigated whether more polar groups, conveying favourable physicochemical properties to the molecule (**10a-g**), are able to bind the WPF shelf. We were particularly interested in 4,4-difluoropiperidinyl analogue (**10d**) as the two geminal fluorine substituents were predicted to lower basicity of the tertiary amine ( $pK_a = 4.67$  (conjugated acid of the tertiary amine)), predicted using ACD/Labs I-Lab 2.0 software [Algorithm Version: v12.1.0.50374], Table S3), which suggests that the compound will exist in a predominantly deprotonated state at physiological pH, allowing binding of the WPF shelf. We also designed two amide-based compounds (**11a-b**) to investigate the importance of the tetrahedral carbon atom proximal to the WPF shelf-binding group.

### 2.3. Synthesis

Our general synthetic strategy is based on that previously reported for the OXFBD02 (**1a**).<sup>21</sup> The synthesis of aldehyde **17** has been optimised (Scheme 1A and Supporting Information) as this is a

key intermediate in the synthesis of the secondary alcohols **9a-n**, and the amines **10a-d**. The secondary alcohols **9o-p** were generated by reaction of the TIPS-protected analogue **18** with organolithium reagents (Scheme 1A), followed by deprotection.



**Scheme 1.** Synthesis of the 3,5-dimethylisoxazole-based compounds **9-11**. (A) Synthesis of the secondary alcohols **9a-p** (**9a**: R = 4-chlorophenyl, **9b**: R = 2-methoxyphenyl; **9c**: R = 3-methoxyphenyl; **9d**: R = 4-methoxyphenyl; **9e**: R = 4-tolyl; **9f**: R = 3,4-dichlorophenyl; **9g**: R = 4-fluorophenyl; **9h**: R = cyclohexyl; **9i**: R = cyclopropyl; **9j**: R = 3-pyridyl; **9k**: R = 4-pyridyl; **9l**: R = 3-fluorophenyl; **9m**: R = 4-cyanophenyl; **9n**: R = 4-chloro-2-pyridyl, **9o**: R = 2-fluorophenyl, **9p**: R = 2-pyridyl) and the amines

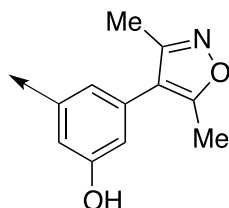
**10a-f** (**10a**: R = N-methylpiperazinyl; **10b**: R = morpholinyl; **10c**: R = N-benzylamino; **10d**: R = 4,4-difluoropiperidinyl; **10e**: R = piperidinyl; **10f**: R = pyrrolidinyl). *Reagents and conditions*: (a) KF, L-(+)-tartaric acid, CH<sub>3</sub>CN/THF, rt, 30 min, 59-73% (n =2); (b) BH<sub>3</sub>·THF, THF, 0 °C then rt, 18 h, 80-96% (n=3); (c) MnO<sub>2</sub>, CHCl<sub>3</sub>/EtOAc, reflux, 2 h, 49-78% (n=3), (d) Pd(OAc)<sub>2</sub>, RuPhos, Na<sub>2</sub>CO<sub>3</sub>, EtOH, 80 °C, 85%; (e) for **9a-e**: RMgBr, THF, rt, 3-19 h, 51-80%; for **9f**: 3,4-dichlorophenylmagnesium bromide, THF, 50 °C, 14 h, 11%; for **9g-i**: Aryl/alkyl bromide, Mg, I<sub>2</sub>, THF, rt to reflux, 30-60 min, then **17**, THF, 0 °C to rt, 2-18 h, 72-85%; for **9j**: 3-bromopyridine, isopropylmagnesium chloride lithium chloride complex, THF, rt, 2 h, then **17**, THF, rt, 4 h, 73%; for **9k**: 4-iodopyridine, isopropylmagnesium chloride, THF, rt, 1 h, then **17**, THF, rt to 50 °C, 22 h, 9%; for **9l-n**: Aryl iodide, isopropylmagnesium chloride lithium chloride complex, THF, -10 °C to rt, 2-5 h, then **17**, THF, rt to 50 °C, 3 h to 2 d, 11-23%; (f) for **10a-c**: amine, AcOH, EtOH, pH = 4, rt, 20-40 min, then NaBH<sub>3</sub>CN, rt, 17-23 h, 20-69%; for **10d**: 4,4-difluoropiperidine hydrochloride, EtOH, rt, 30 min, then NaBH<sub>3</sub>CN, rt, 19 h, 33%; (g) TIPSCl, imidazole, DMF, 0 °C to rt, 13 h, 84%; (h) Amine, AcOH, EtOH, rt, 1 h, then NaBH<sub>3</sub>CN, rt, 22 h, then TBAF, THF, 0 °C to rt, 1-2 h, 8-33%; (i) Aryl bromide, <sup>n</sup>BuLi, THF, -78 °C, 40 min, then **18**, THF, -78 °C to rt, 3-16 h, then TBAF, THF, 0 °C, 0.5-2 h, 17-89%; (B) Synthesis of **10g**. *Reagents and conditions*: (a) Et<sub>3</sub>SiH, TFA, rt, 15 min, 70%; (C) Synthesis of **11a-b**. *Reagents and conditions*: (a) **13**, Pd(OAc)<sub>2</sub>, RuPhos, Na<sub>2</sub>CO<sub>3</sub>, EtOH, 90 °C, mw, 1.5 h, 68%; (b); LiOH, THF, rt, 24 h, 96%; (c) EDC hydrochloride, HOBt hydrate, THF, rt, 20 min, then amine, 55 °C, 3 d, 52-56% (see Experimental Section for more detailed procedures).

Reductive amination of **18** with subsequent deprotection furnished the amines **10e-f** (Scheme 1A). The methylene derivative **10g** was synthesised by treating OXFBD02 (**1a**) with TFA and Et<sub>3</sub>SiH to reduce the secondary alcohol (Scheme 1B). To obtain the amides **11a-b** we coupled the carboxylic acid **21** to the appropriate secondary amine using 1-ethyl-3-(3-dimethylaminopropyl)carbodiimide (EDC) (Scheme 1C). Detailed information for the synthesis of all final compounds (**9a-p**, **10a-f**, **11a-b**) as well as the intermediates (**13**, **15-18**, **20-21**) can be found in the Experimental Section.

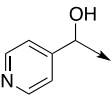
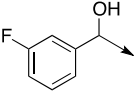
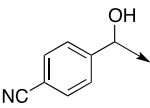
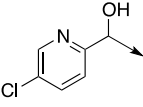
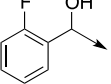
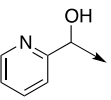
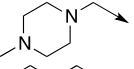
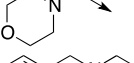
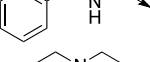
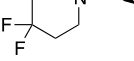
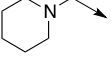
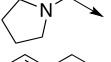
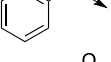
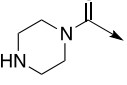
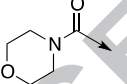
## 2.4. *In vitro* inhibition and SAR studies

A well-validated Amplified Luminescence Proximity Homogeneous Assay (AlphaScreen™) peptide displacement assay was used to measure the BRD4(1) IC<sub>50</sub> values for the synthesised compound, and the data obtained are shown in Table 1.<sup>47</sup>

**Table 1.** IC<sub>50</sub> values, pIC<sub>50</sub> values, ligand efficiencies (LE), clogP values, lipophilic ligand efficiencies (LLE), cLogD<sub>pH7.4</sub> values, and solubility forecast index (SFI) for **9a-p**, **10a-g**, **11a-b**, including **1a** as a reference compound. Heat map shows relative IC<sub>50</sub> values obtained in an AlphaScreen assay.<sup>47</sup> Red indicates low IC<sub>50</sub> values, and green indicates high IC<sub>50</sub> values. Quoted IC<sub>50</sub> values are a mean of three technical repeats. Ranges in parentheses represent 95% confidence intervals resulting from sigmoidal curve fitting to the triplicate data.



Compound	Substituent	BRD4(1) IC <sub>50</sub> (μM) <sup>a</sup>	pIC <sub>50</sub>	LE	cLogP <sup>b</sup>	LLE	cLogD <sub>pH7.4</sub> <sup>b</sup>	SFI
<b>1a</b>		0.384 (0.346-0.420) <sup>c</sup>	6.42	0.41	2.53	3.89	3.62	6.62
<b>9a</b>		0.631 (0.539-0.739)	6.20	0.38	3.13	3.07	4.28	7.28
<b>9b</b>		0.270 (0.223-0.327)	6.57	0.38	2.45	4.12	3.80	6.80
<b>9c</b>		0.478 (0.402-0.570)	6.32	0.37	2.45	3.87	3.80	6.80
<b>9d</b>		0.585 (0.531-0.644)	6.23	0.36	2.45	3.78	3.80	6.80
<b>9e</b>		0.296 (0.264-0.332)	6.53	0.40	2.99	3.54	4.32	7.32
<b>9f</b>		0.945 (0.865-1.03)	6.02	0.35	3.60	2.42	5.01	8.01
<b>9g</b>		0.842 (0.697-1.02)	6.07	0.37	2.59	3.48	4.00	7.00
<b>9h</b>		0.166 (0.158-0.175)	6.78	0.43	3.24	3.54	4.24	6.24
<b>9i</b>		0.377 (0.339-0.420)	6.42	0.47	1.54	4.88	3.26	5.26
<b>9j</b>		0.166 (0.142-0.193)	6.78	0.43	1.04	5.74	2.96	5.96

9k		0.303 (0.262-0.349)	6.52	0.41	1.04	5.48	2.86	5.86
9l		0.793 (0.685-0.919)	6.10	0.37	2.59	3.51	4.00	7.00
9m		0.604 (0.536-0.680)	6.22	0.36	1.97	4.25	3.53	6.53
9n		0.495 (0.427-0.574)	6.31	0.38	1.89	4.42	3.49	6.49
9o		1.42 (1.21-1.68)	5.85	0.36	2.59	3.26	4.00	7.00
9p		4.68 (3.40-6.45)	5.33	0.34	1.04	4.29	2.96	5.96
10a		1.23 (1.02-1.47)	5.91	0.38	0.72	5.19	1.41	3.41
10b		0.956 (0.802-1.14)	6.02	0.40	0.97	5.05	2.34	4.34
10c		2.25 (1.82-2.77)	5.65	0.34	3.21	2.44	2.34	5.34
10d		0.235 (0.210-0.263)	6.63	0.40	1.37	5.26	3.62	5.62
10e		4.28 (3.39-5.40)	5.37	0.36	2.55	2.82	2.22	4.22
10f		3.27 (2.43-4.38)	5.49	0.38	1.98	3.51	1.27	3.27
10g		1.10 (0.990-1.22)	5.96	0.40	4.00	1.96	4.96	7.96
11a		0.722 (0.568-0.918)	6.14	0.39	1.62	4.52	3.21	5.21
11b		3.80 (3.04-4.74)	5.42	0.34	0.07	5.35	2.38	4.38

<sup>a</sup>Protein concentration was adjusted to a final assay concentration of 10 nM, peptide concentration was 4 nM (see Supporting Information for detailed assay procedures). <sup>b</sup>cLogP and cLogD<sub>pH7.4</sub> values were calculated using ACD/Labs I-Lab 2.0 software (Algorithm Version: 5.0.0.184). <sup>c</sup>Values taken from Hewings *et al.*<sup>21</sup>

Addition of a 4-chloro substituent (**9a**, Table 1) resulted in a small drop in BRD4(1) affinity ( $IC_{50}$  = 0.631  $\mu$ M). Addition of a methoxy group was generally well tolerated, with 2-position (**9b**) substitution preferred ( $IC_{50}$  = 0.270  $\mu$ M) over 3- (**9c**) or 4-position (**9d**) substitution. The 4-tolyl derivative (**9e**) showed similar affinity to **1a**, indicating that lipophilic substituents are favourable for BRD4(1) binding. Interestingly, fluorine was less well tolerated than other substituents (**9g**, **l**, **o**), with the 2-fluoro derivative (**9o**) displaying the lowest BRD4(1) affinity ( $IC_{50}$  = 1.42  $\mu$ M). The 3-pyridyl (**9j**,  $IC_{50}$  = 0.166  $\mu$ M) and 4-pyridyl (**9k**,  $IC_{50}$  = 0.303  $\mu$ M) derivatives showed high BRD4(1)

affinity. Intriguingly the 2-pyridyl derivative (**9p**) showed substantially reduced BRD4(1) affinity ( $IC_{50} = 4.68 \mu M$ ). Both the cyclopropyl (**9i**) and cyclohexyl substituents (**9h**) were well tolerated. The cyclohexyl derivative displayed the joint highest affinity ( $IC_{50} = 0.166 \mu M$ ) for BRD4(1), albeit at the expense of increased lipophilicity ( $clogD_{7.4} = 4.24$ ,  $LLE = 3.54$ ) compared to the equipotent 3-pyridyl derivative (**9j**,  $clogD_{7.4} = 2.96$ ,  $LLE = 5.74$ ). The phenyl derivative in which the secondary hydroxyl group is removed (**10g**) showed a significantly reduced BRD4(1) affinity ( $IC_{50} = 1.10 \mu M$ ) compared to the matched pair of compound **1a**. In general, other more polar substituents were poorly tolerated and displayed higher  $IC_{50}$  values. The piperazine amide derivative (**11a**) was relatively well tolerated, whereas the morpholine derivative (**11b**) was not.

We determined a BRD4(1) dissociation constant ( $K_d$ ) for **9j** of  $0.247 \mu M \pm 0.08 \mu M$  using isothermal titration calorimetry (ITC) (Fig. S4A), which is consistent with the AlphaScreen results. For **1a** we determined a  $K_d$  value of  $0.435 \mu M \pm 0.16 \mu M$  (Fig. S4B). Selectivity profiling in a BROMOScan assay against 12 phylogenetically diverse bromodomains confirmed that both **1a** and **9j** potent BET bromodomain ligands, with additional modest affinity for the CREBBP bromodomain, but no significant affinity for any of the other of the selected bromodomains investigated (Table S4).

## 2.5. Structural studies

To understand the structural basis of our SAR observations we obtained X-ray crystal structures of the 3-pyridyl derivative (**9j**; PDB code 6FSY), the cyclopropyl derivative (**9i**; PDB code 6FT3), and the difluorinated piperidine derivative (**10d**; PDB code 6FT4) in complex with BRD4(1). In all cases the molecules bind to BRD4(1) broadly as expected. The 3,5-dimethylisoxazole acts as the KAc mimic and forms a hydrogen bond with N140 and a water-mediated hydrogen bond with Y97 (Fig. 4A). Interestingly in the case of **9j** and **9i**, only the (*R*)-enantiomer is observed in the X-ray crystal structure, despite a racemate being submitted to crystallisation. It should be noted that despite these two molecules having the same absolute configuration, they have the opposite sense of stereochemistry due to the priority assignment of the pyridine ring compared to the cyclopropyl ring.



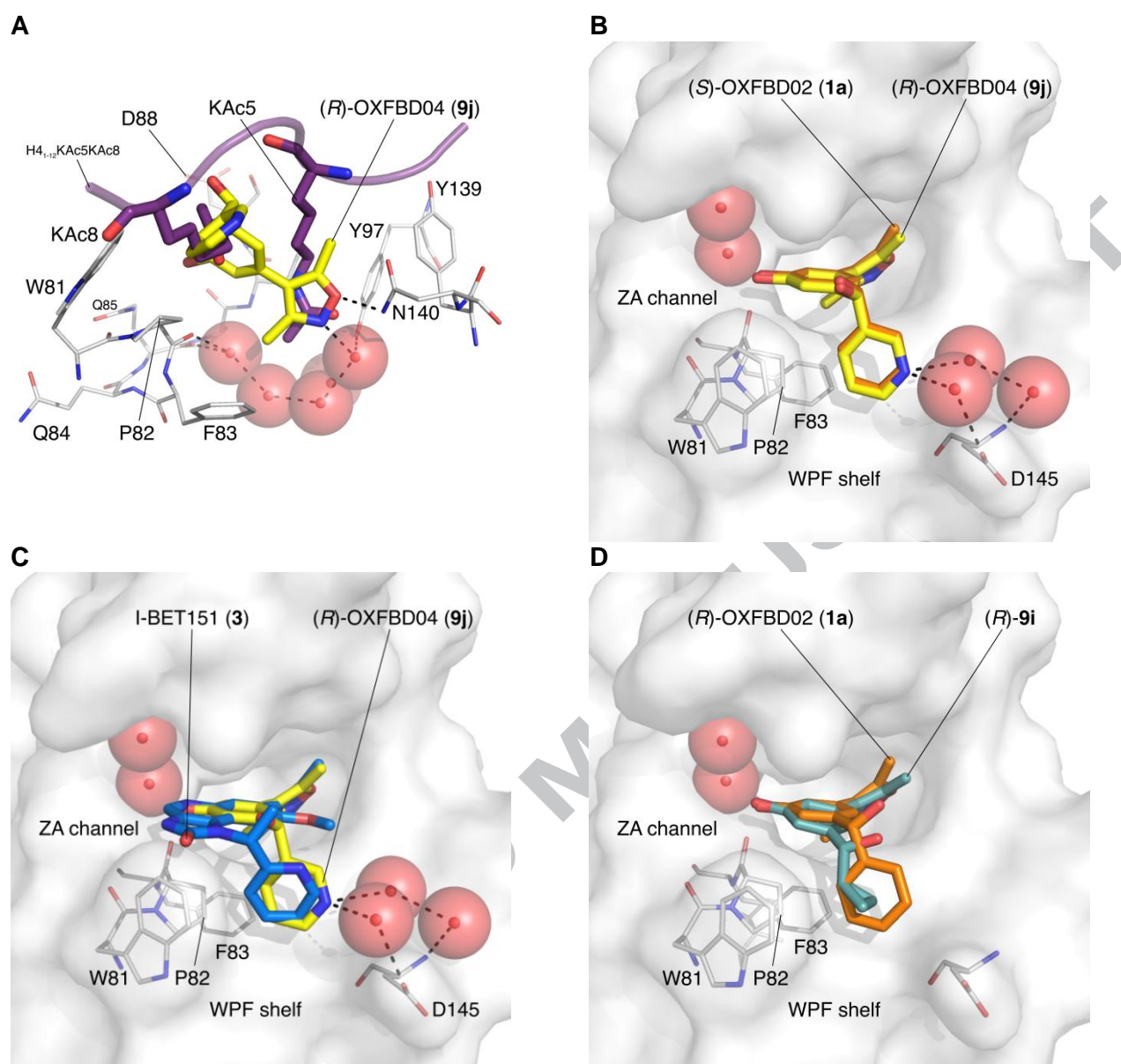


**Fig. 4A.** Overlaid X-ray crystal structures of (*R*)-OXFBD04 [(*R*)-**9j**, PDB code 6FSY, carbon = yellow; resolution: 1.34 Å] and the diacetylated histone H4-mimicking peptide H4<sub>1-12</sub>KAc5KAc8 (PDB code 3UVW, carbon = purple) bound to BRD4(1). **B.** Overlaid X-ray crystal structures of (*R*)-OXFBD04 [(*R*)-**9j**, PDB code 6FSY, carbon = yellow) and (*S*)-OXFBD02 [(*S*)-**1a**, PDB code 4J0S, carbon = orange]<sup>21</sup> bound to BRD4(1), showing that the molecules have very similar binding modes to BRD4(1). (*R*)-**9j** forms additional water-mediated interactions with D145, which are not possible for **1a**. **C.** Overlaid X-ray crystal structures of (*R*)-OXFBD04 [(*R*)-**9j**, PDB code 6FSY, carbon = yellow) and the I-BET151 (**3**, PDB code 3ZYU, carbon = marine blue) bound to BRD4(1), showing that the pyridine nitrogen does not overlay with that of I-BET151. **D.** Overlaid X-ray crystal structures of the cyclopropyl derivative (*R*)-**9i** (PDB code 6FT3, carbon = light teal; 1.28 Å) and (*R*)-OXFBD02 (**1a**, PDB code 4J0S, carbon = orange) bound to BRD4(1), showing that the molecules do not overlay precisely when binding to BRD4(1).

Compound **9j** overlays precisely with (*S*)-OXFBD02 (which has the same sense of stereochemistry; PDB code 4J0S) with the pyridine ring occupying the WPF shelf (Fig. 4B). The pyridine nitrogen is oriented away from the W81 and forms a water-mediated hydrogen bond with D145. It is feasible that this additional interaction, which is not present in OXFBD02, is responsible (at least in part) for the increase in BRD4(1) affinity displayed by **9j**. Interestingly, the pyridine

nitrogen does not overlay with that of I-BET151 (**3**) when bound to BRD4(1) (PDB code 3ZYU) (Fig. 4C), and the nitrogen atom in I-BET151 does not appear to form any interactions with BRD4(1). The phenol moiety of **9j** forms a hydrogen bond to the ZA-channel water molecule in the same manner as OXFBD02 (**1a**). The cyclopropyl derivative (**9i**) does not overlay so precisely with (*R*)-OXFBD02, with the hydroxyl group oxygen atoms displaced by 1.4 Å. The cyclopropyl group occupies the WPF shelf and is oriented towards W81. However, analysis of the B-factors for the ligand indicates that the cyclopropyl ring is the most flexible component of the molecule, and that in general **9i** is more flexible than **9j**, perhaps reflecting the higher affinity of the latter for BRD4(1).

The SAR of the pyridyl derivatives (**9j**, **k**, **p**) is particularly intriguing given the significant difference in BRD4(1) resulting from moving the nitrogen atom one position around the ring. We hypothesised that the decreased potency of 2-pyridyl derivative **9p** could be affected by the formation of an intramolecular H-bond between the nitrogen lone pair of the 2-pyridyl substituent and the secondary hydroxyl group. This interaction cannot form in the 3-pyridyl derivative **9j**. We conducted <sup>1</sup>H NMR experiments to determine whether we could detect formation of an internal hydrogen bond in **9p** in solution. To assess the presence and strength of a solution-phase hydrogen bond we observed the change in chemical shift of the given hydrogen atom when the <sup>1</sup>H NMR solvent is changed from CDCl<sub>3</sub> to D<sub>6</sub>-DMSO.<sup>48</sup> The chemical shift of hydrogen atoms that are not engaged in hydrogen bonds typically show a  $\Delta_{\text{ppm}} \text{CDCl}_3 \rightarrow \text{D}_6\text{-DMSO} = 2\text{-}4$  ppm, as their environment is predominantly dictated by the surrounding solvent. Hydrogen atoms that are involved in a hydrogen bond typically show  $\Delta_{\text{ppm}} \text{CDCl}_3 \rightarrow \text{D}_6\text{-DMSO} < 1$  ppm, as their environment is mainly dictated by the intramolecular interaction, and hence less affected by the surrounding solvent. This technique is especially powerful when combined with structural studies, as it allows comparison between intramolecular hydrogen bonds formed in solution phase and those present when a ligand is bound to a protein.

In D<sub>6</sub>-DMSO, the signal for the phenolic hydroxyl group of **9p** shifts downfield ( $\Delta_{\text{ppm}} \text{CDCl}_3 \rightarrow \text{D}_6\text{-DMSO} = +4.2$  ppm) consistent with this group being solvent exposed. In contrast, only a small change was seen for the secondary alcohol ( $\Delta_{\text{ppm}} \text{CDCl}_3 \rightarrow \text{D}_6\text{-DMSO} = +0.8$  ppm), which supports the idea that this group is engaged in an intramolecular hydrogen bond (Fig. 5A). We hypothesised



that the 4-chloro-2-pyridyl derivative (**9n**) would have a less basic nitrogen atom due to the inductive electron withdrawing effects of the 4-chloro substituent, and that this would result in a weaker internal H-bond. Consistent with this prediction, we observed an increased  $\Delta_{\text{ppm}}$   $\text{CDCl}_3 \rightarrow \text{D}_6\text{-DMSO}$  of +1.6 ppm for the secondary alcohol, indicating a weaker internal hydrogen bond ( $\Delta_{\text{ppm}} \text{CDCl}_3 \rightarrow \text{D}_6\text{-DMSO} = +4.7$  ppm for the phenol of **9n**). This compound shows intermediate BRD4(1) affinity ( $\text{IC}_{50} = 495$  nM) between **9j** and **9p**.

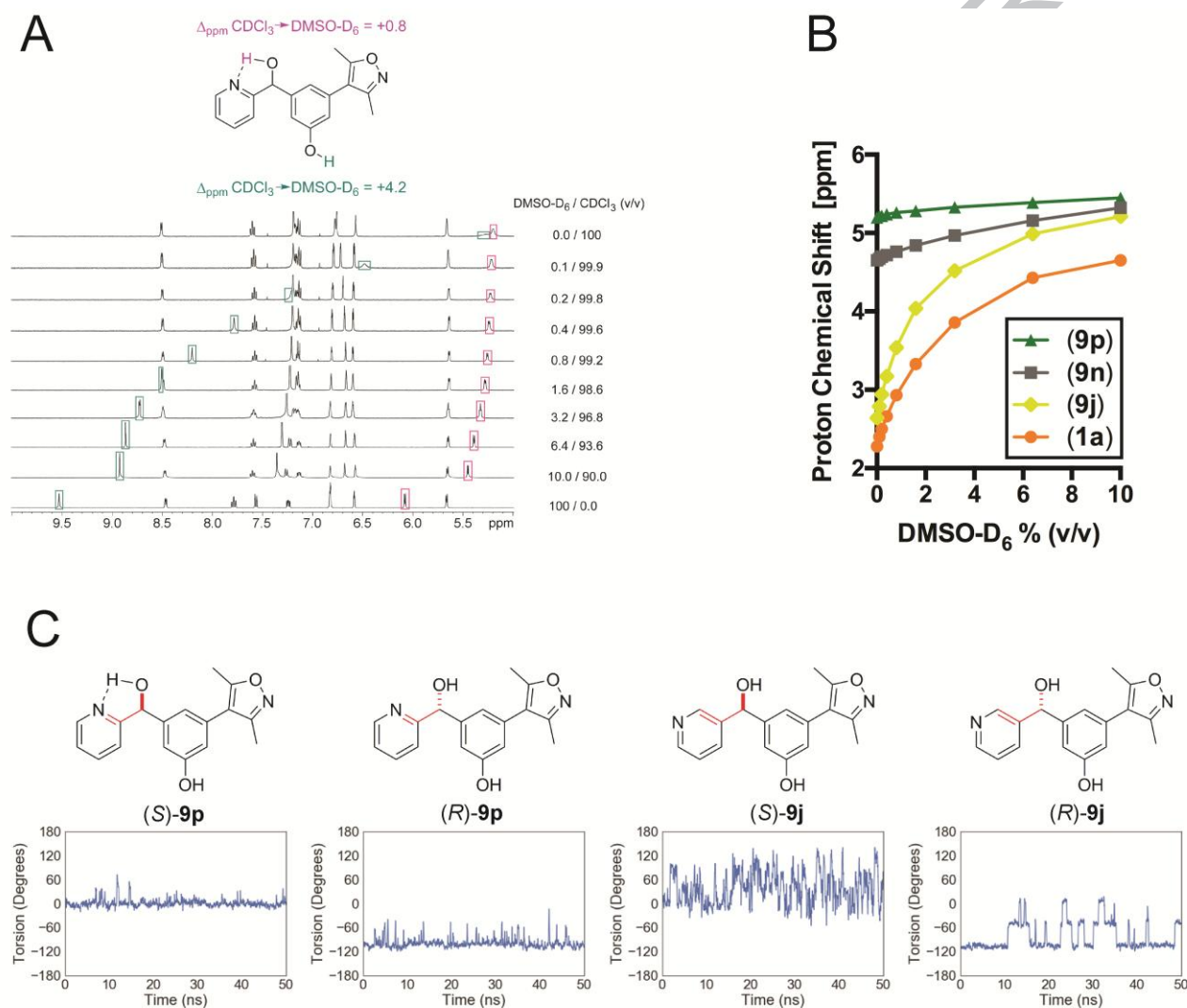


**Fig. 5.** Studies to rationalise the observed structure-activity relationship. A)  $^1\text{H}$  NMR spectra of **9p** dissolved in different mixtures of  $\text{CDCl}_3$  and  $\text{D}_6\text{-DMSO}$  displayed in a range from 5.0-10.0 ppm. (B) Chemical shifts of  $-\text{CHOH}$  protons of pyridyl analogues **9p**, **9n**, **9j**, and **1a**, which was used as a control for a compound that is not able to form an intramolecular H-bond, plotted against  $\text{D}_6\text{-DMSO}$  concentration. All experiments were performed at a compound concentration of 2 mg/mL. See Figure S5-8 for additional information. (C) Molecular dynamics studies for the enantiomers of **9p** and **9j** bound to BRD4(1). Representative plots showing the moving average of the dihedral angle between the bonds shown in red during three 50 ns MD simulations. A graph summarising the results of all randomised MD simulations that have been performed can be found in Figure S9-10.

We proposed that the internal hydrogen bond present in **9p** would result in the molecule adopting a solution state conformation that was unfavourable for protein binding. To investigate this idea, we conducted molecular dynamics (MD) simulations to predict the conformation that both enantiomers of **9p** would adopt when bound to BRD4(1). A 50 ns simulation indicates that (*S*)-**9p** adopts a very similar conformation to (*R*)-OXBDF02, and that in this conformation the internal hydrogen bond is intact (Fig. 6A). In this conformation the pyridine nitrogen atom is facing towards the solvent and away from W81, which is also the case in the X-ray crystal structure of **9j**, and an X-ray crystal structure of I-BET151 (**3**) which contains a 2-pyridyl substituent (Fig. 4C).

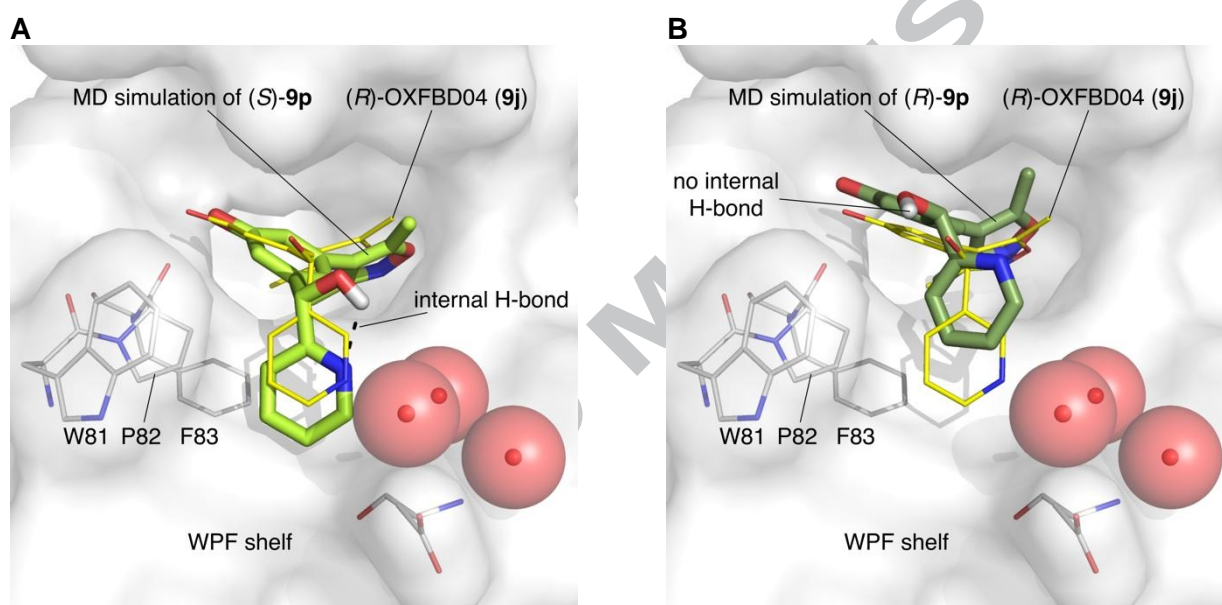


**Fig. 6A.** A representative image of a 45 ns MD simulation of (*S*)-**9p** overlaid with the X-ray crystal structures of (*R*)-OXFBD04 [(*R*)-**9j**, PDB code 6FSY, carbon = yellow] bound to BRD4(1). The predicted internal hydrogen-bond is present in (*S*)-**9p**. **B.** A representative image of a 50 ns MD simulation of (*R*)-**9p** overlaid with the X-ray crystal structures of (*R*)-OXFBD04 [(*R*)-**9j**, PDB code 6FSY, carbon = yellow] bound to BRD4(1). The simulation indicates that it is favourable for the pyridine nitrogen atom of (*S*)-**9p** to orient away from W8, requiring the internal hydrogen bond to be broken.

We reasoned that the orientation of the nitrogen atom away from the hydrophobic W81 residue is likely favourable. However, while the (*S*)-enantiomer of **9p** can adopt this orientation and maintain the internal hydrogen bond, the (*R*)-enantiomer would not be able to bind to BRD4(1) and maintain the internal hydrogen bond. This was shown to be the case in a 50 ns MD simulation, where the pyridine nitrogen is oriented away from W81, and consequently the internal hydrogen bond is broken (Fig. 6B). This observation provides an explanation for the low BRD4(1) affinity displayed by racemic **9p**, as only half the concentration of the ligand can bind to BRD4(1) with the internal hydrogen bond intact. In the opposite enantiomer a large enthalpic penalty to break the hydrogen

bond must first be overcome before the ligand can bind to BRD4(1). This observation predicts that (*S*)-**9p** should have a much higher affinity for BRD4(1) than (*R*)-**9p**. Work to investigate this is ongoing but is beyond the scope of these studies.

Compounds **10a-f** were designed to investigate whether more polar groups would be tolerated on the WPF shelf. As might be expected, most of these compounds show low BRD4(1) affinity, in line with the idea that a lipophilic group is preferred in this region. The notable exception in this series is the geminal difluorinated piperidine (**10d**), which has an IC<sub>50</sub> value of 235 nM for BRD4(1). We attribute this to the electron-withdrawing effects of the fluorine atoms resulting in reduced basicity that suppresses amine protonation, allowing the piperidine to interact better with the lipophilic WPF shelf. An X-ray crystal structure of **10d** bound to BRD4(1) (PDB code 6FT4; Fig. 7A) confirms that the difluoropiperidine moiety does reside on the WPF shelf, as predicted. We calculated the p*K*<sub>a</sub> values of the amine analogues (Table S3) and plotted the predicted appearance of the non-ionic state under assay conditions against the detected IC<sub>50</sub> values (Fig. 7B). These data suggest that positively charged amines do not bind well to the WPF shelf, with a correlation (linear regression  $R^2 = 0.8162$ ) between BRD4(1) affinity and the p*K*<sub>a</sub> of the conjugated acid of the tertiary amine observed.

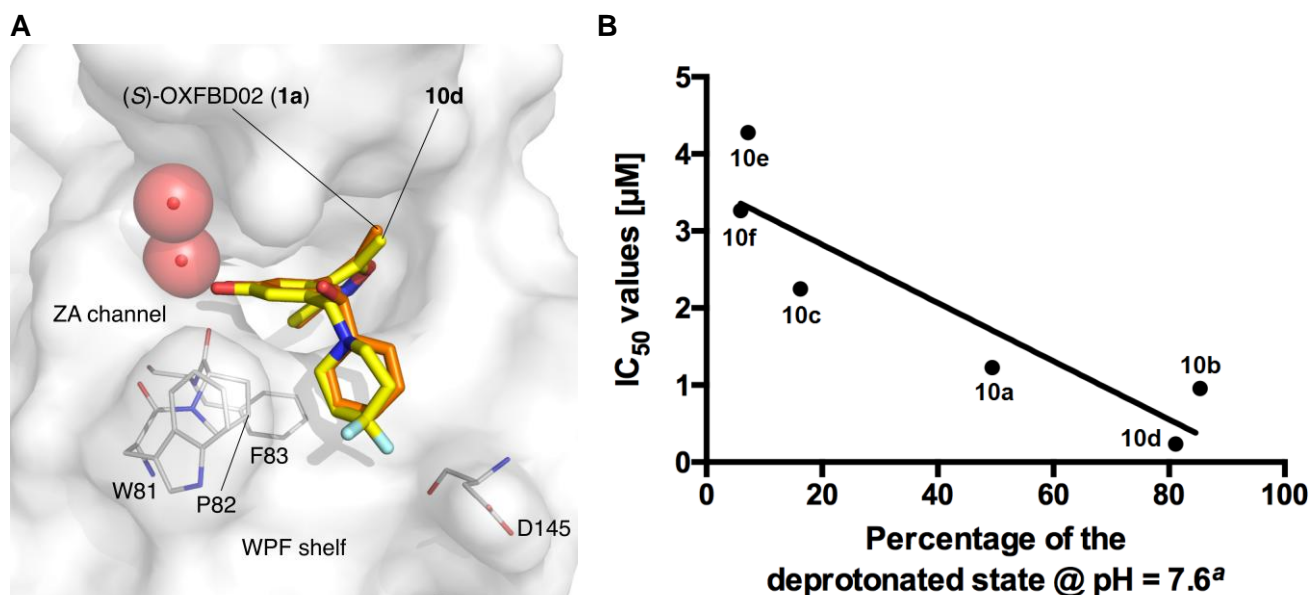


**Fig. 7A.** Overlaid X-ray crystal structures of **10b** (PDB code 6FT4, carbon = yellow; resolution: 1.34 Å) and (S)-OXFBD02 (**1a**, PDB code 4J0S, carbon = orange)<sup>21</sup> bound to BRD4(1). The inductive electron-withdrawing effect of the fluorine atoms reduces the basicity of the piperidine sufficiently for it to remain unprotonated and bind to the WPF shelf. **B.** BRD4(1) IC<sub>50</sub> values of amines (**10a-f**) plotted against the predicted appearance of the non-ionic state under assay conditions (pH = 7.6). Linear regression gives a R<sup>2</sup> value of 0.8162, indicating a good correlation between reduced basicity and increased BRD4(1) affinity. <sup>a</sup>Calculated using ACD/Labs I-Lab 2.0 software (Algorithm Version: v5.0.0.184).

While the cyclopropyl-derived **9i** shows the highest LE of the series, the 3-pyridyl derivative **9j** and the cyclohexyl analogue **9h** have the highest BRD4(1) affinity. However, while **9h** has a LLE of 3.54, **9j** shows a LLE of 5.74, indicating that this BRD4(1) ligand has an optimised balance of affinity and physicochemical properties.

## 2.6. Metabolism and cellular studies

The metabolic stability of our most promising compounds (**9j**, **10d**) was tested in a human microsomal stability assay using OXFBD02 (**1a**) as a reference. The cyclohexyl derivative **9h** was excluded from these studies as its more lipophilic nature limits its solubility and increases the likelihood of a poor metabolic profile. OXFBD02 (**1a**) and the 4,4-difluoropiperidinyl derivative (**10d**) exhibited similar metabolic half-lives, with  $t_{1/2}$  = 39.8 min and  $t_{1/2}$  = 27.0 min, respectively. Compounds **1a** and **10d** displayed CL<sub>int</sub> values of 34.8 and 51.4  $\mu$ L/min/mg protein and are consequently considered to be medium and high clearance compounds, respectively.<sup>49</sup> In contrast, the 3-pyridyl analogue (**9j**) displayed a significantly longer metabolic half-life of 388 min (Table 2). With an intrinsic clearance (CL<sub>int</sub>) of 3.57  $\mu$ L/min/mg protein, **9j** is therefore classified as a low

clearance compound. These properties indicate that **9j** is the optimal ligand in this series for progression to use in cellular and potentially *in vivo* studies. However, it should be noted that the microsomal stability assay only provides insights into phase I metabolism. More comprehensive metabolic characterisation, including phase II conjugation reactions, will be included in future studies.

**Table 2.** Metabolic stability data of **1a**, **9j**, and **10d** including the intrinsic clearance ( $CL_{int} \pm$  standard error) and the apparent half-life ( $t_{1/2}$ ) detected by means of a microsomal stability assay using human liver microsomes. Dextromethorphan and verapamil were used as medium and high clearance controls, respectively. Compounds were tested at a concentration of 3  $\mu$ M.

Compound	$CL_{int}$ ( $\mu$ L/min/mg protein)	$t_{1/2}$ (min)	n
OXFBD02 ( <b>1a</b> )	$34.8 \pm 3.76$	39.8	5
<b>9j</b>	$3.57 \pm 2.21$	388	5
<b>10d</b>	$51.4 \pm 2.6$	27.0	5
dextromethorphan	$25.4 \pm 4.23$	54.5	5
verapamil	$192 \pm 11.3$	7.20	3

To rationalise the selection of compounds used for further cellular studies we have predicted the cell permeability of all final compounds presented herein. All compounds were predicted to have an absorption rate constant ( $K_a$ ) between 0.053 – 0.058  $\text{min}^{-1}$  which suggests excellent cellular uptake (Table S5). As there is no significant difference in permeability among the synthesised compounds we decided to further study the compound **9j** displaying to most promising results in our previous studies in a cellular setup. In a cell growth assay using A498 (renal), HT-29 (colon), and MCF7 (breast) cancer cell lines, **9j** showed low micromolar activity (Table 3 and Fig. S11). OXFBD02 was used as a positive control, and the data for OXFBD02 are in line with that obtained in the NCI-60 screen. To address the mechanism of cytotoxicity, we probed the effect of **9j** and **1a** on *MYC* suppression in MCF7 cells. We show that **9j** exerts a potent and time-dependent effect of *MYC* suppression similar to **1a** and (+)-JQ1, which was used as a positive control (Fig. 8). These data indicate that OXFBD04 (**9j**) shows similar cellular efficacy to OXFBD02 (**1a**), which combined with its enhanced metabolic stability makes OXFBD04 (**9j**) a useful tool compound for studying the function of the BET bromodomains.

**Table 3.** GI<sub>50</sub> data for OXFBD02 (**1a**) and OXFBD04 (**9j**). A498 (renal), HT-29 (colon), and MCF7 (breast) cancer cell lines were used. Values quoted are a mean of three repeats. The standard deviation is shown.

Compound	GI <sub>50</sub> (μM) A498	GI <sub>50</sub> (μM) HT-29	GI <sub>50</sub> (μM) MCF7
OXFBD02 ( <b>1a</b> )	1.58 ± 1.35	5.79 ± 0.84	1.25 ± 0.47
OXFBD04 ( <b>9j</b> )	4.88 ± 1.54	4.40 ± 0.81	1.40 ± 0.60

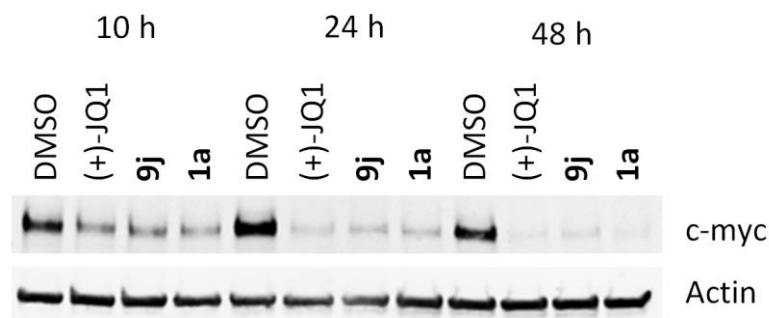


**Fig. 8.** Inhibition of BET bromodomains by means of 3,5-dimethylisoxazole-based ligands OXFDD02 (**1a**) or OXFBD04 (**9j**) induces *MYC* suppression in MCF7 breast cancer cells. Representative western blot detection of c-myc after treatment with OXFBD02 (**1a**), OXFBD04 (**9j**), or (+)-JQ1 as a reference. Compounds were tested at a concentration of 10 μM.

### 3. Conclusion

In conclusion, we have shown that the BET bromodomain ligand OXFBD02 (**1a**) displays a promising profile in the NCI-60 panel of cancer cell lines, but a short metabolic half-life of 40 minutes in human liver microsomes. To optimise the metabolic stability of this compound series, we investigated the SAR of WPF-binding groups, with a view to optimising the overall compound properties. In the pyridyl series we showed that an intramolecular hydrogen bond detrimentally affects the affinity of 2-pyridyl derivative (**9p**), by holding the (*R*)-enantiomer in a conformation that disfavors BRD4(1) binding. However, the 3-pyridyl derivative, OXFBD04 (**9j**), displays higher BRD4(1) affinity than the parent compound and an LLE value of 5.74, indicating that it is a BRD4(1) ligand with an optimised balance of affinity and physicochemical properties. The addition of the pyridine ring led to an increased metabolic half-life of 6.5 hours in human liver microsomes. These data indicate that the 3,5-dimethylisoxazole group is not inherently metabolically labile, and optimisation of the overall compound properties can lead to compounds with useful metabolic stabilities. In cancer cell lines, OXFBD04 (**9j**) showed similar effects on cytotoxicity and *MYC* suppression compared to the parent compound OXFBD02 (**1a**). Consequently, we report



OXFDB04 (**9j**) as an improved tool compound to study BRD4 in *in vitro* and potentially *in vivo* settings.

ACCEPTED MANUSCRIPT

## 4. Experimental

### 4.1. General chemistry experimental details

$^1\text{H}$  NMR spectra were recorded on Bruker AVIII HD 400 (400 MHz) or Bruker AVII 500 (500 MHz). Chemical shifts are reported as  $\delta_{\text{H}}$  part per million (ppm) relative to the solvent reference peak as internal deuterium lock.<sup>50</sup> The multiplicity of each signal is indicated by: s (singlet), d (doublet), t (triplet), dd (doublet of doublets), q (quartet), sp (septet) or m (multiplet). Identical proton coupling constants ( $J$ ) are averaged in each spectrum and are reported to the nearest 0.1 Hz. Coupling constants were determined using Bruker TopSpin software.  $^{13}\text{C}$  NMR spectra were recorded on Bruker AVIII HD 400 (101 MHz) or Bruker AVII 500 (126 MHz). Chemical shifts are reported as  $\delta_{\text{C}}$  part per million (ppm) relative to the solvent reference peak as internal deuterium lock. Coupling constants ( $J$ ) are quoted in Hz and are recorded to the nearest 1 Hz. Identical coupling constants ( $J$ ) are averaged in each spectrum and reported to the nearest 1 Hz. The coupling constants are determined by analysis using Bruker TopSpin software.  $^{19}\text{F}$  NMR spectra were recorded on a Bruker AVII 500 (470 MHz) using a broadband proton decoupling pulse sequence and deuterium internal lock. The chemical shift data for each signal are given as  $\delta_{\text{F}}$  in units of parts per million (ppm).  $^{11}\text{B}$  NMR spectra were recorded on a Bruker DRX500 (160 MHz). The chemical shift data for each signal are given as  $\delta_{\text{B}}$  in units of parts per million (ppm). Coupling constants ( $J$ ) are quoted in Hz and are recorded to the nearest 1 Hz. Identical coupling constants ( $J$ ) are averaged in each spectrum and reported to the nearest 1 Hz. The coupling constants are determined by analysis using Bruker TopSpin software. Note: in all isoxazole-containing compounds, positions on the central aromatic ring are numbered first, the isoxazole ring with primes (') and any additional rings with double primes (') etc. Low-resolution mass spectra (LRMS) using electron spray ionisation were recorded on a Micromass LCT Premier spectrometer. Electrospray Ionisation (ESI) High-Resolution Mass Spectrometry (HRMS) spectra were acquired on either a Bruker MicroTOF spectrometer or a Thermo Exactive mass spectrometer, equipped with Agilent 1100 liquid chromatography systems for flow injection analysis, from solutions of MeOH, H<sub>2</sub>O or MeCN as stated. MicroTOF data were processed using Bruker Hystar software, while Exactive data were analysed using Thermo Xcalibur software. Melting points on crystallised samples were determined using either a) a Leica Galen III hot stage microscope or b) a Griffin capillary tube melting point apparatus and are uncorrected. The solvents of



crystallisation are shown in parentheses. Infrared spectra were obtained from thin films using a diamond attenuated total reflectance module. The spectra were recorded on a Bruker Tensor 27 spectrometer. Absorption maxima ( $\nu_{\max}$ ) are reported in wavenumbers ( $\text{cm}^{-1}$ ) and are classified as broad (br), strong (s), medium (m) or weak (w). Analytical HPLC was carried out on a PerkinElmer Flexar system with a Binary LC Pump and UV/VIS LC Detector. For determination of compound purity following methods were applied. Method 1 (M1): a Dionex Acclaim<sup>®</sup> 120 column (C18, 5  $\mu\text{m}$ , 120 Å, 4.6  $\times$  150 mm) was used and the solvents employed were A = 0.1% (v/v) solution of formic acid in 95%  $\text{H}_2\text{O}$ /5% MeCN; B = 0.1% (v/v) solution of formic acid in 95% MeCN/5%  $\text{H}_2\text{O}$ , and the gradient (A:B). A 10-minute linear gradient of 0-100% B was run with a flow rate of 1 mL/min and detection at 254 nm. Samples were injected in DMSO, MeOH, DMSO/MeOH or DMSO/ $\text{CHCl}_3$ . Method 2 (M2): a Dionex Acclaim<sup>®</sup> 120 column (C18, 5  $\mu\text{m}$ , 120 Å, 4.6  $\times$  150 mm) was used and the solvents employed were A =  $\text{H}_2\text{O}$ ; B = MeCN. Linear gradient conditions (0–10 min, linear increase from 5% to 95% of B; 10–15 min, B = 95%) with a flow rate of 1.5 mL/min and detection at 254 nm. Samples were injected in DMSO, MeOH, DMSO/MeOH or DMSO/ $\text{CHCl}_3$ . Method 3 (M3): a Dionex Acclaim<sup>®</sup> 120 column (C18, 5  $\mu\text{m}$ , 120 Å, 4.6  $\times$  150 mm) was used and the solvents employed were A =  $\text{H}_2\text{O}$ ; B = MeCN. Linear gradient conditions (0–10 min, linear increase from 5% to 95% of B; 10–15 min, B = 95%) with a flow rate of 1.5 mL/min and detection at 220 nm. Samples were injected in DMSO, MeOH, DMSO/MeOH or DMSO/ $\text{CHCl}_3$ . All compounds that were subjected to biological evaluation had purity of  $\geq 95\%$  determined by HPLC and LCMS analysis.

Anhydrous solvents were obtained under the following conditions: anhydrous DMF, anhydrous MeOH and anhydrous EtOH were purchased from Sigma-Aldrich UK in SureSeal<sup>™</sup> bottles and used without further purification; anhydrous THF and  $\text{CH}_2\text{Cl}_2$  were dried over activated 3 Å molecular sieves under an argon or nitrogen atmosphere; where stated, THF was distilled from sodium and benzophenone and pyridine was distilled from  $\text{CaH}_2$ . Chemicals were purchased from Acros, Sigma-Aldrich, Alfa Aesar, Fisher, Apollo Scientific or Fluorochem. Where appropriate and if not stated otherwise, all non-aqueous reactions were performed in a flame-dried flask under an inert atmosphere of nitrogen or argon.  $\text{MnO}_2$  was activated at 250 °C overnight prior to use. Organolithium reagents were titrated against diphenylacetic acid,<sup>51</sup> and commercially-available organomagnesium compounds were titrated against salicylaldehyde phenylhydrazone.<sup>52</sup> Where stated,  $\text{NEt}_3$  was dried with KOH and distilled onto KOH pellets.

Isolute® SCX-2 cartridges for cation exchange were purchased from Biotage UK and were used according to manufacturers' protocols.

## 4.2. Synthetic procedures

### 4.2.1. 3-(3,5-Dimethyl-1,2-oxazol-4-yl)-5-[hydroxyl(phenyl)methyl]phenol (**1a**)<sup>21</sup>

Following the procedure of Hewings *et al.*,<sup>21</sup> to a solution of **17** (2.63 g, 12.1 mmol, 1.0 eq) in anhydrous THF at 0 °C was added dropwise a 1 M solution of phenylmagnesium bromide (34.0 mL, 34.0 mmol, 2.8 eq) in THF. The reaction solution was warmed to rt and stirred for 4 h. After this time, the volatile components were removed *in vacuo*. The resulting solid was crystallised from hot MeCN and the mother liquor was purified by silica gel chromatography, eluting with 1% AcOH and EtOAc in petroleum ether (gradient elution 15 → 40%). The combined solids were crystallised from hot MeCN yielding **1a** (1.43 g, 40%) as an off-white crystalline solid: *R*<sub>f</sub> (50% EtOAc/petroleum ether) 0.38; mp 187-190 °C (MeCN) [lit. mp 187-188 °C<sup>21</sup>]; <sup>1</sup>H NMR (400 MHz, D<sub>6</sub>-acetone) δ 8.44 (1H, br s, C(1)OH), 7.49-7.43 (2H, m, C(2'')H & C(6'')H), 7.34-7.28 (2H, m, C(3'')H and C(5'')H), 7.24-7.19 (1H, m, C(4'')H), 6.94-6.91 (1H, m, C(6)H), 6.91-6.88 (1H, m, C(4)H), 6.67 (1H, dd, *J* = 1.9, 1.9 Hz, C(2)H), 5.83-5.79 (1H, m, CHOH), 4.90 (1H, d, *J* = 3.9 Hz, CHOH), 2.36 (3H, s, C(5')CH<sub>3</sub>), 2.18 (3H, s, C(3')CH<sub>3</sub>); LRMS *m/z* (ES<sup>+</sup>) 296 ([M + H]<sup>+</sup>, 100%). Data are in good agreement with literature values.<sup>21</sup>

### 4.2.2. 3-(3,5-Dimethyl-1,2-oxazol-4-yl)-5-[(4-chlorophenyl)(hydroxy)methyl]phenol (**9a**)

To a solution of **17** (96 mg, 442 μmol, 1.0 eq) in anhydrous THF (2 mL) was added a 1 M solution of 4-chlorophenylmagnesium bromide (1.00 mL, 216 mg, 1.00 mmol, 2.3 eq) in Et<sub>2</sub>O at rt, and the reaction solution was stirred for 19 h. The reaction was quenched with a saturated aqueous solution of NH<sub>4</sub>Cl (15 mL), and the aqueous phase was extracted with EtOAc (3 × 15 mL). The combined organic layers were washed with H<sub>2</sub>O (45 mL), passed through an anhydrous frit and concentrated *in vacuo*. Purification by silica gel chromatography, eluting with EtOAc in cyclohexane (gradient elution 5 → 100%) followed by mass-directed autopurification (0.1% formic acid, gradient elution MeCN/H<sub>2</sub>O 30 → 85%) afforded the desired product **9a** (74 mg, 51%) as a clear and colourless oil that solidified under vacuum to give a colourless amorphous solid: *R*<sub>f</sub> (50%

EtOAc/cyclohexane) 0.35;  $\nu_{\max}$  (thin film)/ $\text{cm}^{-1}$ : 3457 (br) (O–H), 3015 (br), 2970 (w), 2949 (br);  $^1\text{H}$  NMR (400 MHz,  $\text{CD}_3\text{OD}$ )  $\delta$  7.42–7.36 (2H, m,  $\text{C}(2'')\text{H}$  &  $\text{C}(6'')\text{H}$ ), 7.34–7.28 (2H, m,  $\text{C}(3'')\text{H}$  &  $\text{C}(5'')\text{H}$ ), 6.88–6.83 (1H, m,  $\text{C}(6)\text{H}$ ), 6.82–6.77 (1H, m,  $\text{C}(4)\text{H}$ ), 6.64 (1H, dd,  $J = 2.2, 1.6$  Hz,  $\text{C}(2)\text{H}$ ), 5.75 (1H, s,  $\text{CHOH}$ ), 2.36 (3H, s,  $\text{C}(5')\text{CH}_3$ ), 2.21 (3H, s,  $\text{C}(3')\text{CH}_3$ );  $^{13}\text{C}$  NMR (101 MHz,  $\text{CD}_3\text{OD}$ )  $\delta$  166.9 ( $\text{C}(5')$ ), 160.0 ( $\text{C}(3')$ ), 159.0 ( $\text{C}(1)$ ), 148.0 ( $\text{C}(5)$ ), 144.7 ( $\text{C}(4'')$ ), 134.0 ( $\text{C}(1'')$ ), 132.6 ( $\text{C}(3)$ ), 129.4 ( $\text{C}(3'')$  &  $\text{C}(5'')$ ), 129.3 ( $\text{C}(2'')$  &  $\text{C}(6'')$ ), 119.7 ( $\text{C}(4)$ ), 117.9 ( $\text{C}(4')$ ), 115.9 ( $\text{C}(2)$ ), 114.0 ( $\text{C}(6)$ ), 75.9 ( $\text{CHOH}$ ), 11.5 ( $\text{C}(5')\text{CH}_3$ ), 10.8 ( $\text{C}(3')\text{CH}_3$ ); HRMS  $m/z$  ( $\text{ES}^+$ ) Found: 352.0715 & 354.0698.  $\text{C}_{18}\text{H}_{16}\text{ClNNaO}_3^+$  requires  $[\text{M}(^{35}\text{Cl})]^+$  &  $[\text{M}(^{37}\text{Cl})]^+$  352.0711 & 354.0683; LRMS  $m/z$  ( $\text{ES}^-$ ) 328 ( $[\text{M}(^{35}\text{Cl}) - \text{H}]^-$ , 100%), 330 ( $[\text{M}(^{37}\text{Cl}) - \text{H}]^-$ , 39%]; HPLC RT = 11.55 min, purity 95.5% (M1).

#### 4.2.3. 3-(3,5-Dimethyl-1,2-oxazol-4-yl)-5-[hydroxy(2-methoxyphenyl)methyl]phenol (9b)

To a solution of **17** (94 mg, 433  $\mu\text{mol}$ , 1.0 eq) in anhydrous THF (2 mL) was added a 1 M solution 2-methoxyphenylmagnesium bromide (1.00 mL, 211 mg, 1.00 mmol, 2.3 eq) in THF at rt, and the reaction solution was stirred for 3 h. The reaction was quenched with a saturated aqueous solution of  $\text{NH}_4\text{Cl}$  (15 mL), and the aqueous phase was extracted with EtOAc (3  $\times$  15 mL). The combined organic layers were washed with  $\text{H}_2\text{O}$  (45 mL), passed through an anhydrous frit and concentrated *in vacuo*. Purification by silica gel chromatography, eluting with EtOAc in cyclohexane (gradient elution 10  $\rightarrow$  60%) afforded **9b** (113 mg, 80%) as a colourless solid:  $R_f$  (50% EtOAc/cyclohexane) 0.36;  $\nu_{\max}$  (thin film)/ $\text{cm}^{-1}$ : 3196 (br) (O–H), 2993 (w), 2837 (w), 1642 (m) 1596 (s); mp 167–169  $^\circ\text{C}$  (EtOAc);  $^1\text{H}$  NMR (400 MHz,  $\text{CD}_3\text{OD}$ )  $\delta$  7.49 (1H, dd,  $J = 7.5, 1.5$  Hz,  $\text{C}(6'')\text{H}$ ), 7.25 (1H, ddd,  $J = 7.8, 7.8, 1.5$  Hz,  $\text{C}(3'')\text{H}$ ), 7.01–6.92 (2H, m,  $\text{C}(4'')\text{H}$  &  $\text{C}(5'')\text{H}$ ), 6.88–6.84 (1H, m,  $\text{C}(6)\text{H}$ ), 6.80–6.76 (1H, m,  $\text{C}(4)\text{H}$ ), 6.60 (1H, dd,  $J = 1.9, 1.9$  Hz,  $\text{C}(2)\text{H}$ ), 6.12 (1H, s,  $\text{CHOH}$ ), 3.81 (3H, s,  $\text{OCH}_3$ ), 2.37 (3H, s,  $\text{C}(5')\text{CH}_3$ ), 2.21 (3H, s,  $\text{C}(3')\text{CH}_3$ );  $^{13}\text{C}$  NMR (101 MHz,  $\text{CD}_3\text{OD}$ )  $\delta$  166.7 ( $\text{C}(5')$ ), 160.0 ( $\text{C}(3')$ ), 158.8 ( $\text{C}(1)$ ), 157.7 ( $\text{C}(2'')$ ), 148.1 ( $\text{C}(5)$ ), 133.9 ( $\text{C}(1'')$ ), 132.0 ( $\text{C}(3)$ ), 129.5 ( $\text{C}(3'')$ ), 127.9 ( $\text{C}(6'')$ ), 121.6 ( $\text{C}(4'')$  or  $\text{C}(5'')$ ), 119.9 ( $\text{C}(4)$ ), 118.0 ( $\text{C}(4')$ ), 115.4 ( $\text{C}(2)$ ), 114.2 ( $\text{C}(6)$ ), 111.7 ( $\text{C}(5')$  or  $\text{C}(4'')$ ), 70.5 ( $\text{CHOH}$ ), 55.9 ( $\text{OCH}_3$ ), 11.4 ( $\text{C}(5')\text{CH}_3$ ), 10.7 ( $\text{C}(3')\text{CH}_3$ ); HRMS  $m/z$  ( $\text{ES}^+$ ) Found: 326.1386.  $\text{C}_{19}\text{H}_{20}\text{NO}_4^+$  requires  $\text{M}^+$  326.1387; LCMS (formic acid) RT = 0.88,  $[\text{M} + \text{H}]^+ = 326$ ; HPLC RT = 10.95 min, purity 98.0% (M1).

**4.2.4. 3-(3,5-Dimethyl-1,2-oxazol-4-yl)-5-[hydroxy(3-methoxyphenyl)methyl]phenol (9c)**

To a solution of **17** (103 mg, 474  $\mu$ mol, 1.0 eq) in anhydrous THF (2 mL) was added a 1 M solution of 3-methoxyphenylmagnesium bromide (1.00 mL, 211 mg, 1.00 mmol, 2.1 eq) in THF at rt, and the reaction solution was stirred for 5 h. The reaction was quenched with a saturated aqueous solution of  $\text{NH}_4\text{Cl}$  (15 mL), and the aqueous phase was extracted with EtOAc ( $3 \times 15$  mL). The combined organic layers were washed with  $\text{H}_2\text{O}$  (45 mL), passed through an anhydrous frit and concentrated *in vacuo*. Purification by silica gel chromatography, eluting with EtOAc in cyclohexane (gradient elution 10  $\rightarrow$  60%) afforded **9c** (106 mg, 68%) as a colourless solid:  $R_f$  (50% EtOAc/cyclohexane) 0.34;  $\nu_{\text{max}}$  (thin film)/ $\text{cm}^{-1}$ : 3176 (br) (O–H), 2933 (w), 1640 (w), 1596 (w); mp 94–96  $^{\circ}\text{C}$  (EtOAc);  $^1\text{H}$  NMR (400 MHz,  $\text{CD}_3\text{OD}$ )  $\delta$  7.24 (1H, dd,  $J = 7.8, 7.8$  Hz, C(2'')H), 7.05–6.93 (2H, m, C(4'')H & C(5'')H or C(4'')H & C(6'')H or C(5'')H & C(6'')H), 6.89–6.84 (1H, m, C(6)H), 6.84–6.76 (2H, m, C(4)H & C(4'')H, C(5'')H or C(6'')H), 6.67–6.59 (1H, m, C(2)H), 5.72 (1H, s, CHOH), 3.78 (3H, s,  $\text{OCH}_3$ ), 2.73 (3H, s, C(5') $\text{CH}_3$ ), 2.22 (3H, s, C(3') $\text{CH}_3$ );  $^{13}\text{C}$  NMR (101 MHz,  $\text{CD}_3\text{OD}$ )  $\delta$  166.8 (C(5')), 161.2 (C(3')), 160.0 (C(3')), 158.9 (C(1)), 148.3 (C(1')), 147.4 (C(5)), 132.4 (C(3)), 130.3 (C(2')), 120.0 (C(4''), C(5'') or C(6'')), 119.8 (C(4''), C(5'') or C(6'')), 118.0 (C(4')), 115.7 (C(2)), 114.1 (C(6)), 113.7 (C(4)), 113.2 (C(4''), C(5'') or C(6'')), 76.6 (CHOH), 55.7 ( $\text{OCH}_3$ ), 11.4 (C(5') $\text{CH}_3$ ), 10.7 (C(3') $\text{CH}_3$ ); HRMS  $m/z$  ( $\text{ES}^+$ ) Found: 326.1386.  $\text{C}_{19}\text{H}_{20}\text{NO}_4^+$  requires  $M^+$  326.1387; LCMS (formic acid) RT = 0.87,  $[\text{M} + \text{H}]^+ = 326$ ; HPLC RT = 10.84 min, purity 98.5% (M1).

**4.2.5. 3-(3,5-Dimethyl-1,2-oxazol-4-yl)-5-[hydroxy(4-methoxyphenyl)methyl]phenol (9d)**

To a solution of **17** (102 mg, 470  $\mu$ mol, 1.0 eq) in anhydrous THF (2 mL) was added a 0.5 M solution of 4-methoxyphenylmagnesium bromide (2.00 mL, 211 mg, 1.00 mmol, 2.1 eq) in THF at rt, and the reaction solution was stirred for 3 h. The reaction was quenched with a saturated aqueous solution of  $\text{NH}_4\text{Cl}$  (15 mL), and the aqueous phase was extracted with EtOAc ( $3 \times 15$  mL). The combined organic layers were washed with  $\text{H}_2\text{O}$  (45 mL), passed through an anhydrous frit and concentrated *in vacuo*. Purification by silica gel chromatography, eluting with EtOAc in cyclohexane (gradient elution 10  $\rightarrow$  60%) afforded **9d** (104 mg, 68%) as a clear and colourless oil. Precipitation from  $\text{Et}_2\text{O}$  and hexane afforded a colourless amorphous solid:  $R_f$  (50% EtOAc/cyclohexane) 0.44;  $\nu_{\text{max}}$  (thin film)/ $\text{cm}^{-1}$ : 3016 (w) (O–H), 2970 (w), 1739 (s);  $^1\text{H}$  NMR (400

MHz, CD<sub>3</sub>OD)  $\delta$  7.34-7.26 (2H, m, C(3'')H & C(5'')H), 6.91-6.84 (3H, m, C(2'')H, C(6'')H & C(6)H), 6.81-6.78 (1H, m, C(4)H), 6.65-6.60 (1H, m, C(2)H), 5.72 (1H, s, CHOH), 3.74 (3H, s, OCH<sub>3</sub>), 2.35 (3H, s, C(5')CH<sub>3</sub>), 2.20 (3H, s, C(3')CH<sub>3</sub>); <sup>13</sup>C NMR (126 MHz, CD<sub>3</sub>OD)  $\delta$  166.8 (C(5')), 160.4 (C(4'')), 160.0 (C(3')), 158.9 (C(1)), 148.6 (C(5) or C(1'')), 137.9 (C(1'') or C(5)), 132.3 (C(3)), 129.0 (C(3'') & C(5'')), 119.6 (C(4)), 118.0 (C(4')), 115.5 (C(2)), 114.7 (C(2'') & C(6'')), 113.9 (C(6)), 76.2 (CHOH), 55.7 (OCH<sub>3</sub>), 11.4 (C(5')CH<sub>3</sub>), 10.7 (C(3')CH<sub>3</sub>); HRMS *m/z* (ES<sup>-</sup>) Found: 324.1243. C<sub>19</sub>H<sub>18</sub>NO<sub>4</sub><sup>-</sup> requires M<sup>-</sup>, 324.1241; LRMS *m/z* (ES<sup>-</sup>) 324 ([M - H]<sup>-</sup>, 100%); HPLC RT = 10.74 min, purity 97.1% (M1).

#### 4.2.6. 3-(3,5-Dimethyl-1,2-oxazol-4-yl)-5-[hydroxy(4-methylphenyl)methyl]phenol (9e)

To a solution of **17** (93 mg, 428  $\mu$ mol, 1.0 eq) in anhydrous THF (2 mL) was added a 1 M solution of 4-tolylmagnesium bromide (1.00 mL, 195 mg, 1.00 mmol, 2.3 eq) in THF at rt, and the reaction solution was stirred for 1 h. To aid solubility, additional THF (2 mL) was added and the reaction solution was stirred at rt for 17 h. The reaction was quenched with a saturated aqueous solution of NH<sub>4</sub>Cl (15 mL), and the aqueous phase was extracted with EtOAc (3  $\times$  15 mL). The combined organic layers were washed with H<sub>2</sub>O (45 mL), passed through an anhydrous frit and concentrated *in vacuo*. Purification by silica gel chromatography, eluting with acetone in petroleum ether (gradient elution 10  $\rightarrow$  50%) afforded **9e** (75 mg, 56%) as a clear and colourless oil. Precipitation from Et<sub>2</sub>O and hexane gave a colourless, amorphous solid: R<sub>f</sub> (20% EtOAc/cyclohexane) 0.08;  $\nu_{\max}$  (thin film)/cm<sup>-1</sup>: 3280 (br) (O-H), 1596 (s), 1421 (s); <sup>1</sup>H NMR (400 MHz, CD<sub>3</sub>OD)  $\delta$  7.27 (2H, d, *J* = 7.9 Hz, C(3'')H & C(5'')H), 7.12 (2H, d, *J* = 7.9 Hz, C(2'')H & C(6'')H), 6.90-6.85 (1H, m, C(6)H), 6.82-6.77 (1H, m, C(4)H), 6.65-6.60 (1H, m, C(2)H), 5.72 (1H, s, CHOH), 2.33 (3H, s, C(5')CH<sub>3</sub>), 2.28 (3H, s, C(4'')CH<sub>3</sub>), 2.19 (3H, s, C(3')CH<sub>3</sub>); <sup>13</sup>C NMR (126 MHz, CD<sub>3</sub>OD)  $\delta$  166.4 (C(5')), 159.9 (C(3')), 158.5 (C(1)), 148.1 (C(5)), 142.4 (C(1'')), 137.7 (C(4'')), 131.9 (C(3)), 129.5 (C(2'') & C(6'')), 127.3 (C(3'') & C(5'')), 119.3 (C(4)), 117.6 (C(4')), 115.2 (C(2)), 113.6 (C(6)), 76.1 (CHOH), 20.7 (C(4'')), 11.1 (C(5')), 10.4 (C(3')); HRMS *m/z* (ES<sup>+</sup>) Found: 310.1433. C<sub>19</sub>H<sub>20</sub>NO<sub>3</sub><sup>+</sup> requires M<sup>+</sup> 310.1438; LRMS (formic acid) RT = 0.92, [M + H]<sup>+</sup> = 310; HPLC RT = 11.29 min, purity 98.5% (M1).

**4.2.7. 3-(3,5-Dimethyl-1,2-oxazol-4-yl)-5-[(3,4-dichlorophenyl)(hydroxy)methyl]phenol (9f)**

To a solution of **17** (110 mg, 506  $\mu$ mol, 1.0 eq) in anhydrous THF (2 mL) was added a 0.5 M solution of 3,4-dichlorophenylmagnesium bromide (2.50 mL, 313 mg, 1.25 mmol, 2.5 eq) in THF at rt, and the reaction solution was stirred for 7 h, then was heated at 50 °C for 15 h. Additional 3,4-dichlorophenylmagnesium bromide (1.00 mL, 125 mg, 500  $\mu$ mol, 1.0 eq) was added and the reaction solution was stirred at 50 °C for 7 h. The reaction was quenched with a saturated aqueous solution of NH<sub>4</sub>Cl (15 mL), and the aqueous phase was extracted with EtOAc (3  $\times$  15 mL). The combined organic layers were washed with H<sub>2</sub>O (45 mL), passed through an anhydrous frit and concentrated *in vacuo*. The residue was resuspended in MeOH, filtered and the filtrate was concentrated *in vacuo*. Purification by silica gel chromatography, eluting with EtOAc in cyclohexane (gradient elution 5  $\rightarrow$  55%) followed by mass-directed autopurification (0.1% formic acid, gradient elution MeCN/H<sub>2</sub>O 30  $\rightarrow$  85%) afforded **9f** (20 mg, 11%) as a colourless solid: R<sub>f</sub> (50% EtOAc/cyclohexane) 0.49;  $\nu_{\max}$  (thin film)/cm<sup>-1</sup>: 3198 (br) (O–H), 1637 (m), 1596 (s); <sup>1</sup>H NMR (400 MHz, CD<sub>3</sub>OD)  $\delta$  7.58 (1H, d, *J* = 1.8 Hz, C(2'')H), 7.47 (1H, d, *J* = 8.3 Hz, C(5'')H), 7.31 (1H, dd, *J* = 8.3, 1.8 Hz, C(6'')H), 6.86–6.82 (1H, m, C(6)H), 6.82–6.78 (1H, m, C(4)H), 6.69–6.63 (1H, m, C(2)H), 5.74 (1H, s, CHOH), 2.38 (3H, s, C(5')CH<sub>3</sub>), 2.23 (3H, s, C(3')CH<sub>3</sub>); <sup>13</sup>C NMR (101 MHz, CD<sub>3</sub>OD)  $\delta$  166.9 (C(5')), 160.0 (C(3')), 159.2 (C(1)), 147.5 (C(3'')), 146.9 (C(4'')), 133.2 (C(3)), 132.7 (C(5)), 131.9 (C(1'')), 131.4 (C(5'')), 129.6 (C(2'')), 127.5 (C(6'')), 119.7 (C(4)), 117.9 (C(4')), 116.2 (C(2)), 113.9 (C(6)), 75.3 (CHOH), 11.5 (C(5')CH<sub>3</sub>), 10.7 (C(3')CH<sub>3</sub>); HRMS *m/z* (ES<sup>+</sup>) Found: 386.0322, C<sub>18</sub>H<sub>15</sub>Cl<sub>2</sub>NNaO<sub>3</sub><sup>+</sup> requires M<sup>+</sup> 386.0321; LCMS (formic acid) RT = 1.05, [M + H]<sup>+</sup> 364; HPLC RT = 13.52 min, purity 99.2% (M1).

**4.2.8. 3-(3,5-Dimethyl-1,2-oxazol-4-yl)-5-[(4-fluorophenyl)(hydroxyl)methyl]phenol (9g)**

Magnesium turnings (63 mg, 2.49 mmol, 6.0 eq) and a crystal of iodine were added to anhydrous THF (5 mL) and the mixture was stirred. 1-Bromo-4-fluorobenzene (314  $\mu$ L, 500 mg, 2.85 mmol, 6.6 eq) in anhydrous THF (5 mL) were added to the dropping funnel. The solution was added dropwise at rt, and the funnel was rinsed with further anhydrous THF (0.5 mL). The reaction mixture was heated under reflux with stirring for 1 h. After this time, the Mg turnings had dissolved and the solution became cloudy. The solution was cooled to 0 °C and an ice-cooled solution of **17**



(94 mg, 433  $\mu$ mol, 1.0 eq) in anhydrous THF (10 mL) added *via* cannulation. The reaction solution was warmed to rt and stirred for 16 h, then the reaction was quenched with H<sub>2</sub>O (20 mL) and neutralised with an aqueous 1 M solution of HCl. The THF was removed *in vacuo*, and the aqueous phase was extracted with EtOAc (3  $\times$  20 mL). The combined organic layers were washed with brine (30 mL), dried over anhydrous MgSO<sub>4</sub>, filtered, and concentrated *in vacuo*. Purification by silica gel chromatography, eluting with EtOAc in petroleum ether (gradient elution 25  $\rightarrow$  40%) afforded a colorless oil, from which **9g** was precipitated by the addition of CHCl<sub>3</sub> to give a colourless solid (98 mg, 72%): *R*<sub>f</sub> (50% EtOAc/petroleum ether) 0.24;  $\nu_{\text{max}}$  (thin film)/cm<sup>-1</sup>: 3285 (br) (O–H), 2985 (m), 2972 (m), 2939 (m), 2923 (m), 2866 (m), 2844 (m), 2826 (m), 1597 (w); <sup>1</sup>H NMR (400 MHz, CD<sub>3</sub>OD)  $\delta$  7.34-7.25 (2H, m, C(2'')H & C(6'')H), 6.98-6.89 (2H, m, C(3'')H & C(5'')H), 6.74-6.70 (1H, m, C(6)H), 6.69-6.64 (1H, m, C(4)H), 6.52-6.50 (1H, m, C(2)H), 5.63 (1H, s, CHOH), 2.25 (3H, s, C(5')CH<sub>3</sub>), 2.10 (3H, s, C(3')CH<sub>3</sub>); <sup>13</sup>C NMR (126 MHz, CDCl<sub>3</sub>)  $\delta$  166.4 (C(5')), 163.1 (d, *J* = 243.8 Hz, C(4')), 159.6 (C(3')), 158.7 (C(1)), 147.8 (C(5)), 141.6 (d, *J* = 2.9 Hz, C(1')), 132.1 (C(3)), 129.2 (d, *J* = 8.2 Hz, C(2'') & C(6'')), 119.2 (C(4)H), 117.6 (C(4')), 115.51 (d, *J* = 29.3 Hz, C(3'') & C(5'')), 115.45 (C(2)H), 113.6 (C(6)H), 75.5 (CHOH), 11.1 (C(5')CH<sub>3</sub>), 10.4 (C(3')CH<sub>3</sub>); <sup>19</sup>F NMR (377 MHz, CD<sub>3</sub>OD)  $\delta$  -117.7; HRMS *m/z* (ES<sup>+</sup>) Found: 336.1011. C<sub>18</sub>H<sub>16</sub>FNNaO<sub>3</sub><sup>+</sup> requires *M*<sup>+</sup> 336.1006; LRMS *m/z* (ES<sup>-</sup>) 312 ([*M* – H]<sup>-</sup>, 100%); HPLC RT = 11.03 min, purity 95.7% (M1).

#### 4.2.9. 3-[Cyclohexyl(hydroxyl)methyl]-5-(3,5-dimethyl-1,2-oxazol-4-yl)phenol (**9h**)

Cyclohexanecarbonyl bromide (0.39 mL, 0.51 g, 3.1 mmol, 6.8 eq) in dry THF (1.0 mL) was added dropwise to a flask containing magnesium turnings (69 mg, 2.8 mmol, 6.1 eq) and a crystal of iodine in anhydrous THF (1.0 mL) at rt. Following initiation, the reaction solution was stirred for 1 h, then **17** (0.10 g, 0.46 mmol, 1.0 eq) in dry THF (2.0 mL) was added dropwise. The reaction solution was stirred at rt for 2 h then the reaction was quenched with a saturated aqueous solution of NH<sub>4</sub>Cl (15 mL), and the aqueous phase was extracted with EtOAc (3  $\times$  50 mL). The combined organic layers were washed with brine (50 mL), dried over anhydrous MgSO<sub>4</sub>, filtered, and concentrated *in vacuo*. Purification by silica gel chromatography, eluting with EtOAc in petroleum ether (gradient elution 0  $\rightarrow$  80%) afforded **9h** (103 mg, 74%) as a colourless solid foam: *R*<sub>f</sub> (50% EtOAc/petroleum ether)

0.51; mp 84–86°C (CHCl<sub>3</sub>);  $\nu_{\max}$  (thin film)/cm<sup>-1</sup> 3273 (br) (O–H), 2927 (m), 2852 (w), 2363 (br), 1632 (w), 1595 (s), 1422 (s), 730 (s); <sup>1</sup>H NMR (500 MHz, CD<sub>3</sub>OD)  $\delta$  6.77–6.74 (1H, m, C(4)*H*), 6.71–6.68 (1H, m, C(6)*H*), 6.53–6.50 (1H, m, C(2)*H*), 4.26 (1H, d, *J* = 7.2 Hz, CHOH), 2.39 (3H, s, C(5')CH<sub>3</sub>), 2.24 (3H, s, C(3')CH<sub>3</sub>), 2.03–1.96 (1H, m, CH), 1.80–1.73 (1H, m, CH), 1.72–1.61 (2H, m, 2 × CH), 1.61–1.52 (1H, m, CH), 1.45–1.37 (1H, m, CH), 1.31–0.84 (5H, m, 5 × CH); <sup>13</sup>C NMR (126 MHz, CD<sub>3</sub>OD)  $\delta$  166.7 (C(5')), 160.0 (C(3')), 158.8 (C(1)), 147.7 (C(5)), 132.0 (C(3)), 119.9 (C(4)), 118.1 (C(4')), 115.6 (C(2)), 114.2 (C(6)), 79.8 (CHOH), 46.4 (CHCHOH), 30.6 (CH<sub>2</sub>), 30.2 (CH<sub>2</sub>), 27.6 (CH<sub>2</sub>), 27.3 (CH<sub>2</sub>), 27.2 (CH<sub>2</sub>), 11.5 (C(5')CH<sub>3</sub>), 10.8 (C(3')CH<sub>3</sub>); LRMS *m/z* (ES<sup>-</sup>) 300 ([M – H]<sup>-</sup>, 100%); HRMS *m/z* (ES<sup>+</sup>) found 302.17507 (100%), 303.17851 (30%); C<sub>18</sub>H<sub>23</sub>NO<sub>3</sub> requires [M + H]<sup>+</sup> 302.17507; HPLC RT = 9.11 min, purity 99.3% (M2).

#### 4.2.10. 3-[Cyclopropyl(hydroxyl)methyl]-5-(3,5-dimethyl-1,2-oxazol-4-yl)phenol (9i)

To a flask containing magnesium turnings (55 mg, 2.26 mmol, 6.1 eq) and a crystal of iodine was added dropwise bromocyclopropane (200  $\mu$ L, 302 mg, 2.50 mmol, 6.8 eq) in anhydrous THF (2 mL). Following initiation, the reaction solution was stirred for 30 min, then **17** (80 mg, 368  $\mu$ mol, 1.0 eq) and distilled THF (2 mL) were added. The reaction solution was stirred at rt for 18 h then the reaction was quenched with a saturated aqueous solution of NH<sub>4</sub>Cl (15 mL), and the aqueous phase was extracted with EtOAc (3 × 15 mL). The combined organic layers were washed with H<sub>2</sub>O (45 mL) and brine (45 mL), dried over anhydrous MgSO<sub>4</sub>, filtered, and concentrated *in vacuo*. Purification by silica gel chromatography, eluting with EtOAc in petroleum ether (gradient elution 20 → 80%) afforded **9i** (81 mg, 85%) as a clear and colourless oil: R<sub>f</sub> (50% EtOAc/petroleum ether) 0.24;  $\nu_{\max}$  (thin film)/cm<sup>-1</sup>: 3240 (br) (O–H), 3001 (w), 2361 (w), 2343 (w), 1638 (w), 1597 (m); <sup>1</sup>H NMR (400 MHz, CD<sub>3</sub>OD)  $\delta$  6.80–6.76 (1H, m, C(6)*H*), 6.74–6.70 (1H, m, C(4)*H*), 6.53 (1H, dd, *J* = 1.8, 1.8 Hz, C(2)*H*), 3.82 (1H, d, *J* = 8.3 Hz, CHOH), 2.30 (3H, s, C(5')CH<sub>3</sub>), 2.15 (3H, s, C(3')CH<sub>3</sub>), 1.09–0.98 (1H, m, CHCHOH), 0.55–0.46 (1H, m, CH), 0.45–0.31 (2H, m, 2 × CH), 0.29–0.22 (1H, m, CH); <sup>13</sup>C NMR (101 MHz, CD<sub>3</sub>OD)  $\delta$  166.8 (C(5')), 160.0 (C(3')), 158.9 (C(1)), 148.3 (C(5)), 132.2 (C(3)), 119.3 (C(4)), 118.1 (C(4')), 115.7 (C(2)), 113.6 (C(6)), 78.9 (CHOH), 19.8 (CHCHOH), 11.5 (C(5')CH<sub>3</sub>), 10.8 (C(3')CH<sub>3</sub>), 4.4 (CH<sub>2</sub>), 3.1 (CH<sub>2</sub>); HRMS *m/z* (ES<sup>+</sup>) Found: 282.1110. C<sub>15</sub>H<sub>17</sub>NaO<sub>3</sub><sup>+</sup>



requires  $M^+$  282.1101; LRMS  $m/z$  ( $ES^+$ ) 260 ( $[M + H]^+$ , 97%), 282 ( $[M + Na]^+$ , 100%); HPLC RT = 9.98 min, purity 98.7% (M1).

#### 4.2.11. 3-(3,5-Dimethyl-1,2-oxazol-4-yl)-5-[hydroxy(pyridine-3-yl)methyl]phenol (9j)

To a solution of 3-bromopyridine (351 mg, 2.22 mmol, 5.1 eq) in anhydrous THF (2 mL) was added a 1.3 M solution of isopropylmagnesium chloride lithium chloride complex (2.00 mL, 378 mg, 2.60 mmol, 6.0 eq) in THF dropwise at rt. The reaction mixture was stirred for 2 h, after which time a solution of **17** (94 mg, 433  $\mu$ mol, 1.0 eq) in anhydrous THF (2 mL) was added dropwise, and the reaction solution stirred at rt for 4 h. The reaction was quenched with a saturated aqueous solution of  $NH_4Cl$  (15 mL), and the aqueous phase was extracted with EtOAc ( $3 \times 15$  mL). The combined organic layers were washed with  $H_2O$  (45 mL), brine (45 mL), dried over anhydrous  $MgSO_4$ , filtered, and concentrated *in vacuo*. Purification by silica gel chromatography, eluting with MeOH in  $CH_2Cl_2$  (gradient elution 0  $\rightarrow$  10%) afforded **9j** (94 mg, 73%) as a colourless solid:  $R_f$  (10% MeOH/ $CH_2Cl_2$ ) 0.46;  $\nu_{max}$  (thin film)/ $cm^{-1}$ : 2970 (br), 2949 (w), 2923 (br), 2866 (br), 2844 (w);  $^1H$  NMR (400 MHz,  $DMSO-D_6$ )  $\delta$  9.57 (1H, s, C(1)OH), 8.62 (1H, d,  $J = 2.0$  Hz, C(2'')H), 8.44 (1H, dd,  $J = 4.8, 2.0$  Hz, C(6'')H), 7.76 (1H, ddd,  $J = 7.9, 2.0, 2.0$  Hz, C(4'')H), 7.35 (1H, dd,  $J = 7.9, 4.8$  Hz, C(5'')H), 6.87-6.76 (2H, m, C(4)H & C(6)H), 6.61 (1H, dd,  $J = 2.3, 1.6$  Hz, C(2)H), 6.07 (1H, d,  $J = 4.0$ , CHOH), 5.75 (1H, d,  $J = 4.0$ , CHOH), 2.37 (3H, s, C(5') $CH_3$ ), 2.19 (3H, s, C(3') $CH_3$ );  $^{13}C$  NMR (101 MHz,  $CD_3OD$ )  $\delta$  166.9 (C(5')), 159.9 (C(3')), 159.3 (C(1)), 148.8 (C(6'')), 148.6 (C(2'')), 147.4 (C(3'') or C(5)), 142.4 (C(5) or C(3'')), 136.4 (C(4'')), 132.8 (C(3)), 125.1 (C(5'')), 119.5 (C(4)), 117.8 (C(4')), 116.2 (C(2)), 113.9 (C(6)), 74.3 (CHOH), 11.5 (C(5') $CH_3$ ), 10.7 (C(3') $CH_3$ ); HRMS  $m/z$  ( $ES^-$ ) Found: 295.1092.  $C_{17}H_{17}N_2O_3^-$  requires  $M^-$  295.1088; LRMS  $m/z$  ( $ES^-$ ) 295 ( $[M - H]^-$ , 100%); HPLC RT = 8.29 min, purity 97.8% (M1).

#### 4.2.12 3-(3,5-Dimethyl-1,2-oxazol-4-yl)-5-[hydroxy(pyridine-4-yl)methyl]phenol (9k)

To a solution of 4-iodopyridine (242 mg, 1.18 mmol, 5.1 eq) in anhydrous THF (4 mL) was added a 2 M solution of isopropylmagnesium chloride (1.20 mL, 247 mg, 2.40 mmol, 10.3 eq) in THF dropwise at rt and the reaction solution was stirred for 1 h. To a solution of **17** (50 mg, 230  $\mu$ mol, 1.0 eq) in anhydrous THF (4 mL) was added a portion of the above Grignard solution (2.60 mL,

590  $\mu$ mol, 2.6 eq), and the solution was stirred at rt for 4 h, then was heated at 50 °C for 18 h. The reaction was quenched with a saturated aqueous solution of  $\text{NH}_4\text{Cl}$  (15 mL), and the aqueous phase was extracted with EtOAc (3  $\times$  15 mL). The combined organic layers were washed with  $\text{H}_2\text{O}$  (45 mL), passed through an anhydrous frit and concentrated *in vacuo*. Purification by silica gel chromatography, eluting with MeOH in  $\text{CH}_2\text{Cl}_2$  (gradient elution 0  $\rightarrow$  20%) afforded **9k** (6 mg, 9%) as a yellow oil:  $R_f$  (10% EtOAc/cyclohexane) 0.40;  $\nu_{\text{max}}$  (thin film)/ $\text{cm}^{-1}$ : 3356 (br) (O–H), 2482 (br), 2244 (w), 2072 (m), 1598 (m);  $^1\text{H}$  NMR (400 MHz,  $\text{CD}_3\text{OD}$ )  $\delta$  8.56–8.43 (2H, m, C(2'')H & C(6'')H), 7.53–7.48 (2H, m, C(3'')H & C(5'')H), 6.87–6.84 (1H, m, C(6)H), 6.84–6.81 (1H, m, C(4)H), 6.67 (1H, dd,  $J$  = 2.2, 1.6 Hz, C(2)H), 5.78 (1H, s, CHOH), 2.38 (3H, s, C(5')CH<sub>3</sub>), 2.22 (3H, s, C(3')CH<sub>3</sub>);  $^{13}\text{C}$  NMR (101 MHz,  $\text{CD}_3\text{OD}$ )  $\delta$  166.9 (C(5')), 159.9 (C(3')), 159.3 (C(1)), 156.4 (C(5) or C(4'')), 150.0 (C(2'')H & C(6'')H), 147.0 (C(4'') or C(5)), 132.9 (C(3)), 123.0 (C(3'') & C(5'')), 119.8 (C(4)), 117.8 (C(4')), 116.4 (C(2)), 114.1 (C(6)), 75.2 (CHOH), 11.4 (C(5')CH<sub>3</sub>), 10.7 (C(3')CH<sub>3</sub>); HRMS  $m/z$  ( $\text{ES}^+$ ) Found: 297.1238.  $\text{C}_{17}\text{H}_{17}\text{N}_2\text{O}_3^+$  requires  $M^+$  297.11234; LRMS  $m/z$  ( $\text{ES}^+$ ) 297 ( $[\text{M} + \text{H}]^+$ , 100%); HPLC RT = 8.27 min, purity 95.4% (M1).

#### 4.2.13. 3-(3,5-Dimethyl-1,2-oxazol-4-yl)-5-[(3-fluorophenyl)(hydroxyl)methyl]phenol (**9l**)

To a solution of 1-fluoro-3-iodobenzene (270  $\mu$ L, 511 mg, 2.30 mmol, 5.3 eq) in anhydrous THF (8 mL) was added a 1.3 M solution of isopropylmagnesium chloride lithium chloride (2.00 mL, 378 mg, 2.60 mmol, 5.8 eq) in THF dropwise at –10 °C. The reaction solution was warmed to rt and stirred for 5 h. To a solution of **17** (94 mg, 433  $\mu$ mol, 1.0 eq) in anhydrous THF (8 mL) was added dropwise a portion of the above Grignard solution (4.00 mL, 909  $\mu$ mol, 2.1 eq). The reaction was stirred at rt for 3 h, then was heated at 50 °C for 18 h. Additional Grignard solution (1.00 mL, 227  $\mu$ mol, 0.5 eq) was added and the reaction solution was heated at 50 °C for 2 h, before addition of the remaining Grignard solution (5.00 mL, 1.15 mmol, 2.7 eq). The reaction solution was stirred at 50 °C for 1 h, then the reaction was quenched with a saturated aqueous solution of  $\text{NH}_4\text{Cl}$  (15 mL), and the aqueous phase was extracted with EtOAc (3  $\times$  15 mL). The combined organic layers were washed with  $\text{H}_2\text{O}$  (45 mL), passed through an anhydrous frit and concentrated *in vacuo*. Purification by silica gel chromatography, eluting with EtOAc in cyclohexane (gradient elution 5  $\rightarrow$  100%) followed by mass-directed autopurification (0.1% formic acid, gradient elution

MeCN / H<sub>2</sub>O 15 → 55%) afforded **9l** (15 mg, 11%) as a clear and colourless oil that solidified under vacuum to give a colourless, amorphous solid: *R<sub>f</sub>* (50% EtOAc/petroleum ether) 0.49; *v*<sub>max</sub> (thin film)/cm<sup>-1</sup>: 3291 (br) (O–H), 2470 (br), 1593 (s); <sup>1</sup>H NMR (400 MHz, CD<sub>3</sub>OD) δ 7.37-7.29 (1H, m, C(5'')H), 7.24-7.19 (1H, m, C(6)H), 7.19-7.13 (1H, m, C(2'')H or C(4'')H), 7.01-7.93 (1H, m, C(4'')H or C(2'')H), 6.88-8.83 (1H, m, C(6)H), 6.82-6.78 (1H, m, C(4)H), 6.67-6.62 (1H, m, C(2)H), 5.76 (1H, s, CHOH), 2.38 (3H, s, C(5')CH<sub>3</sub>), 2.22 (3H, s, C(3')CH<sub>3</sub>); <sup>13</sup>C NMR (101 MHz, CD<sub>3</sub>OD) δ 168.8 (C(5')), 164.3 (d, *J* = 245 Hz, C(3'')), 159.9 (C(3')), 159.1 (C(1)), 148.9 (d, *J* = 7 Hz, C(1'')), 147.9 (C(5)), 132.5 (C(3)), 131.0 (d, *J* = 8 Hz, C(5'')), 123.4 (d, *J* = 3 Hz, C(6'')), 119.7 (C(4)), 117.9 (C(4')), 115.9 (C(2)), 114.8 (d, *J* = 21 Hz, C(2'') or C(4'')), 114.1 (d, *J* = 22 Hz, C(4'') or C(2'')), 114.0 (C(6)), 75.9 (CHOH), 11.4 (C(5')CH<sub>3</sub>), 10.7 (C(3')CH<sub>3</sub>); <sup>19</sup>F NMR (377 MHz, CD<sub>3</sub>OD) δ –115.4; HRMS *m/z* (ES<sup>–</sup>) Found: 312.1043. C<sub>18</sub>H<sub>15</sub>FNO<sub>3</sub><sup>–</sup> requires *M*<sup>–</sup> 312.1041; LRMS *m/z* (ES<sup>–</sup>) 312 ([*M* – H]<sup>–</sup>, 100%); HPLC RT = 11.08 min, purity 95.4% (M1).

#### 4.2.14. 3-[[3-(3,5-Dimethyl-1,2-oxazol-4-yl)-5-hydroxyphenyl](hydroxyl)methyl]benzonitrile (**9m**)

To a solution of 4-iodobenzonitrile (484 mg, 2.11 mmol, 4.4 eq) in anhydrous THF (2 mL) was added a 1.3 M solution of isopropylmagnesium chloride lithium chloride complex (2.00 mL, 378 mg, 2.60 mmol, 5.4 eq) in THF dropwise at –10 °C. The reaction solution was stirred for 4 h. To a solution of **17** (105 mg, 483 μmol, 1.0 eq) in anhydrous THF (8 mL) at –10 °C was added dropwise the Grignard solution. The solution was stirred for 3 h, then was warmed to rt and quenched with a saturated aqueous solution of NH<sub>4</sub>Cl (15 mL), and the aqueous phase was extracted with EtOAc (3 × 15 mL). The combined organic layers were washed with H<sub>2</sub>O (45 mL) and brine (45 mL), dried over anhydrous MgSO<sub>4</sub>, filtered, and concentrated *in vacuo*. Purification by silica gel chromatography, eluting with EtOAc in petroleum ether (gradient elution 10 → 60%) afforded **9m** (34 mg, 23%) as a clear and colourless oil: *R<sub>f</sub>* (50% EtOAc/petroleum ether) 0.32; *v*<sub>max</sub> (thin film)/cm<sup>-1</sup>: 3319 (br) (O–H), 2972 (w), 2230 (w) (C≡N), 1632 (w), 1595 (m); <sup>1</sup>H NMR (400 MHz, CD<sub>3</sub>OD) δ 7.71-7.66 (2H, m, C(3'')H & C(5'')H), 7.62-7.57 (2H, m, C(2'')H & C(6'')H), 6.83-6.80 (1H, m, C(6)H), 6.79-6.77 (1H, m, C(4)H), 6.79-6.77 (1H, m, C(2)H), 5.79 (1H, s, CHOH), 2.36 (3H, s,

$C(5')CH_3$ ), 2.20 (3H, s,  $C(3')CH_3$ );  $^{13}C$  NMR (126 MHz,  $CD_3OD$ )  $\delta$  165.5 ( $C(5')$ ), 158.5 ( $C(3')$ ), 157.8 ( $C(1)$ ), 150.3 ( $C(5)$ ), 146.0 ( $C\equiv N$ ), 131.9 ( $C(3'')$  and  $C(5'')$ ), 131.3 ( $C(3)$ ), 127.0 ( $C(2'')$  and  $C(6'')$ ), 118.4 ( $C(4'')$ ), 118.3 ( $C(4)$ ), 116.4 ( $C(4')$ ), 114.7 ( $C(2)$ ), 112.6 ( $C(6)$ ), 110.5 ( $C(1'')$ ), 74.5 (CHOH), 10.0 ( $C(5')CH_3$ ), 9.3 ( $C(3')CH_3$ ); HRMS  $m/z$  ( $ES^+$ ) Found: 343.1061.  $C_{19}H_{16}N_2NaO_3^+$  requires  $M^+$  343.1053; LRMS  $m/z$  ( $ES^-$ ) 319 ( $[M - H]^-$ , 52%), 639 ( $[2M - H]^-$ , 100%); HPLC RT = 10.83 min, purity 95.7% (M1).

#### 4.2.15. 3-[(5-Chloropyridin-2-yl)(hydroxyl)methyl]-5-(3,5-dimethyl-1,2-oxazol-4-yl)phenol (9n)

To a solution of 5-chloro-2-iodopyridine (532 mg, 2.22 mmol, 5.1 eq) in anhydrous THF (2 mL) was added a 1.3 M solution of isopropylmagnesium chloride lithium chloride complex (2.00 mL, 378 mg, 2.60 mmol, 6.0 eq) in THF dropwise at rt. The reaction solution was stirred for 2 h. To a solution of **17** (94 mg, 433  $\mu$ mol, 1.0 eq) in anhydrous THF (2 mL) was added dropwise a portion of the above Grignard solution (2.00 mL, 1.11 mmol, 2.6 eq). The reaction was stirred at rt for 23 h, then was heated at 50 °C for 21 h, before the remaining Grignard solution (2.00 mL, 1.11 mmol, 2.6 eq) was added. The reaction solution was stirred for a further 5 h at 50 °C, then the reaction was quenched with a saturated aqueous solution of  $NH_4Cl$  (15 mL), and the aqueous phase was extracted with EtOAc (3  $\times$  15 mL). The combined organic layers were washed with  $H_2O$  (45 mL) and brine (45 mL), dried over anhydrous  $MgSO_4$ , filtered, and concentrated *in vacuo*. Purification by silica gel chromatography, eluting with acetone in petroleum ether (gradient elution 20  $\rightarrow$  80%) afforded **9n** (22 mg, 15%) as a clear and colourless oil. Precipitation from  $CHCl_3$  and hexane afforded **9n** as a colourless amorphous solid:  $R_f$  (50% EtOAc/cyclohexane) 0.35;  $\nu_{max}$  (thin film)/ $cm^{-1}$ : 3457 (br), 3016 (br) (O–H), 2970 (w), 2837 (w), 1631 (m), 1369 (s);  $^1H$  NMR (400 MHz,  $CD_3OD$ )  $\delta$  8.45 (1H, d,  $J = 2.4$  Hz,  $C(6'')H$ ), 7.85 (1H, dd,  $J = 8.5, 2.4$  Hz,  $C(4'')H$ ), 7.61 (1H, d,  $J = 8.5$  Hz,  $C(3'')H$ ), 6.87–6.80 (2H, m,  $C(4)H$  and  $C(6)H$ ), 6.61 (1H, dd,  $J = 1.8, 1.8$  Hz,  $C(2)H$ ), 5.76 (1H, s, CHOH), 2.36 (3H, s,  $C(5')CH_3$ ), 2.20 (3H, s,  $C(3')CH_3$ );  $^{13}C$  NMR (126 MHz,  $CD_3OD$ )  $\delta$  166.9 ( $C(5')$ ), 163.1 ( $C(2'')$ ), 159.9 ( $C(3')$ ), 159.2 ( $C(1)$ ), 148.1 ( $C(6'')$ ), 146.6 ( $C(5)$ ), 138.3 ( $C(4'')$ ), 132.6 ( $C(3)$ ), 131.9 ( $C(5'')$ ), 123.1 ( $C(3'')$ ), 119.6 ( $C(6)$ ), 117.8 ( $C(4')$ ), 116.1 ( $C(2)$ ), 114.0 ( $C(4)$ ), 76.7 (CHOH), 11.4 ( $C(5')CH_3$ ), 10.7 ( $C(3')CH_3$ ); HRMS  $m/z$  ( $ES^+$ ) Found: 353.0659.  $C_{17}H_{15}ClN_2NaO_3^+$  requires  $M^+$  353.0663; LRMS  $m/z$  ( $ES^-$ ) 329 ( $[M - H]^-$ , 100%); HPLC RT = 9.93 min, purity 97.2% (M1).

**4.2.16. 3-(3,5-Dimethyl-1,2-oxazol-4-yl)-5-[(2-fluorophenyl)(hydroxyl)methyl]phenol (9o)**

To a solution of 1-bromo-2-fluorobenzene (27.0  $\mu$ L, 43 mg, 247  $\mu$ mol, 1.2 eq) in anhydrous THF (2 mL) at  $-78^{\circ}\text{C}$  was added a 2.3 M solution of  $n\text{BuLi}$  in THF (12.0  $\mu$ L, 28 mg, 431  $\mu$ mol, 2.1 eq). The reaction solution was stirred at  $-78^{\circ}\text{C}$  for 40 min before a solution of **18** (75 mg, 201  $\mu$ mol, 1.0 eq) in anhydrous THF (2 mL) was added. The solution was stirred at  $-78^{\circ}\text{C}$  for 3 h, then was warmed to rt and quenched with  $\text{H}_2\text{O}$  (5 mL) and neutralised with an aqueous 1 M solution of HCl. The THF was removed *in vacuo*, and the aqueous phase was extracted with EtOAc (3  $\times$  10 mL). The combined organic layers were washed with  $\text{H}_2\text{O}$  (30 mL) and brine (30 mL), dried over anhydrous  $\text{MgSO}_4$ , filtered, and concentrated *in vacuo*. To a solution of the resulting residue in distilled THF (5 mL) at  $0^{\circ}\text{C}$  was added a 1 M solution of TBAF (65.0  $\mu$ L, 59 mg, 224  $\mu$ mol, 1.1 eq) in THF. The solution was stirred at  $0^{\circ}\text{C}$  for 2 h, then the volatile components were removed *in vacuo*. The resulting residue was partitioned between  $\text{H}_2\text{O}$  (10 mL) and EtOAc (10 mL). The phases were separated, the aqueous layer was extracted with EtOAc (2  $\times$  10 mL) and the combined organic layers were washed with brine (30 mL), dried over anhydrous  $\text{MgSO}_4$ , filtered, and concentrated *in vacuo*. Purification by silica gel chromatography, eluting with EtOAc in petroleum ether (gradient elution 20  $\rightarrow$  100%) afforded **9o** (11 mg, 17%) as a clear and colourless oil, which was precipitated from  $\text{CHCl}_3$  with hexane to give a colourless, amorphous solid:  $R_f$  (50% EtOAc/petroleum ether) 0.45;  $\nu_{\text{max}}$  (thin film)/ $\text{cm}^{-1}$ : 2970 (w), 2866 (br), 2844 (br), 1739 (s), 1435 (w), 1371 (w);  $^1\text{H}$  NMR (500 MHz,  $\text{CD}_3\text{OD}$ )  $\delta$  7.56 (1H, ddd,  $J = 7.6, 7.6, 1.6$  Hz, C(6'')H), 7.30-7.24 (1H, m, C(4'')H), 7.17 (1H, ddd,  $J = 7.6, 7.6, 1.0$  Hz, C(5'')H), 7.04 (1H, ddd,  $J = 10.5, 8.1, 1.0$  Hz, C(3'')H), 6.84-6.82 (1H, m, C(6)H), 6.78-6.76 (1H, m, C(4)H), 6.62-6.60 (1H, m, C(2)H), 6.03 (1H, s, CHOH), 2.35 (3H, s, C(5')CH<sub>3</sub>), 2.19 (3H, s, C(3')CH<sub>3</sub>);  $^{13}\text{C}$  NMR (126 MHz,  $\text{CD}_3\text{OD}$ )  $\delta$  166.8 (C(5')), 161.2 (d,  $J = 244$  Hz, C(2'')), 159.9 (C(3')), 159.0 (C(1)), 147.3 (C(5)), 132.9 (d,  $J = 13$  Hz, C(1'')), 132.4 (C(3)), 130.1 (d,  $J = 8$  Hz, C(5'')), 128.8 (d,  $J = 4$  Hz, C(3'')), 125.4 (d,  $J = 3$  Hz, C(4'')), 119.5 (C(4)), 117.9 (C(4')), 116.1 (d,  $J = 22$  Hz, C(6')), 115.8 (C(2)), 113.9 (C(6)), 69.9 (d,  $J = 3$  Hz, CHOH), 11.4 (C(5')CH<sub>3</sub>), 10.7 (C(3')CH<sub>3</sub>);  $^{19}\text{F}$  NMR (377 MHz,  $\text{CD}_3\text{OD}$ )  $\delta$  -120.6; HRMS  $m/z$  (ES<sup>+</sup>) Found: 336.1013.  $\text{C}_{18}\text{H}_{16}\text{FNNaO}_3^+$  requires  $M^+$  336.1006; LRMS  $m/z$  (ES<sup>+</sup>) 314 ([M + H]<sup>+</sup>, 100%); HPLC RT = 11.00 min, purity 95.2% (M1).

**4.2.17. 3-(3,5-Dimethyl-1,2-oxazol-4-yl)-5-[hydroxy(pyridine-2-yl)methyl]phenol (9p)**

To a solution of 2-bromopyridine (38.0  $\mu$ L, 64 mg, 402  $\mu$ mol, 1.5 eq) in Et<sub>2</sub>O (3 mL) at -78 °C was added a 2.3 M solution of *n*BuLi in hexanes (180  $\mu$ L, 420 mg, 414  $\mu$ mol, 1.5 eq). The reaction solution was stirred at -78 °C for 40 min, then was warmed to rt and stirred for a further 40 min before cooling to -78 °C. To this was added a solution of **18** (100 mg, 268  $\mu$ mol, 1.0 eq) in Et<sub>2</sub>O (5 mL). The solution was allowed to warm to rt, over 16 h then the reaction was quenched with H<sub>2</sub>O (5 mL) and neutralised with an aqueous 20% (w/v) solution of NH<sub>4</sub>Cl. The aqueous phase was extracted with EtOAc (4  $\times$  10 mL). The combined organic layers were washed with brine (40 mL), dried over anhydrous Na<sub>2</sub>SO<sub>4</sub>, filtered, and concentrated *in vacuo*. Purification by silica gel chromatography, eluting with EtOAc in 30-40 °C petroleum ether (gradient elution 4  $\rightarrow$  50%) afforded the TIPS-protected intermediate (65 mg, 54%) as a yellow oil. To a solution of this intermediate (50 mg, 110  $\mu$ mol, 1.0 eq) in distilled THF (2 mL) at 0 °C was added a 1 M solution of TBAF (121  $\mu$ L, 110 mg, 121  $\mu$ mol, 1.1 eq). The reaction was stirred at 0 °C for 30 min, then the volatile components were removed *in vacuo*. Purification by silica gel chromatography, eluting with acetone in 30-40 °C petroleum ether (gradient elution 20  $\rightarrow$  60%) afforded **9p** (29 mg, 89%) as a colourless solid: R<sub>f</sub> (40% EtOAc/petroleum ether) 0.26; mp 221-223 °C (acetone);  $\nu_{\max}$  (thin film)/cm<sup>-1</sup>: 3389 (br), 2925 (w), 1593 (s); <sup>1</sup>H NMR (400 MHz, DMSO-D<sub>6</sub>)  $\delta$  9.53 (1H, s, C(1)OH), 8.48-8.43 (1H, m, C(6'')H), 7.78 (1H, ddd, *J* = 9.5, 7.6, 1.8 Hz, C(4'')H), 7.59-7.54 (1H, m, C(3'')H), 7.24 (1H, ddd, *J* = 7.6, 4.9, 1.1 Hz, C(5'')H), 6.84-6.79 (2H, m, C(4)H & C(6)H), 6.59-6.56 (1H, m, C(2)H), 6.08 (1H, d, *J* = 4.1 Hz, CHOH), 5.66 (1H, d, *J* = 4.1, CHOH), 2.35 (3H, s, C(5')CH<sub>3</sub>), 2.17 (3H, s, C(3')CH<sub>3</sub>); <sup>13</sup>C NMR (126 MHz, DMSO-D<sub>6</sub>)  $\delta$  164.9 (C(5')), 163.9 (C(3')), 157.9 (C(1)), 157.4 (C(2'')), 148.3 (C(6'')), 146.4 (C(5)), 136.8 (C(4'')), 130.5 (C(3)), 122.2 (C(5'')), 120.0 (C(3'')), 117.7 (C(4)), 115.9 (C(4')), 114.1 (C(2)), 112.4 (C(6)), 75.4 (CHOH), 11.3 (C(5')CH<sub>3</sub>), 10.5 (C(3')CH<sub>3</sub>); HRMS *m/z* (ES<sup>+</sup>) Found: 319.1048. C<sub>17</sub>H<sub>17</sub>N<sub>2</sub>NaO<sub>3</sub><sup>+</sup> requires M<sup>+</sup> 319.1053; LRMS *m/z* (ES<sup>+</sup>) 297 ([M + H]<sup>+</sup>, 100%), 319 ([M + Na]<sup>+</sup>, 20%); HPLC RT = 8.42 min, purity 98.9% (M1).

**4.2.18. 3-(3,5-Dimethyl-1,2-oxazol-4-yl)-5-[(4-methylpiperazin-1-yl)methyl]phenol (10a)**

To a solution of **17** (106 mg, 488  $\mu$ mol, 1.0 eq) and 1-methylpiperazine (70.0  $\mu$ L, 63 mg, 631  $\mu$ mol, 1.3 eq) in EtOH (5 mL) was added AcOH dropwise until the solution was pH 4. The reaction



solution was stirred at rt for 20 min before addition of NaBH<sub>3</sub>CN (20 mg, 318  $\mu$ mol, 0.7 eq). The solution was stirred for a further 17 h and the volatile components were removed *in vacuo*. Purification by silica gel chromatography, eluting with MeOH in CH<sub>2</sub>Cl<sub>2</sub> (gradient elution 0  $\rightarrow$  20%) yielded **10a** (101 mg, 69%) as an oil that crystallised under vacuum. A small sample of **10a** was purified by semi-preparative HPLC for biological testing. The degree of TFA salt formation was quantified using 1,4-difluorobenzene (DFB) as an internal standard in <sup>19</sup>F NMR and gave a TFA content of 19.2% (w/w). The difference in relaxation times of <sup>19</sup>F nuclei of TFA and DFB was addressed by an external calibration using samples containing known amounts of TFA and DFB. R<sub>f</sub> (20% MeOH/CH<sub>2</sub>Cl<sub>2</sub>) 0.43; mp free amine 144-146 °C (MeOH), TFA salt (from MeCN) > 250 °C;  $\nu_{\max}$  (thin film)/cm<sup>-1</sup>: 2965 (w), 2813 (w), 1589 (m); <sup>1</sup>H NMR (400 MHz, CD<sub>3</sub>OD)  $\delta$  6.91-6.84 (2H, m, C(4)H & C(6)H), 6.79-6.74 (1H, m, C(2)H), 3.99 (2H, s, CH<sub>2</sub>Ar), 3.53-3.36 (4H, m, 4  $\times$  NCH<sub>2</sub>), 3.28-3.04 (4H, m, 4  $\times$  NCH<sub>2</sub>), 2.92 (3H, s, NCH<sub>3</sub>), 2.41 (3H, s, C(5')CH<sub>3</sub>), 2.25 (3H, s, C(3')CH<sub>3</sub>); <sup>13</sup>C NMR (126 MHz, CD<sub>3</sub>OD)  $\delta$  167.0 (C(5')H), 159.9 (C(3')H), 159.5 (C(1)), 137.6 (C(3)), 132.5 (C(5)), 122.5 (C(4)), 117.6 (C(2)), 115.8 (C(6)), 114.1 (C(4')), 62.0 (CH<sub>2</sub>Ar), 53.8 (2  $\times$  NCH<sub>2</sub>), 50.5 (2  $\times$  NCH<sub>2</sub>), 43.5 (CH<sub>3</sub>), 11.4 (C(5')CH<sub>3</sub>), 10.7 (C(3')CH<sub>3</sub>); <sup>19</sup>F NMR (377 MHz, CD<sub>3</sub>OD)  $\delta$  -77.3; HRMS *m/z* (ES<sup>+</sup>) Found: 302.1858. C<sub>17</sub>H<sub>24</sub>N<sub>3</sub>O<sub>2</sub><sup>+</sup> requires M<sup>+</sup> 302.1863; LRMS *m/z* (ES<sup>+</sup>) 302 ([M + H]<sup>+</sup>, 100%); HPLC RT = 8.14 min, purity 99.7% (M1).

#### 4.2.19. 3-(3,5-Dimethyl-1,2-oxazol-4-yl)-5-(morpholin-4-ylmethyl)phenol (**10b**)

To a solution of **17** (100 mg, 460  $\mu$ mol, 1.0 eq) and morpholine (50.0  $\mu$ L, 50 mg, 572  $\mu$ mol, 1.2 eq) in EtOH (5 mL) was added AcOH dropwise until the solution was pH 4. The reaction solution was stirred at rt for 40 min before addition of NaBH<sub>3</sub>CN (23 mg, 366  $\mu$ mol, 0.8 eq). The solution was stirred for a further 23 h and the volatile components were removed *in vacuo*. Purification by silica gel chromatography, eluting with EtOAc in petroleum ether (gradient elution 40  $\rightarrow$  100%) yielded **10b** (27 mg, 20%) as a yellow oil. A small sample of **10b** was purified by semi-preparative HPLC for biological testing. The degree of TFA salt formation was quantified using 1,4-difluorobenzene (DFB) as an internal standard in <sup>19</sup>F NMR and gave a TFA content of 23.9% (w/w). The difference in relaxation times of <sup>19</sup>F nuclei of TFA and DFB was addressed by an external calibration using samples containing known amounts of TFA and DFB. R<sub>f</sub> (80% EtOAc/petroleum ether) 0.10;  $\nu_{\max}$

(thin film)/cm<sup>-1</sup>: 2982 (m), 2886 (w), 2359 (m), 2344 (m), 1673 (m); mp TFA salt (MeCN) > 250 °C; <sup>1</sup>H NMR (400 MHz, CD<sub>3</sub>OD) δ 6.97 (1H, dd, *J* = 1.9, 1.9 Hz, C(4)*H*), 6.94 (1H, dd, *J* = 1.4, 1.4 Hz, C(6)*H*), 6.88 (1H, dd, *J* = 1.9, 1.4 Hz, C(2)*H*), 4.34 (2H, s, CH<sub>2</sub>Ar), 4.19-3.94 (2H, m, 2 × CH<sub>A</sub>H<sub>B</sub>), 3.87-3.63 (2H, m, 2 × CH<sub>A</sub>H<sub>B</sub>), 3.50-3.07 (4H, m, 2 × CH<sub>2</sub>), 2.42 (3H, s, C(5')CH<sub>3</sub>), 2.27 (3H, s, C(3')CH<sub>3</sub>); <sup>13</sup>C NMR (126 MHz, CD<sub>3</sub>OD) δ 167.2 (C(5')), 160.0 (C(3')), 159.8 (C(1)), 133.9 (C(3)), 131.7 (C(5)), 123.8 (C(4)), 118.7 (C(2)H), 118.4 (C(6)), 117.1 (C(4')), 64.9 (2 × CH<sub>2</sub>O), 61.7 (CH<sub>2</sub>Ar), 52.9 (2 × CH<sub>2</sub>N), 11.5 (C(5')CH<sub>3</sub>), 10.7 (C(3')CH<sub>3</sub>); <sup>19</sup>F NMR (377 MHz, CD<sub>3</sub>OD) δ -77.1; HRMS *m/z* (ES<sup>+</sup>) Found: 289.1547. C<sub>16</sub>H<sub>21</sub>N<sub>2</sub>O<sub>3</sub><sup>+</sup> requires M<sup>+</sup> 289.1547; LRMS *m/z* (ES<sup>+</sup>) 289 ([M + H]<sup>+</sup>, 100%); HPLC RT = 8.58 min, purity 99.5% (M1).

#### 4.2.20. 3-[(Benzylamino)methyl]-5-(3,5-dimethyl-1,2-oxazol-4-yl)phenol (**10c**)

To a solution of benzylamine (100 μL, 98 mg, 916 μmol, 1.9 eq) and AcOH (100 μL, 104 mg, 1.75 mmol, 3.6 eq) in EtOH (5 mL) was added **17** (105 mg, 483 μmol, 1.0 eq). The reaction solution was stirred at rt for 30 min, then NaBH<sub>3</sub>CN (39 mg, 621 μmol, 1.3 eq) was added. The solution was stirred for a further 19 h, then the volatile components were removed *in vacuo*. Purification by silica gel chromatography, eluting with EtOH in EtOAc (gradient elution 0 → 50%), followed by ISOLUTE® SCX-2 amine catch and release column yielded **10c** (103 mg, 69%) as a clear and colourless oil. A small sample of **10c** was purified by semi-preparative HPLC for biological testing. The degree of TFA salt formation was quantified using 1,4-difluorobenzene (DFB) as an internal standard in <sup>19</sup>F NMR and gave a TFA content of 18.6% (w/w). The difference in relaxation times of <sup>19</sup>F nuclei of TFA and DFB was addressed by an external calibration using samples containing known amounts of TFA and DFB. R<sub>f</sub> free amine (70% EtOAc/petroleum ether) 0.18; ν<sub>max</sub> (thin film)/cm<sup>-1</sup>: 2982 (w), 2361 (m), 2344 (m), 1670 (m); mp TFA salt > 250 °C (MeCN); <sup>1</sup>H NMR (500 MHz, CD<sub>3</sub>OD) δ 7.52-7.44 (5H, m, C<sub>6</sub>H<sub>5</sub>), 6.95-6.92 (1H, m, C(6)*H*), 6.91-6.88 (1H, m, C(4)*H*), 6.84-6.81 (1H, m, C(2)*H*), 4.26 (2H, s, CH<sub>2</sub>Ph), 4.22 (2H, s, CH<sub>2</sub>Ar), 2.41 (3H, s, C(5')CH<sub>3</sub>), 2.25 (3H, s, C(3')CH<sub>3</sub>); <sup>13</sup>C NMR (126 MHz, CDCl<sub>3</sub>) δ 167.2 (C(5')), 159.8 (C(3')) & (C(1)), 134.5 (C(5)), 133.8 (C(3)), 132.4 (C(1')), 131.1 (C(2'') & C(6'') or C(3'') & C(5'')), 130.8 (C(4'')), 130.3 (C(3'') & C(5'') or C(2'') & C(6'')), 122.4 (C(4)), 118.1 (C(2)), 117.4 (C(4')), 117.2 (C(6)), 52.2 (CH<sub>2</sub>Ph), 51.8 (CH<sub>2</sub>Ar), 11.5 (C(5')CH<sub>3</sub>), 10.7 (C(3')CH<sub>3</sub>); <sup>19</sup>F NMR (377 MHz, CD<sub>3</sub>OD) δ -77.1;



HRMS  $m/z$  ( $ES^+$ ) Found: 309.1592.  $C_{19}H_{21}O_2N_2^+$  requires  $M^+$  309.1598; LRMS  $m/z$  ( $ES^+$ ) 309 ( $[M + H]^+$ , 100%); HPLC RT = 9.67 min, purity 97.7% (M1).

#### 4.2.21. 3-(3,5-Dimethyl-1,2-oxazol-4-yl)-5-(4,4-difluoropiperidin-1-ylmethyl)phenol (10d)

To a solution of 4,4-difluoropiperidine hydrochloride (156 mg, 987  $\mu$ mol, 2.1 eq) in EtOH (5 mL) was added **17** (100 mg, 460  $\mu$ mol, 1.0 eq). The reaction solution was stirred at rt for 30 min, then  $NaBH_3CN$  (49 mg, 780  $\mu$ mol, 1.6 eq) was added. The solution was stirred for a further 19 h, then the volatile components were removed *in vacuo*. Purification by silica gel chromatography, eluting with EtOAc in petroleum ether (gradient elution 15  $\rightarrow$  100%), followed by ISOLUTE<sup>®</sup> SCX-2 amine catch and release column yielded **10d** (49 mg, 33%) as a clear and colourless oil. A small sample of the **10d** was purified by semi-preparative HPLC before biological evaluation. The degree of protonation was quantified by  $^{19}F$  NMR and gave a TFA content of 31.5% (w/w).  $R_f$  free amine (100% EtOAc) 0.69;  $\nu_{max}$  (thin film)/ $cm^{-1}$ : 2982 (m), 2886 (w), 2359 (m), 2344 (m), 2160 (w); mp TFA salt > 250 °C (MeCN);  $^1H$  NMR (400 MHz,  $CD_3OD$ )  $\delta$  6.99-6.96 (1H, m, C(6)*H*), 6.94 (1H, dd,  $J$  = 1.4, 1.4 Hz, C(4)*H*), 6.90-6.87 (1H, m, C(2)*H*), 4.37 (2H, s,  $CH_2Ar$ ), 3.71-3.22 (4H, m, 2  $\times$   $NCH_2$ ), 2.48-2.23 (4H, m, 2  $\times$   $CF_2CH_2$ ), 2.42 (3H, s, C(5') $CH_3$ ), 2.27 (3H, s, C(3') $CH_3$ );  $^{13}C$  NMR (126 MHz,  $CDCl_3$ )  $\delta$  167.2 (C(5')), 160.0 (C(3')), 159.8 (C(1)), 134.0 (C(3)), 132.5 (C(5)), 123.5 (C(4)), 120.2 (t,  $J$  = 242 Hz,  $CF_2$ ), 118.7 (C(6)), 118.2 (C(2)), 117.1 (C(4')), 60.7 ( $CH_2Ar$ ), 50.4 (t,  $J$  = 6 Hz, 2  $\times$   $NCH_2$ ), 32.1 (t,  $J$  = 26 Hz, 2  $\times$   $CF_2CH_2$ ), 11.5 (C(5') $CH_3$ ), 10.7 (C(3') $CH_3$ );  $^{19}F$  NMR (377 MHz,  $CD_3OD$ )  $\delta$  -77.0 ( $CF_3CO_2$ ), -98.7 (1F, d,  $J$  = 195 Hz,  $CF_AFB$ ), -104.9 (1F, d,  $J$  = 195 Hz,  $CF_AFB$ ); HRMS  $m/z$  ( $ES^+$ ) Found: 323.1560.  $C_{17}H_{21}O_2N_2F_2^+$  requires  $M^+$  323.1566; LRMS  $m/z$  ( $ES^+$ ) 323 ( $[M + H]^+$ , 100%); HPLC RT = 9.29 min, purity 99.6% (M1).

#### 4.2.22. 3-(3,5-Dimethyl-1,2-oxazol-4-yl)-5-(piperidin-1-ylmethyl)phenol (10e)

To a solution of piperidine (50.0  $\mu$ L, 43 mg, 506  $\mu$ mol, 1.5 eq) and AcOH (50.0  $\mu$ L, 52 mg, 873  $\mu$ mol, 2.7 eq) in EtOH (5 mL) was added **18** (123 mg, 329  $\mu$ mol, 1.0 eq). The reaction solution was stirred at rt for 1 h, then  $NaBH_3CN$  (11 mg, 175  $\mu$ mol, 0.5 eq) was added. The solution was stirred for a further 22 h, then the volatile components were removed *in vacuo*. Purification by silica gel chromatography, eluting with EtOAc in petroleum ether (gradient elution 0  $\rightarrow$  50%), followed by

ISOLUTE® SCX-2 amine catch and release column yielded an oil that contained a mixture of **10e** (1 mg, 3.49  $\mu$ mol) and the TIPS-protected intermediate (14 mg, 31.6  $\mu$ mol). To a solution of the oil resuspended in distilled THF (1 mL) was added a 1 M solution of TBAF (35.0  $\mu$ L, 32 mg, 35.0  $\mu$ mol, 1.1 eq) in THF dropwise at 0 °C. The reaction was warmed to rt and stirred for 2 h, then the reaction was quenched with H<sub>2</sub>O (5 mL). The aqueous phase was extracted with EtOAc (3  $\times$  5 mL), and the combined organic layers were washed with brine (15 mL), dried over anhydrous MgSO<sub>4</sub>, filtered, and concentrated *in vacuo*. Purification by silica gel chromatography, eluting with EtOH in EtOAc (gradient elution 0  $\rightarrow$  50%) yielded **10e** (11 mg, 8%) as a clear and colourless oil: R<sub>f</sub> (20% MeOH/CH<sub>2</sub>Cl<sub>2</sub>) 0.56;  $\nu_{\max}$  (thin film)/cm<sup>-1</sup>: 2982 (w), 2938 (w), 2361 (m), 2334 (m); <sup>1</sup>H NMR (500 MHz, CD<sub>3</sub>OD)  $\delta$  6.79 (1H, dd, *J* = 1.8, 1.8 Hz, C(4)*H*), 6.77-6.64 (1H, m, C(6)*H*), 6.65 (1H, dd, *J* = 1.8, 1.8 Hz, C(2)*H*), 3.48 (2H, s, CH<sub>2</sub>Ar), 2.52-2.40 (4H, m, 2  $\times$  CH<sub>2</sub>N), 2.40 (3H, s, C(5')CH<sub>3</sub>), 2.25 (3H, s, C(3')CH<sub>3</sub>), 1.61 (4H, tt, *J* = 5.7, 5.7 Hz, 2  $\times$  CH<sub>2</sub>CH<sub>2</sub>N), 1.53-1.32 (2H, m, CH<sub>2</sub>CH<sub>2</sub>CH<sub>2</sub>N); <sup>13</sup>C NMR (126 MHz, CD<sub>3</sub>OD)  $\delta$  166.8 (C(5')), 160.0 (C(3')), 159.1 (C(1)), 140.5 (C(5)), 132.4 (C(3)), 122.6 (C(4)), 117.9 (C(4')), 117.2 (C(6)), 116.0 (C(2)), 64.5 (CH<sub>2</sub>Ar), 55.4 (2  $\times$  CH<sub>2</sub>N), 26.5 (2  $\times$  CH<sub>2</sub>CH<sub>2</sub>N), 25.1 (CH<sub>2</sub>CH<sub>2</sub>CH<sub>2</sub>N), 11.5 (C(5')CH<sub>3</sub>), 10.7 (C(3')CH<sub>3</sub>); HRMS *m/z* (ES<sup>+</sup>) Found: 287.1759. C<sub>17</sub>H<sub>23</sub>N<sub>2</sub>O<sub>2</sub><sup>+</sup> requires M<sup>+</sup> 287.1754; LRMS *m/z* (ES<sup>+</sup>) 287 ([M + H]<sup>+</sup>, 100%); HPLC RT = 9.24 min, purity 99.2% (M1).

#### 4.2.23. 3-(3,5-Dimethyl-1,2-oxazol-4-yl)-5-(pyrrolidin-1-ylmethyl)phenol (**10f**)

To a solution of pyrrolidine (50.0  $\mu$ L, 43 mg, 493  $\mu$ mol, 1.3 eq) and AcOH (50.0  $\mu$ L, 52 mg, 873  $\mu$ mol, 2.4 eq) in EtOH (5 mL) was added **18** (138 mg, 369  $\mu$ mol, 1.0 eq). The reaction solution was stirred at rt for 1 h, then NaBH<sub>3</sub>CN (13 mg, 207  $\mu$ mol, 0.6 eq) was added. The solution was stirred for a further 22 h, then the volatile components were removed *in vacuo*. Purification by silica gel chromatography, eluting with EtOAc in petroleum ether (gradient elution 0  $\rightarrow$  50%), followed by ISOLUTE® SCX-2 amine catch and release column yielded an oil that contained a mixture of **10f** (10 mg, 3.67  $\mu$ mol) and the TIPS-protected intermediate (54 mg, 126  $\mu$ mol). To a solution of the oil resuspended in distilled THF (2 mL) was added a 1 M solution of TBAF (200  $\mu$ L, 181 mg, 200  $\mu$ mol, 1.6 eq) in THF dropwise at 0 °C. The reaction was warmed to rt and stirred for 1 h, then the reaction was quenched with H<sub>2</sub>O (5 mL). The aqueous phase was extracted with EtOAc (3  $\times$  5 mL),

and the combined organic layers were washed with brine (15 mL), dried over anhydrous  $\text{MgSO}_4$ , filtered, and concentrated *in vacuo*. Purification by silica gel chromatography, eluting with EtOH in EtOAc (gradient elution 0  $\rightarrow$  40%) yielded **10f** (33 mg, 33%) as a clear and colourless oil:  $R_f$  (20% MeOH/ $\text{CH}_2\text{Cl}_2$ ) 0.44;  $\nu_{\text{max}}$  (thin film)/ $\text{cm}^{-1}$ : 2961 (m), 2930 (m), 1632 (w), 1593 (s);  $^1\text{H}$  NMR (500 MHz,  $\text{CD}_3\text{OD}$ )  $\delta$  6.81 (1H, dd,  $J = 1.7, 1.7$  Hz, C(4)*H*), 6.79-6.77 (1H, m, C(6)*H*), 6.66 (1H, dd,  $J = 2.2, 1.7$  Hz, C(2)*H*), 3.66 (2H, s,  $\text{CH}_2\text{Ar}$ ), 2.67-2.60 (4H, m,  $2 \times \text{CH}_2\text{N}$ ), 2.39 (3H, s, C(5') $\text{CH}_3$ ), 2.24 (3H, s, C(3') $\text{CH}_3$ ), 1.87-1.80 (4H, m,  $2 \times \text{CH}_2\text{CH}_2\text{N}$ );  $^{13}\text{C}$  NMR (126 MHz,  $\text{CD}_3\text{OD}$ )  $\delta$  166.8 (C(5')), 159.9 (C(3')), 159.2 (C(1)), 141.0 (C(5)), 132.6 (C(3)), 122.3 (C(4)), 117.8 (C(4')), 116.8 (C(6)), 116.2 (C(2)), 61.1 ( $\text{CH}_2\text{Ar}$ ), 54.9 ( $2 \times \text{CH}_2\text{N}$ ), 24.1 ( $2 \times \text{CH}_2\text{CH}_2\text{N}$ ), 11.5 (C(5') $\text{CH}_3$ ), 10.7 (C(3') $\text{CH}_3$ ); HRMS  $m/z$  ( $\text{ES}^+$ ) Found: 273.1597.  $\text{C}_{16}\text{H}_{21}\text{N}_2\text{O}_2^+$  requires  $M^+$  273.1598; LRMS  $m/z$  ( $\text{ES}^+$ ) 273 ( $[\text{M} + \text{H}]^+$ , 100%); HPLC RT = 8.98 min, purity 95.9% (M1).

#### 4.2.24. 3-Benzyl-5-(3,5-dimethylisoxazol-4-yl)phenol (10g)

To a mixture of **1a** (30 mg, 102  $\mu\text{mol}$ , 1.0 eq) and  $\text{Et}_3\text{SiH}$  (81  $\mu\text{L}$ , 59 mg, 510  $\mu\text{mol}$ , 5.0 eq) was added TFA (0.5 mL). The solution was stirred for 15 min, after which time TLC analysis indicated complete consumption of starting material. The reaction was concentrated *in vacuo* and the residues were dissolved in  $\text{CH}_2\text{Cl}_2$  (15 mL), washed with a saturated aqueous solution of  $\text{NaHCO}_3$  (15 mL),  $\text{H}_2\text{O}$  (15 mL), and brine (15 mL), dried ( $\text{MgSO}_4$ ), filtered, and concentrated *in vacuo*.

Purification by silica gel column chromatography (gradient elution, 3  $\rightarrow$  40% EtOAc/40-60  $^\circ\text{C}$  petroleum ether) gave **10g** as a pale brown solid (20 mg, 70%);  $R_f$  (30% EtOAc/petroleum ether) 0.24; mp 100 - 102  $^\circ\text{C}$  (acetone);  $\nu_{\text{max}}$  (thin film)/ $\text{cm}^{-1}$ : 3217 (O-H) (br), 3026, 2929, 2852 (C-H) (w), 1632 (m), 1593 (s), 1420 (s), 1325 (s), 1258 (m);  $^1\text{H}$  NMR (500 MHz,  $\text{D}_6$ -acetone)  $\delta$  8.44 (1H, s, OH), 7.35-7.28 (4H, m, C(2'')*H*, C(6'')*H*, C(3'')*H*, C(5'')*H*), 7.24-7.18 (1H, m, C(4'')*H*), 6.76-6.73 (1H, m, C(4)*H*), 6.73-6.71 (1H, m, C(2)*H*), 6.69-6.66 (1H, m, C(6)*H*), 3.98 (2H, s,  $\text{CH}_2$ ), 2.38 (3H, s, C(5') $\text{CH}_3$ ), 2.21 (3H, s, C(3') $\text{CH}_3$ );  $^{13}\text{C}$  NMR (126 MHz,  $\text{D}_6$ -acetone)  $\delta$  164.8 (C(5')), 158.0, 157.8 (C(3'), C(1)), 143.7 (C(3)), 141.2 (C(1'')), 131.7 (C(5)), 128.9 (C(2''), C(6'')), 128.4 (C(3''), C(5'')), 126.0 (C(4'')), 120.7 (C(4)), 116.2 (C(4')), 114.9 (C(2)), 113.5 (C(6)), 41.3 ( $\text{CH}_2$ ), 10.7 (C(5') $\text{CH}_3$ ), 10.0 (C(3') $\text{CH}_3$ ); HRMS  $m/z$  (ES) found  $[\text{M} + \text{Na}]^+$  302.1151;  $\text{C}_{18}\text{H}_{17}\text{NNaO}_2^+$  requires  $M^+$  302.1151;

LRMS  $m/z$  ( $ES^+$ ) 280 ( $[M + H]^+$ , 100%), 302 ( $[M + Na]^+$ , 88%); HPLC: RT 12.59 min, purity 97.5% (M1).

#### 4.2.25. [3-(3,5-Dimethylisoxazol-4-yl)-5-hydroxyphenyl](piperidin-1-yl)methanone (11a)

To a solution of **21** (50 mg, 214  $\mu$ mol, 1.0 eq) in THF was added EDC·HCl (62 mg, 323  $\mu$ mol, 1.5 eq.) and HOBt hydrate (15 mg, 111  $\mu$ mol, 0.5 eq). The reaction solution was stirred at rt for 20 min, then piperidine (64  $\mu$ L, 55 mg, 644  $\mu$ mol, 3.0 eq). The mixture was then heated at 55 °C for 3 days, then diluted with EtOAc (5 mL), and washed with H<sub>2</sub>O (4  $\times$  5 mL), and brine (3  $\times$  5 mL), dried over anhydrous MgSO<sub>4</sub>, filtered, and concentrated *in vacuo*. Purification by silica gel chromatography, eluting with MeOH in CH<sub>2</sub>Cl<sub>2</sub> (gradient elution 0  $\rightarrow$  10%) yielded **11a** (36 mg, 56%) as a colourless solid:  $R_f$  (1% AcOH/EtOAc) 0.48; mp 189-191 °C (MeOH);  $\nu_{max}$  (thin film)/cm<sup>-1</sup>: 3188 (br), 2969 (w), 2925 (w), 2857 (w), 1587 (s), 1432 (s), 1363 (w), 1324 (s), 1303 (med), 1244 (s), 1113 (s), 1071 (w), 1030 (m); <sup>1</sup>H NMR (400 MHz, MeOD)  $\delta$  6.82 (1H, dd,  $J$  = 2.1, 1.5 Hz, C(2)*H*), 6.79 (1H, dd,  $J$  = 2.1, 1.5 Hz, C(6)*H*), 6.77 (1 H, dd,  $J$  = 1.5, 1.5 Hz, C(4)*H*), 3.77-3.63 (2H, m, CH<sub>2</sub>N), 3.50-3.37 (2H, m, CH<sub>2</sub>N), 2.42 (3H, s, C(5')CH<sub>3</sub>), 2.26 (3H, s, C(3')CH<sub>3</sub>), 1.77-1.62 (4H, m, CH<sub>2</sub>CH<sub>2</sub>N & CH<sub>2</sub>CH<sub>2</sub>CH<sub>2</sub>N), 1.62-1.51 (2H, m, CH<sub>2</sub>CH<sub>2</sub>N); <sup>13</sup>C NMR (101 MHz, MeOD)  $\delta$  171.7 (R<sub>2</sub>NCO-Ar), 167.2 (C(5')), 159.8 (C(3')), 159.4 (C(1)), 139.3 (C(5)), 133.3 (C(3)), 119.1 (C(4)), 118.3 (C(2)), 117.3 (C(4')), 113.8 (C(6)), 50.0 (CH<sub>2</sub>N), 44.3 (CH<sub>2</sub>N), 27.6 (CH<sub>2</sub>CH<sub>2</sub>N), 26.7 (CH<sub>2</sub>CH<sub>2</sub>N), 25.4 (CH<sub>2</sub>CH<sub>2</sub>CH<sub>2</sub>N), 11.4 (C(5')CH<sub>3</sub>), 10.6 (C(3')CH<sub>3</sub>); HRMS  $m/z$  ( $ES^-$ ) Found: 299.14015. C<sub>17</sub>H<sub>19</sub>N<sub>2</sub>O<sub>3</sub><sup>-</sup> requires M<sup>-</sup> 299.1401; LRMS  $m/z$  ( $ES^+$ ) 299 ( $[M - H]^+$ , 100%); HPLC: retention time 7.82 min, purity 97.9% (M3).

#### 4.2.26. [3-(3,5-Dimethylisoxazol-4-yl)-5-hydroxyphenyl](morpholin-4-yl)methanone (11b)

To a solution of **21** (50 mg, 214  $\mu$ mol, 1.0 eq) in THF was added EDC·HCl (62 mg, 323  $\mu$ mol, 1.5 eq) and HOBt hydrate (15 mg, 111  $\mu$ mol, 0.5 eq). The reaction was stirred at rt for 20 min, then morpholine (56  $\mu$ L, 56 mg, 640  $\mu$ mol, 3.0 eq). The reaction mixture was then heated at 55 °C for 3 days, then diluted with EtOAc (5 mL), and washed with H<sub>2</sub>O (4  $\times$  5 mL) and brine (3  $\times$  5 mL), dried over anhydrous MgSO<sub>4</sub>, filtered, and concentrated *in vacuo*. Purification by silica gel chromatography, eluting with MeOH in CH<sub>2</sub>Cl<sub>2</sub> (gradient elution 0  $\rightarrow$  10%) yielded **11b** (34 mg,

52%) as a colourless solid:  $R_f$  (10% MeOH/CH<sub>2</sub>Cl<sub>2</sub>) 0.28; mp 195-197 °C (CH<sub>2</sub>Cl<sub>2</sub>);  $\nu_{\max}$  (thin film)/cm<sup>-1</sup>: 3175 (br) 2999 (med), 2937 (w), 2857 (w), 1585 (s), 1473 (m), 1416 (m), 1324 (m), 1253 (m), 1231 (w), 1206 (w), 1116 (w), 1026 (w); <sup>1</sup>H NMR (400 MHz, MeOD)  $\delta$  6.85-6.81 (3H, m, C(2)H, C(4)H, C(6)H), 3.84-3.44 (8H, m, 2 × OCH<sub>2</sub>CH<sub>2</sub>N), 2.40 (3H, s, C(5')CH<sub>3</sub>), 2.25 (3H, s, C(3')CH<sub>3</sub>); <sup>13</sup>C NMR (101 MHz, CDCl<sub>3</sub>)  $\delta$  171.8 (R<sub>2</sub>NCO-Ar), 167.2 (C(5')), 159.8 (C(3')), 159.4 (C(1)), 138.3 (C(5)), 133.4 (C(3)), 119.3 (C(4)), 118.5 (C(2)), 117.1 (C(4')), 114.1 (C(6)), 67.7 (2 × OCH<sub>2</sub>CH<sub>2</sub>N), 49.5 (OCH<sub>2</sub>CH<sub>2</sub>N), 43.7 (OCH<sub>2</sub>CH<sub>2</sub>N), 11.4, 10.6; HRMS  $m/z$  (ES<sup>-</sup>) Found: 301.1193. C<sub>16</sub>H<sub>17</sub>N<sub>2</sub>O<sub>4</sub><sup>-</sup> requires M<sup>-</sup> 301.1194; LRMS  $m/z$  (ES<sup>-</sup>) 301 ([M - H]<sup>-</sup>, 100%). HPLC: RT 6.63 min, purity 97.4% (M3).

#### 4.2.27. Potassium (3,5-dimethylisoxazol-4-yl)trifluoroborate (13)<sup>53</sup>

Following to the procedure of Lennox *et al.*,<sup>54</sup> to a suspension of (3,5-dimethylisoxazol-4-yl)boronic acid (**12**, 2.5 g, 17.74 mmol, 1.0 eq) in CH<sub>3</sub>CN (15 mL), was added 7 mL of a 10 M aqueous solution of KF (4.12 g, 70.96 mmol, 4.0 eq). The reaction mixture was stirred at rt until the boronic acid had completely dissolved. A solution of L-(+)-tartaric acid (5.46 g, 36.37 mmol, 2.05 eq) in THF (27 mL) was added dropwise to the reaction mixture over a period of 10 minutes. A colourless precipitate formed instantly. The suspension was stirred at room temperature for 20 minutes. After this time the reaction mixture was filtered. The filter cake was rinsed several times with CH<sub>3</sub>CN, the combined filtrates were concentrated *in vacuo* to give **13** as a colourless solid (2.62 g, 12.9 mmol, 73%).  $R_f$  (petroleum ether: Et<sub>2</sub>O 1:1) 0.10; mp >300 °C (acetone) [lit. mp > 200 °C<sup>53</sup>]; <sup>1</sup>H NMR (400 MHz, D<sub>6</sub>-DMSO)  $\delta$  2.19 (3H, s, C(5')CH<sub>3</sub>), 2.04 (3H, s, C(3')CH<sub>3</sub>); <sup>11</sup>B NMR (160 MHz, D<sub>6</sub>-DMSO)  $\delta$  2.33 (q,  $J$  = 49 Hz); <sup>19</sup>F NMR (377 MHz, D<sub>6</sub>-DMSO)  $\delta$  -134.1 - -134.9 (m); LRMS  $m/z$  (ES<sup>-</sup>) 164 ([M - K]<sup>-</sup>, 82%), 367 ([2M - K]<sup>-</sup>, 100%). Data are in good agreement with literature values.<sup>53</sup>

#### 4.2.28. 3-Bromo-5-hydroxybenzylalcohol (15)<sup>20, 55</sup>

Following the procedure of Hewings *et al.*,<sup>20</sup> to a solution of 3-bromo-5-hydroxybenzoic acid (5.15 g, 23.7 mmol, 1.0 eq) in anhydrous THF (200 mL) was added a 1 M solution of borane (70.0

mL, 6.02 g, 70.0 mmol, 3.0 eq) in THF dropwise at 0 °C. The reaction solution was warmed to rt and stirred for 44 h, then was cooled to 0 °C. This was followed by slow addition of MeOH (200 mL), then an aqueous 1 M solution of HCl (100 mL), and then the volatile components were removed *in vacuo*. The resulting residue was resuspended in H<sub>2</sub>O (150 mL) and extracted with EtOAc (3 × 150 mL). The combined organic layers were washed with a saturated aqueous solution of NaHCO<sub>3</sub> (450 mL), and brine (450 mL), dried over anhydrous MgSO<sub>4</sub>, filtered, and concentrated *in vacuo* to give **15** (4.65 g, 22.9 mmol, 96%) as an oil that was deemed pure enough for use in the next step: R<sub>f</sub> (30% EtOAc/petroleum ether) 0.22; <sup>1</sup>H NMR (400 MHz, D<sub>6</sub>-DMSO) δ 9.81 (1H, s, C(5)OH), 6.93-6.88 (1H, m, C(2)H), 6.79 (1H, dd, *J* = 1.9, 1.9 Hz, C(4)H), 6.74-6.70 (1H, m, C(6)H), 5.25 (1H, t, *J* = 5.7 Hz, CH<sub>2</sub>OH), 4.40 (2H, d, *J* = 5.7 Hz, CH<sub>2</sub>OH); LRMS *m/z* (ES<sup>-</sup>) 201 & 203 ([M(<sup>79</sup>Br) – H]<sup>-</sup> & [M(<sup>81</sup>Br) – H]<sup>-</sup>, 79%), 403 & 405 & 407 ([M(<sup>79</sup>Br)M(<sup>79</sup>Br) – H]<sup>-</sup> & [M(<sup>79</sup>Br)M(<sup>81</sup>Br) – H]<sup>-</sup> & [M(<sup>81</sup>Br)M(<sup>81</sup>Br) – H]<sup>-</sup>, 100%). Data are in good agreement with literature values.<sup>20</sup>

#### 4.2.29. 3-Bromo-5-hydroxybenzaldehyde (**16**)<sup>21</sup>

To a solution of 3-bromo-5-hydroxybenzylalcohol **15** (1.79 g, 8.77 mmol, 1.0 eq) in CHCl<sub>3</sub> (15 mL) and ethyl acetate (3 mL) was added activated MnO<sub>2</sub> (5.34 g, 61.4 mmol, 7 eq). The reaction mixture was heated under reflux for 3 h after which time the reaction was judged to be complete by TLC analysis. After this time the suspension was cooled to rt and filtered through Celite<sup>®</sup>, eluting with CH<sub>2</sub>Cl<sub>2</sub>. The volatile components were removed *in vacuo*, and the resulting solid was purified by silica gel chromatography, ethyl acetate: petroleum ether 1:3, to yielded **16** (1.39 g, 78%) as an off-white solid: R<sub>f</sub> (30% EtOAc/petroleum ether) 0.50; mp (from CHCl<sub>3</sub>) 137-139 °C [lit. mp 137-140 °C<sup>21</sup>]; <sup>1</sup>H NMR (400 MHz, D<sub>6</sub>-DMSO) δ 10.45 (1H, s, CHO), 9.86 (1H, s, C(5)OH), 7.52-7.45 (1H, m, C<sub>Ar</sub>H), 7.30-7.19 (2H, m, 2 × C<sub>Ar</sub>H); LRMS *m/z* (ES<sup>-</sup>) 199 & 201 ([M(<sup>79</sup>Br) – H]<sup>-</sup> & [M(<sup>81</sup>Br) – H]<sup>-</sup>, 31%), 399 & 401 & 403 ([M(<sup>79</sup>Br)M(<sup>79</sup>Br) – H]<sup>-</sup> & [M(<sup>79</sup>Br)M(<sup>81</sup>Br) – H]<sup>-</sup> & [M(<sup>81</sup>Br)M(<sup>81</sup>Br) – H]<sup>-</sup>, 100%). Data are in good agreement with literature values.<sup>21</sup>

#### 4.2.30. 3-(3,5-Dimethyl-1,2-oxazol-4-yl)-5-hydroxybenzaldehyde (**17**)<sup>21</sup>

Na<sub>2</sub>CO<sub>3</sub> (1.41 g, 13.3 mmol, 3.0 eq) was ground to fine powder and added together with **16** (0.890 g, 4.43 mmol, 1.0 eq) and **13** (1.36 g, 6.64 mmol, 1.5 eq) into a Schlenk flask. The



atmosphere in the Schlenk flask was removed by applying a vacuum and replaced by N<sub>2</sub>. This process was repeated three times. Ethanol (4 mL) was added and the mixture was heated to 80 °C for 10-30 min. RuPhos (0.394 g, 0.531 mmol, 0.12 eq) and Pd(OAc)<sub>2</sub> (60 mg, 0.531 mmol, 0.12 eq) were added to a scintillation vial, which was capped with a septum. The atmosphere in the scintillation vial was removed by applying a vacuum and replaced by N<sub>2</sub>. This process was repeated three times. Ethanol (2 mL) was added to the scintillation vial and the mixture was stirred until the solution was colored deep red. This solution was transferred from the scintillation vial to Schlenk flask using a syringe. Ethanol (2 mL) was used to transfer the residual catalyst from the scintillation vial to Schlenk flask. The reaction mixture was heated for 1 h at 80 °C. After completion, the reaction mixture was cooled to rt and diluted with ethyl acetate. The volatile components were removed *in vacuo*. The residue was dissolved in ethyl acetate (50 mL). The organic layer was washed with water (3 × 20 mL). The organic layer was concentrated *in vacuo*. Purification by silica gel chromatography, eluting with EtOAc in petroleum ether (gradient elution 0 → 50%) yielded **17** (803 mg, 85%) as a yellow solid. R<sub>f</sub> (20% EtOAc/petroleum ether) 0.13; mp (from EtOAc) 184-186 °C [lit. mp 184-187 °C<sup>21</sup>]; <sup>1</sup>H NMR (400 MHz, D<sub>6</sub>-acetone) δ 10.02 (1H, s, CHO), 9.11 (1H, br s, C(5)OH), 7.42 (1H, dd, *J* = 1.4, 1.4 Hz, C(6)H), 7.36 (1H, dd, *J* = 2.3, 1.4 Hz, C(2)H), 7.15 (1H, dd, *J* = 2.3, 1.4 Hz, C(4)H), 2.44 (3H, s, C(5')CH<sub>3</sub>), 2.26 (3H, s, C(3')CH<sub>3</sub>); LRMS *m/z* (ES<sup>-</sup>) 216 ([M - H]<sup>-</sup>, 100%). Data are in good agreement with literature values.<sup>21</sup>

#### 4.2.31. 3-(3,5-Dimethylisoxazol-4-yl)-5-((triisopropylsilyl)oxy)benzaldehyde (**18**)

To a solution of **17** (475 mg, 2.19 mmol, 1.0 eq) and imidazole (420 mg, 6.17 mmol, 2.8 eq) in DMF (2 mL) at 0 °C, was added TIPSCI (500 μL, 451 mg, 2.34 mmol, 1.1 eq) dropwise. The reaction was allowed to warm to rt, and stirred for 22 h, then was diluted with H<sub>2</sub>O (25 mL). The aqueous phase was extracted with EtOAc (3 × 25 mL) and the combined organic layers were washed with brine (75 mL), dried over anhydrous MgSO<sub>4</sub>, filtered, and concentrated *in vacuo*, to yield **18** (683 mg, 84%) as a volatile liquid that was used without purification: R<sub>f</sub> (20% EtOAc/ petroleum ether) 0.69; ν<sub>max</sub> (thin film)/cm<sup>-1</sup>: 2946 (s), 2868 (s), 1702 (s), 1590 (s); <sup>1</sup>H NMR (500 MHz, D<sub>6</sub>-acetone) δ 10.06 (1H, s, CHO), 7.56-7.54 (1H, m, C(6)H), 7.45-7.42 (1H, m, C(2)H), 7.23-7.20 (1H, m, C(4)H), 2.44 (3H, s, C(5')CH<sub>3</sub>), 2.26 (3H, s, C(3')CH<sub>3</sub>), 1.42-1.31 (3H, m, 3 × CH), 1.16 (9H, s, 3 × CH<sub>3</sub>), 1.14 (9H, s, 3 × CH<sub>3</sub>); <sup>13</sup>C NMR (126 MHz,



D<sub>6</sub>-acetone)  $\delta$  192.6 (CHO), 166.5 (C(5')), 158.8 (C(5)), 157.9 (C(3')), 139.7 (C(3)), 134.0 (C(1)), 127.0 (C(2)), 124.6 (C(4)), 119.2 (C(6)), 116.1 (C(4')), 18.2 (3  $\times$  CH), 13.4 (6  $\times$  CH<sub>3</sub>), 11.6 (C(5')CH<sub>3</sub>), 10.8 (C(5')CH<sub>3</sub>); HRMS  $m/z$  (ES<sup>+</sup>) Found: 396.1956. C<sub>21</sub>H<sub>31</sub>NNaO<sub>3</sub>Si<sup>+</sup> requires [M + Na]<sup>+</sup>, 396.1965; LRMS  $m/z$  (ES<sup>+</sup>) 374 ([M + H]<sup>+</sup>, 100%).

#### 4.2.32. Ethyl 3-(3,5-dimethylisoxazol-4-yl)-5-hydroxybenzoate (20)

To a dry 10-20 mL microwave vial were added ethyl 3-bromo-5-hydroxybenzoate (**19**, 500 mg, 2.04 mmol, 1.0 eq), **13** (435 mg, 2.14 mmol, 1.05 eq), Pd(OAc)<sub>2</sub> (5 mg, 20.0  $\mu$ mol, 0.01 eq), RuPhos (29 mg, 61.1  $\mu$ mol, 0.03 eq) and anhydrous Na<sub>2</sub>CO<sub>3</sub> (649 mg, 6.12 mmol, 3.0 eq). The vial was sealed and purged with nitrogen, before the addition of ethanol (10 mL). The reaction solution was degassed, by bubbling with nitrogen for 40 min, then heated at 90 °C with microwave irradiation for 90 min. The mixture was allowed to cool to rt and filtered through a thin pad of silica gel, eluting with CH<sub>2</sub>Cl<sub>2</sub>, and the volatile components were removed *in vacuo*. Purification by silica gel chromatography, eluting with Et<sub>2</sub>O in petroleum ether (gradient elution 30  $\rightarrow$  80%) yielded **20** (224 mg, 68%) as a yellow solid: R<sub>f</sub> (1% AcOH/EtOAc) 0.53;  $\nu_{\max}$  (thin film)/cm<sup>-1</sup>: 3214 (br), 2983 (w), 2935 (w), 1718 (s), 1633 (m), 1421 (m), 1329 (s), 1265 (s), 1235 (s), 1108 (w), 1023 (w); <sup>1</sup>H NMR (400 MHz, MeOD)  $\delta$  7.43 (1H, dd,  $J$  = 2.4, 1.5 Hz, C(2)H), 7.41 (1H, dd,  $J$  = 1.5, 1.5 Hz, C(6)H), 6.97 (1 H, dd,  $J$  = 2.4, 1.5 Hz, C(4)H), 4.36 (2H, q,  $J$  = 7.1 Hz, CH<sub>2</sub>CH<sub>3</sub>), 2.42 (3H, s, C(5')CH<sub>3</sub>), 2.26 (3H, s, C(3')CH<sub>3</sub>), 1.39 (3H, t,  $J$  = 7.1 Hz, CH<sub>2</sub>CH<sub>3</sub>); <sup>13</sup>C NMR (101 MHz, CDCl<sub>3</sub>)  $\delta$  167.6 (C=O), 167.1 (C(5')), 159.7 (C(5)), 159.3 (C(3')), 133.5 (C(3)), 132.9 (C(1)), 122.0 (C(2)), 121.5 (C(4)), 117.1 (C(6)), 116.2 (C(4')), 62.2 (CH<sub>2</sub>CH<sub>3</sub>), 14.5 (CH<sub>2</sub>CH<sub>3</sub>), 11.3 (C(5')CH<sub>3</sub>), 10.6 (C(3')CH<sub>3</sub>); HRMS  $m/z$  (ES<sup>-</sup>) Found: 260.0927. C<sub>14</sub>H<sub>14</sub>NO<sub>4</sub><sup>-</sup> requires M<sup>-</sup> 260.0928; LRMS  $m/z$  (ES<sup>-</sup>) 260 ([M - H]<sup>-</sup>, 100%).

#### 4.2.33. 3-(3,5-Dimethylisoxazol-4-yl)-5-hydroxybenzoic acid (21)

To a solution of **20** (295 mg, 1.13 mmol, 1.0 eq) in THF (5 mL) and H<sub>2</sub>O (2.5 mL) was added LiOH (81 mg, 3.38 mmol, 3.0 eq). The reaction mixture was stirred for 25 h, then Et<sub>2</sub>O (10 mL) and an aqueous 2 M LiOH solution (10 mL) was added. The phases were separated, and the aqueous phase was washed with Et<sub>2</sub>O (2  $\times$  10 mL), then acidified to pH 3 with an aqueous 1 M HCl solution.

The aqueous suspension was then extracted with EtOAc (5 × 10 mL). The combined organic layers were dried over anhydrous MgSO<sub>4</sub>, filtered, and concentrated *in vacuo*, yielding **21** (260 mg, 98%) as a colourless solid: R<sub>f</sub> (1% AcOH/EtOAc) 0.53;  $\nu_{\max}$  (thin film)/cm<sup>-1</sup>: 3169 (br), 2661 (w), 1695 (s), 1595 (s), 1489 (s), 1325 (s), 1231 (s), 1205 (s), 1078 (w); <sup>1</sup>H NMR (400 MHz, MeOD)  $\delta$  7.44 (1H, dd, *J* = 2.3, 1.5 Hz, C(2)*H*), 7.43 (1H, dd, *J* = 1.5, 1.5 Hz, C(6)*H*), 6.96 (1 H, dd, *J* = 2.3, 1.5 Hz, C(4)*H*), 2.42 (3H, s, C(5')CH<sub>3</sub>), 2.26 (3H, s, C(3')CH<sub>3</sub>); <sup>13</sup>C NMR (101 MHz, CDCl<sub>3</sub>)  $\delta$  169.3 (C=O), 167.1 (C(5')), 159.8 (C(5)), 159.2 (C(3')), 133.8 (C(3)), 123.8 (C(1)), 122.3 (C(2)), 121.4 (C(4)), 117.2 (C(6)), 116.6 (C(4')), 11.4 (C(5')CH<sub>3</sub>), 10.6 (C(3')CH<sub>3</sub>); HRMS *m/z* (ES<sup>-</sup>) Found: 232.0615. C<sub>12</sub>H<sub>12</sub>NO<sub>4</sub><sup>-</sup> requires M<sup>-</sup> 232.0615; LRMS *m/z* (ES<sup>-</sup>) 232 ([M – H]<sup>-</sup>, 100%).

### 4.3. Biological evaluation

#### 4.3.1. Cloning, protein expression and purification.

cDNA encoding human BRD4 (NCBI accession numbers NP 055114.1) was obtained from FivePrime and was used as the template to amplify the N-terminal bromodomain region of the protein. Protein expression and purification was carried out as previously described.<sup>37</sup> CREBBP was expressed and purified as previously described.<sup>23</sup>

#### 4.3.2. Bromodomain AlphaScreen™ assay

Bromodomain AlphaScreen™ assays were carried out as previously described<sup>20, 47</sup> with minor modifications using the following peptide: H4KAc4 peptide (H<sub>2</sub>N-YSGRGK(Ac)GGK(Ac)GLGK(Ac)GGAK(Ac)RHRK(Biotin)-CONH<sub>2</sub>). All experiments were carried out in triplicate and OXFBD02 (**1a**) was used as a positive control on every plate. This compound afforded IC<sub>50</sub> values in a range from 307-358 nM, which is in line with published values [BRD4(1) IC<sub>50</sub> = 384 nM<sup>21</sup>]. AlphaScreen™ buffer (25 mM HEPES, 100 mM NaCl, 0.05% w/v CHAPS, 0.1% w/v BSA; pH 7.6) was prepared fresh each day by supplementing HEPES base with BSA, filter sterilisation through a 0.22 µm filter, and storage at 4 °C, with equilibration to room temperature before use. Biotinylated peptides employed and final assay concentrations were: his<sub>6</sub>BRD4(1)

10 nM, H4[1-20](KAc)<sub>4</sub> 4 nM; donor beads 5 µg/mL; acceptor beads 5 µg/mL; DMSO < 0.5%.

Compounds were prepared as 30 mM DMSO stocks. Inhibition was reported as a reduction in signal arising from peptide-bromodomain interaction, with all plates including buffer and DMSO controls. Concentration-response curves against BRD4 were performed in triplicate on a ProxiPlate-384 Plus (Perkin Elmer), which was read using a Perkin Elmer Wallac Multilabel reader 2104. For incubation steps, the plate was sealed, shaken for 10 seconds at 600 rpm, and incubated at room temperature in the dark for 1 h.

#### 4.3.3. Isothermal titration calorimetry

All calorimetric experiments were performed on a MicroCal PEAQ-ITC Automated (Malvern) and analysed with the MicroCal PEAQ-ITC Analysis software (Malvern 1.1.0.1262) using a single binding site model. The first data point was excluded from the analysis. BRD4(1) was dialysed at 4 °C overnight in a Slide-A-Lyzer® MINI Dialysis Device (2000 MWCO; Thermo Scientific Life Technologies) into 50 mM HEPES, 150 mM NaCl containing 0.2% DMSO; pH 7.4. Proteins were centrifuged to remove aggregates (3 min, 3,000 rpm, 25 °C). Protein concentrations were determined by measuring the absorbance at 280 nm using a NanoDrop Lite spectrophotometer (Nanodrop® Technologies Inc.) by using the predicted protein absorbance (BRD4(1):  $\epsilon_{280} = 28420 \text{ M}^{-1} \text{ cm}^{-1}$ , CREBBP:  $\epsilon_{280} = 26930 \text{ M}^{-1} \text{ cm}^{-1}$ ). Small molecules ligand were dissolved as 5 to 10 mM DMSO stock solution and diluted to the required concentration using dialysis buffer. The cell was stirred at 750 rpm, reference power set to 5 µcal/sec and temperature held at 25 °C. After an initial delay of 60 sec, 19 × 2 µL injections (first injection 0.4 µL) were performed with a spacing of 180 sec. Heated dilutions were measured under the same conditions and subtracted for analysis. Small molecule solutions in the calorimetric cell (250 µL, (10 to 20 µM)) were titrated with the protein solutions in the syringe (60 µL, 109 to 160 µM).

#### 4.3.4. Crystallisation

Aliquots of the purified proteins were set up for crystallisation using a mosquito® crystallisation robot (TTP Labtech, Royston UK). Coarse screens were typically setup onto Greiner 3-well plates using three different drop ratios of precipitant to protein per condition (100+50 nL, 75+75 nL and

50+100 nL). Initial hits were optimised further using Greiner 1-well plates and scaling up the drop sizes in steps. All crystallisations were carried out using the sitting drop vapor diffusion method at 4 °C. BRD4(1) crystals with **9j** (1 mM final concentration) were grown by mixing 200 nL of the protein (7.3 mg/ml) with 100 nL of reservoir solution containing 20% PEG 3350 and 0.1 M citrate pH 5.5. BRD4(1) crystals with **9i** (1 mM final concentration) were grown by mixing 200 nL of the protein (7.3 mg/ml) with an 100 nL of reservoir solution containing 0.1 M K(citrate), 0.1 M cacodylate pH 6.5. BRD4(1) crystals with **10d** (1 mM final concentration) were grown by mixing 200 nL of the protein (6.6 mg/ml) with an 100 nL of reservoir solution containing 24.0% PEG1K and 20.0% glycerol.

#### 4.3.5. Data collection and structure solution

Crystals were cryo-protected using the well solution supplemented with additional ethylene glycol and were flash frozen in liquid nitrogen. Data were collected at Diamond beamline I24 using a Pilatus6M detector at 0.96861 Å. Indexing and integration were carried out using XDS<sup>56, 57</sup> and scaling was performed with SCALA.<sup>58</sup> Initial phases were calculated by molecular replacement with PHASER<sup>59</sup> using an ensemble of known bromodomain models (PDB codes 2OSS, 2OUO, 2GRC, 2OO1, 3DAI, 3D7C, 3DWY). Initial models were built by ARP/wARP<sup>60</sup> and building was completed manually with COOT.<sup>61</sup> Refinement was carried out in REFMAC5.<sup>62</sup> Data collection and refinement statistics can be found in Supplemental Table S6. The models and structure factors have been deposited with PDB accession codes: 6FSY (BRD4(1)/ **9j** complex), 6FT3 (BRD4(1)/ **9i** complex) and 6FT4 (BRD4(1)/ **10d** complex).

#### 4.3.6. Human microsomal stability assay

These assays were performed by Cyprotex (Nether Alderley, UK) according to standard operating protocols.

#### 4.3.7. Luciferase reporter assay

The NF-κB luciferase reporter plasmid carrying 6 tandem κB-sites, NF-κB-luc, CMV-β-Gal, and pBSSK were generously provided by Dr Jorge Iñigues-Lluhí (The University of Michigan

Pharmacology Department).<sup>63</sup> All cells were maintained in 5% CO<sub>2</sub> at 37 °C. HeLa cells were grown in Dulbecco's modified Eagle's medium (DMEM, Invitrogen) supplemented with 10% FBS. For luciferase assays, 4×10<sup>5</sup> cells were seeded in a 6-well dish and allowed to adhere overnight. The media was removed, and cells were transfected in Opti-Mem (Invitrogen) with 400 ng NF-κB-luc, 200 ng CMV-β-Gal, and 1,400 ng pBSSK using Lipofectamine 2000 (Life Technologies) according to manufacturer's instructions. After 4.5 h, transfection solution was removed and replaced with DMEM containing 10% FBS. At 24 h after transfection, cells were trypsinized and resuspended in DMEM supplemented with 10% FBS and seeded into a 96-well plate at a density of 8×10<sup>3</sup> cells per well. After an additional 16 h, media was removed and replaced with Opti-Mem containing vehicle or the indicated compounds delivered in DMSO (1% v/v) at the indicated concentrations. After cells incubated with either vehicle or compound for 1 h, cells were treated with either PBS or IL-1β at a final concentration of 2 ng/mL. After an additional 3 h, media was removed and cells were lysed with 60 μL of passive lysis buffer. Luciferase and β-Galactosidase activities were determined as previously described.<sup>64</sup> NF-κB luciferase activity and response curve analysis was performed using GraphPad software.

#### 4.3.8. Cell growth assay

Growth inhibition was assessed by sulforhodamine B colorimetric assay as previously described.<sup>65</sup> Briefly, cells were seeded into 96-well plates at a density appropriate for exponential growth at the start of the assay, and treated with a range of concentrations of OXFBD02 (**1a**) or OXFBD04 (**9j**) for 48 h. Cells were then fixed in 10% (w/v) TCA and stained with sulforhodamine B. The concentrations required to inhibit cell growth by 50% compared to control cells were calculated using GraphPad Prism software (SanDiego, CA, USA).

#### 4.3.9. Western blot assay to detect MYC suppression

MCF7 cells were treated with 10 μM of (+)-JQ1, OXFBD04 (**9j**) or OXFBD02 (**1a**) for 10, 24, or 48 h. Cells were lysed in UTB (9 M urea, 75 mM Tris-HCl pH 7.5, 0.15 M β-mercaptoethanol) and briefly sonicated. Protein expression was assessed by immunoblotting with primary antibodies c-

myc (Cell Signaling, 5605) and Actin (Santa Cruz, sc-69879), and secondary antibodies IRDye® 800CW Donkey anti-Rabbit IgG (H+L) and IRDye® 680RD Goat anti-Mouse IgG (H+L) from LI-COR Biosciences. Odyssey IR imaging technology (LI-COR Biosciences) was used for imaging.

#### 4.4. Computational methods

##### 4.4.1. Molecular dynamics

The protein and ligand co-ordinates were taken from the crystal structures of **1a** bound to BRD4(1), where ligand models for **9j** and **9p** were prepared by substituting the atoms of **1a**. The AMBER99SB-IDLN forcefield was used for the protein.<sup>66</sup> The ligands were protonated at pH 7.4 using the Marvin Suite 16.16.6.0 from ChemAxon (<https://www.chemaxon.com>) and parameterised using the General Amber forcefield (v. 1.8) found in AmberTools16.<sup>67</sup> All crystallographic water molecules were retained and the TIP3P water model was used.<sup>68</sup> The system was solvated within a dodecahedral box, with a minimum distance of 1.2 nm between the protein and the edge of the box. Water molecules were substituted with a sodium ion to neutralise the net charge and to maintain an overall salt concentration of 150 mM sodium chloride. The systems were subject to energy minimisation using the steepest decent algorithm, with a maximum force cut off of 100 kJ mol<sup>-1</sup> nm<sup>-1</sup>. The systems then underwent 200 ps equilibration in the isothermal-isobaric ensemble. The temperature was coupled using a Langevin thermostat, with a target temperature of 300 K, and the pressure was coupled using the Berendsen weak coupling algorithm to a target pressure of 1 atm.<sup>69-71</sup> Simulations were then carried out for 50 ns using GROMACS 2016.4, in triplicate.<sup>72</sup> Torsions were calculated using the MDAnalysis package for Python and a rolling average calculated over 10 time points.<sup>73</sup>

#### Acknowledgments

We thank Dr Angelina Sekirnik and Dr Liam O'Connor for conducting some initial biological experiments in this project. L.E.J. and J.P.B. thank the EPSRC and GlaxoSmithKline for studentship support *via* the Systems Approaches to Biomedical Sciences Centre for Doctoral



Training (EP/G037280/1). M.S. is supported by the Deutsche Forschungsgemeinschaft (SCHL 1408/1-1). D.S.H. thanks Cancer Research UK for a studentship. C.M.C.L. thanks the BBSRC and GlaxoSmithKline for the award of a BBSRC iCASE studentship (BB/M015157/1). A.R.S., J.K.R., and M.M. thank the EPSRC Centre for Doctoral Training in Synthesis for Biology and Medicine (EP/L015838/1) for studentship support, generously supported by AstraZeneca, Diamond Light Source, Defence Science and Technology Laboratory, Evotec, GlaxoSmithKline, Janssen, Novartis, Pfizer, Syngenta, Takeda, UCB, and Vertex. C.N.G.E. thanks Cancer Research UK and the EPSRC for studentship support through the CR-UK and EPSRC Cancer Imaging Centre in Oxford. I.N.M., S.J.C., and E.M.H. thank the MRC (MR/N009460/1) for funding. This project has received funding from the European Union's Horizon 2020 research and innovation programme under grant agreement No 658825. P.F. and S.P. are supported by a Wellcome Trust Career Development Fellowship (095751/Z/11/Z) and the SGC, a registered charity (number 1097737) that receives funds from AbbVie, Bayer Pharma AG, Boehringer Ingelheim, Canada Foundation for Innovation, Eshelman Institute for Innovation, Genome Canada, Innovative Medicines Initiative (EU/EFPIA) [ULTRA-DD grant no. 115766], Janssen, Merck & Co., Novartis Pharma AG, Ontario Ministry of Economic Development and Innovation, Pfizer, São Paulo Research Foundation-FAPESP, Takeda, and the Wellcome Trust (092809/Z/10/Z). The authors would like to thank Diamond Light Source for beamtime (proposal mx15433), and the staff of beamlines I24 for assistance with crystal testing and data collection. We would like to acknowledge the use of the University of Oxford Advanced Research Computing (ARC) facility in carrying out this work: <http://dx.doi.org/10.5281/zenodo.22558>. P.C.B. thanks Lady Margaret Hall, Oxford for research funding. E.M.H. thanks Cancer Research UK (C9720/A18513) for funding. S.J.C. thanks St Hugh's College, Oxford, for research funding.

## A. Supplementary data

Supplementary data (synthesis of compounds and characterisations, supplementary figures, and supplementary tables) associated with this article can be found in the online version, at <http://doi.org/XXXXXXXXXXXXXX>.

## References

1. Weinert BT, Wagner SA, Horn H, et al. Proteome-wide mapping of the Drosophila acetylome demonstrates a high degree of conservation of lysine acetylation. *Sci Signal*. 2011;4: ra48.
2. Kouzarides T. Acetylation: a regulatory modification to rival phosphorylation? *EMBO J*. 2000;19: 1176-1179.
3. Strahl BD, Allis CD. The language of covalent histone modifications. *Nature*. 2000;403: 41-45.
4. Gardner KE, Allis CD, Strahl BD. Operating on chromatin, a colorful language where context matters. *J Mol Biol*. 2011;409: 36-46.
5. Filippakopoulos P, Knapp S. The bromodomain interaction module. *FEBS Lett*. 2012;586: 2692-2704.
6. Mujtaba S, Zeng L, Zhou MM. Structure and acetyl-lysine recognition of the bromodomain. *Oncogene*. 2007;26: 5521-5527.
7. Hewings DS, Rooney TP, Jennings LE, et al. Progress in the development and application of small molecule inhibitors of bromodomain-acetyl-lysine interactions. *J Med Chem*. 2012;55: 9393-9413.
8. Conway SJ. Bromodomains: are readers right for epigenetic therapy? *ACS Med Chem Lett*. 2012;3: 691-694.
9. Jennings LE, Measures AR, Wilson BG, Conway SJ. Phenotypic screening and fragment-based approaches to the discovery of small-molecule bromodomain ligands. *Future Med Chem*. 2014;6: 179-204.
10. Gallenkamp D, Gelato KA, Haendler B, Weinmann H. Bromodomains and their pharmacological inhibitors. *ChemMedChem*. 2014;9: 438-464.
11. Zhang G, Smith SG, Zhou MM. Discovery of chemical inhibitors of human bromodomains. *Chem Rev*. 2015;115: 11625-11668.
12. Romero FA, Taylor AM, Crawford TD, Tsui V, Cote A, Magnuson S. Disrupting acetyl-lysine recognition: progress in the development of bromodomain inhibitors. *J Med Chem*. 2016;59: 1271-1298.
13. Brand M, Measures AM, Wilson BG, et al. Small molecule inhibitors of bromodomain-acetyl-lysine interactions. *ACS Chem Biol*. 2015;10: 22-39.
14. Theodoulou NH, Tomkinson NC, Prinjha RK, Humphreys PG. Progress in the development of non-BET bromodomain chemical probes. *ChemMedChem*. 2016;11: 477-487.
15. Palmer WS. Development of small molecule inhibitors of BRPF1 and TRIM24 bromodomains. *Drug Discov Today Technol*. 2016;19: 65-71.
16. Theodoulou NH, Tomkinson NC, Prinjha RK, Humphreys PG. Clinical progress and pharmacology of small molecule bromodomain inhibitors. *Curr Opin Chem Biol*. 2016;33: 58-66.
17. Filippakopoulos P, Knapp S. Targeting bromodomains: epigenetic readers of lysine acetylation. *Nat Rev Drug Discov*. 2014;13: 337-356.
18. Jones PA, Issa JP, Baylin S. Targeting the cancer epigenome for therapy. *Nat Rev Genet*. 2016;17: 630-641.
19. Fujisawa T, Filippakopoulos P. Functions of bromodomain-containing proteins and their roles in homeostasis and cancer. *Nat Rev Mol Cell Biol*. 2017;18: 246-262.
20. Hewings DS, Wang M, Philpott M, et al. 3,5-dimethylisoxazoles act as acetyl-lysine-mimetic bromodomain ligands. *J Med Chem*. 2011;54: 6761-6770.
21. Hewings DS, Fedorov O, Filippakopoulos P, et al. Optimization of 3,5-dimethylisoxazole derivatives as potent bromodomain ligands. *J Med Chem*. 2013;56: 3217-3227.

22. Hay D, Fedorov O, Filippakopoulos P, et al. The design and synthesis of 5- and 6-isoxazolylbenzimidazoles as selective inhibitors of the BET bromodomains. *MedChemComm*. 2013;4: 140-144.
23. Rooney TP, Filippakopoulos P, Fedorov O, et al. A series of potent CREBBP bromodomain ligands reveals an induced-fit pocket stabilized by a cation- $\pi$  interaction. *Angew Chem Int Ed*. 2014;53: 6126-6130.
24. Hay DA, Fedorov O, Martin S, et al. Discovery and optimization of small-molecule ligands for the CBP/p300 bromodomains. *J Am Chem Soc*. 2014;136: 9308-9319.
25. Sekirnik Nee Measures AR, Hewings DS, Theodoulou NH, et al. Isoxazole-derived amino acids are bromodomain-binding acetyl-lysine mimics: incorporation into histone H4 peptides and histone H3. *Angew Chem Int Ed Engl*. 2016;55: 8353-8357.
26. Dawson MA, Prinjha RK, Dittmann A, et al. Inhibition of BET recruitment to chromatin as an effective treatment for MLL-fusion leukaemia. *Nature*. 2011;478: 529-533.
27. Bamborough P, Diallo H, Goodacre JD, et al. Fragment-based discovery of bromodomain inhibitors part 2: optimization of phenylisoxazole sulfonamides. *J Med Chem*. 2012;55: 587-596.
28. Seal J, Lamotte Y, Donche F, et al. Identification of a novel series of BET family bromodomain inhibitors: binding mode and profile of I-BET151 (GSK1210151A). *Bioorg Med Chem Lett*. 2012;22: 2968-2972.
29. Mirguet O, Lamotte Y, Donche F, et al. From ApoA1 upregulation to BET family bromodomain inhibition: discovery of I-BET151. *Bioorg Med Chem Lett*. 2012;22: 2963-2967.
30. Gehling VS, Hewitt MC, Vaswani RG, et al. Discovery, Design, and Optimization of Isoxazole Azepine BET Inhibitors. *ACS Med Chem Lett*. 2013;4: 835-840.
31. Sharp PP, Garnier J-M, Huang DCS, Burns CJ. Evaluation of functional groups as acetyl-lysine mimetics for BET bromodomain inhibition. *MedChemComm*. 2014;5: 1834-1842.
32. Mirguet O, Lamotte Y, Chung CW, et al. Naphthyridines as novel BET family bromodomain inhibitors. *ChemMedChem*. 2014;9: 580-589.
33. McKeown MR, Shaw DL, Fu H, et al. Biased multicomponent reactions to develop novel bromodomain inhibitors. *J Med Chem*. 2014;57: 9019-9027.
34. Ran X, Zhao Y, Liu L, et al. Structure-based design of gamma-carboline analogues as potent and specific BET bromodomain inhibitors. *J Med Chem*. 2015;58: 4927-4939.
35. Zhao Y, Bai L, Liu L, et al. Structure-based discovery of 4-(6-methoxy-2-methyl-4-(quinolin-4-yl)-9H-pyrimido[4,5-b]indol-7-yl)-3,5-dimethylisoxazole (CD161) as a potent and orally bioavailable BET bromodomain inhibitor. *J Med Chem*. 2017;60: 3887-3901.
36. Picaud S, Da Costa D, Thanasopoulou A, et al. PFI-1, a highly selective protein interaction inhibitor, targeting BET bromodomains. *Cancer Res*. 2013;73: 3336-3346.
37. Filippakopoulos P, Qi J, Picaud S, et al. Selective inhibition of BET bromodomains. *Nature*. 2010;468: 1067-1073.
38. Shoemaker RH. The NCI60 human tumour cell line anticancer drug screen. *Nat Rev Cancer*. 2006;6: 813-823.
39. Lucas X, Wohllwend D, Hugle M, et al. 4-Acyl pyrroles: mimicking acetylated lysines in histone code reading. *Angew Chem Int Ed Engl*. 2013;52: 14055-14059.
40. Huang B, Yang XD, Zhou MM, Ozato K, Chen LF. Brd4 coactivates transcriptional activation of NF-kappaB via specific binding to acetylated RelA. *Mol Cell Biol*. 2009;29: 1375-1387.
41. Zou Z, Huang B, Wu X, et al. Brd4 maintains constitutively active NF-kappaB in cancer cells by binding to acetylated RelA. *Oncogene*. 2014;33: 2395-2404.
42. Perkins ND. Post-translational modifications regulating the activity and function of the nuclear factor kappa B pathway. *Oncogene*. 2006;25: 6717-6730.
43. Huang B, Yang XD, Lamb A, Chen LF. Posttranslational modifications of NF-kappaB: another layer of regulation for NF-kappaB signaling pathway. *Cell Signal*. 2010;22: 1282-1290.

44. Bruno PA, Morriss-Andrews A, Henderson AR, Brooks CL, 3rd, Mapp AK. A synthetic loop replacement peptide that blocks canonical NF-kappaB signaling. *Angew Chem Int Ed Engl.* 2016;55: 14997-15001.
45. Hill AP, Young RJ. Getting physical in drug discovery: a contemporary perspective on solubility and hydrophobicity. *Drug Discov Today.* 2010;15: 648-655.
46. Young RJ, Green DV, Luscombe CN, Hill AP. Getting physical in drug discovery II: the impact of chromatographic hydrophobicity measurements and aromaticity. *Drug Discov Today.* 2011;16: 822-830.
47. Philpott M, Yang J, Tumber T, et al. Bromodomain-peptide displacement assays for interactome mapping and inhibitor discovery. *Mol Biosyst.* 2011;7: 2899-2908.
48. Jansma A, Zhang Q, Li B, et al. Verification of a designed intramolecular hydrogen bond in a drug scaffold by nuclear magnetic resonance spectroscopy. *J Med Chem.* 2007;50: 5875-5877.
49. Houston JB. Utility of in vitro drug metabolism data in predicting in vivo metabolic clearance. *Biochem Pharmacol.* 1994;47: 1469-1479.
50. Gottlieb HE, Kotlyar V, Nudelman A. NMR Chemical Shifts of Common Laboratory Solvents as Trace Impurities. *J Org Chem.* 1997;62: 7512-7515.
51. Kofron WG, Baclawski LM. Convenient Method for Estimation of Alkylolithium Concentrations. *J Org Chem.* 1976;41: 1879-1880.
52. Love BE, Jones EG. The use of salicylaldehyde phenylhydrazine as an indicator for the titration of organometallic reagents. *J Org Chem.* 1999;64: 3755-3756.
53. Molander GA, Canturk B. Organotrifluoroborates and monocoordinated palladium complexes as catalysts--a perfect combination for Suzuki-Miyaura coupling. *Angew Chem Int Ed Engl.* 2009;48: 9240-9261.
54. Lennox AJ, Lloyd-Jones GC. Preparation of organotrifluoroborate salts: precipitation-driven equilibrium under non-etching conditions. *Angew Chem Int Ed Engl.* 2012;51: 9385-9388.
55. Hamann LG, Higuchi RI, Zhi L, et al. Synthesis and biological activity of a novel series of nonsteroidal, peripherally selective androgen receptor antagonists derived from 1,2-dihydropyridono[5,6-g]quinolines. *J Med Chem.* 1998;41: 623-639.
56. Kabsch W. Evaluation of single-crystal X-ray-diffraction data from a position-sensitive detector. *J Appl Crystallogr.* 1988;21: 916-924.
57. Kabsch W. Automatic-indexing of rotation diffraction patterns. *J Appl Crystallogr.* 1988;21: 67-71.
58. Evans P. *SCALA* - scale together multiple observations of reflections, 3.3.0; MRC Laboratory of Molecular Biology: Cambridge. 2007.
59. McCoy AJ, Grosse-Kunstleve RW, Storoni LC, Read RJ. Likelihood-enhanced fast translation functions. *Acta Crystallogr D.* 2005;61: 458-464.
60. Perrakis A, Morris R, Lamzin VS. Automated protein model building combined with iterative structure refinement. *Nat Struct Biol.* 1999;6: 458-463.
61. Emsley P, Cowtan K. Coot: model-building tools for molecular graphics. *Acta Crystallogr D.* 2004;60: 2126-2132.
62. Murshudov GN, Vagin AA, Dodson EJ. Refinement of macromolecular structures by the maximum-likelihood method. *Acta Crystallogr D.* 1997;53: 240-255.
63. Hojfeldt JW, Cruz-Rodriguez O, Imaeda Y, et al. Bifunctional ligands allow deliberate extrinsic reprogramming of the glucocorticoid receptor. *Mol Endocrinol.* 2014;28: 249-259.
64. Iniguez-Lluhi JA, Pearce D. A common motif within the negative regulatory regions of multiple factors inhibits their transcriptional synergy. *Mol Cell Biol.* 2000;20: 6040-6050.
65. Vichai V, Kirtikara K. Sulforhodamine B colorimetric assay for cytotoxicity screening. *Nat Protoc.* 2006;1: 1112-1116.

66. Lindorff-Larsen K, Piana S, Palmo K, et al. Improved side-chain torsion potentials for the Amber ff99SB protein force field. *Proteins Struct Funct Bioinf.* 2010;78: 1950-1958.
67. Wang J, Wolf RM, Caldwell JW, Kollman PA, Case DA. Development and testing of a general amber force field. *J Comput Chem.* 2004;25: 1157-1174.
68. Jorgensen WL, Chandrasekhar J, Madura JD, Impey RW, Klein ML. Comparison of simple potential functions for simulating liquid water. *J Chem Phys.* 1983;79: 926-935.
69. Berendsen HJC, Postma JPM, Vangunsteren WF, Dinola A, Haak JR. Molecular-dynamics with coupling to an external bath. *J Chem Phys.* 1984;81: 3684-3690.
70. Goga N, Rzepiela AJ, de Vries AH, Marrink SJ, Berendsen HJC. Efficient algorithms for Langevin and DPD dynamics. *J Chem Theory Comput.* 2012;8: 3637-3649.
71. Van Gunsteren WF, Berendsen HJC. A Leap-Frog algorithm for stochastic dynamics. *Mol Simulat.* 1988;1: 173-185.
72. Abraham MJ, Murtola T, Schulz R, et al. GROMACS: High performance molecular simulations through multi-level parallelism from laptops to supercomputers. *SoftwareX.* 2015;1-2: 19-25.
73. Gowersk RJ, Linke M, Barnoud J, et al. MDAnalysis: a python package for the rapid analysis of molecular dynamics simulations. *Proc 15th Python Sci Conf.* 2016: 98-105.